



## Offshore Oligo-Miocene volcanic fields within the Corsica-Liguria Basin: Magmatic diversity and slab evolution in the western Mediterranean Sea

Jean-Pierre Réhault, Christian Honthaas, Pol Guennoc, Hervé Bellon, Gilles Ruffet, Joseph Cotten, M. Sosson, René R, R.C. Maury

### ► To cite this version:

Jean-Pierre Réhault, Christian Honthaas, Pol Guennoc, Hervé Bellon, Gilles Ruffet, et al.. Off-shore Oligo-Miocene volcanic fields within the Corsica-Liguria Basin: Magmatic diversity and slab evolution in the western Mediterranean Sea. *Journal of Geodynamics*, 2012, 58, pp.73-95. 10.1016/j.jog.2012.02.003 . insu-00693261

**HAL Id: insu-00693261**

**<https://hal-insu.archives-ouvertes.fr/insu-00693261>**

Submitted on 2 May 2012

**HAL** is a multi-disciplinary open access archive for the deposit and dissemination of scientific research documents, whether they are published or not. The documents may come from teaching and research institutions in France or abroad, or from public or private research centers.

L'archive ouverte pluridisciplinaire **HAL**, est destinée au dépôt et à la diffusion de documents scientifiques de niveau recherche, publiés ou non, émanant des établissements d'enseignement et de recherche français ou étrangers, des laboratoires publics ou privés.

**Offshore Oligo-Miocene volcanic fields within the Corsica-Liguria Basin:  
magmatic diversity and slab evolution in the western Mediterranean Sea**

J.-P. Réhault <sup>a\*</sup>, C. Honthaas <sup>b</sup>, P. Guennoc <sup>c</sup>, H. Bellon <sup>a</sup>, G. Ruffet <sup>d</sup>,  
J. Cotten <sup>a</sup>, M. Sosson <sup>e</sup>, R. C. Maury <sup>a</sup>

<sup>a</sup> Université européenne de Bretagne, UMR 6538 Domaines océaniques, IUEM, Université de Bretagne Occidentale, Place Nicolas Copernic, 29280 Plouzané, France

<sup>b</sup> Institut des Sciences de la Terre de Paris, UMR 7193 – UPMC – CNRS, Equipe Pétrologie, Géochimie, Volcanologie, Tour 46-00, 3<sup>ème</sup> ét., Case 110, 4 place Jussieu, 75252 Paris cedex 05, France

<sup>c</sup> BRGM, BP 6009, 45060 Orléans cedex 2, France

<sup>d</sup> Université européenne de Bretagne, CNRS INSU, UMR 6118, Université de Rennes 1, Géosciences Rennes, 35042 Rennes Cedex, France

<sup>e</sup> CNRS UMR 6526 Géosciences Azur, Université de Nice - Sophia Antipolis, 250 rue Albert Einstein, Sophia Antipolis 06560 Valbonne, France

**Abstract**

The European and Corsica-Sardinia margins of the Ligurian Sea (western Mediterranean) have been affected by a geochemically diverse igneous activity, offshore and onshore, since the Eocene. This magmatism occurred in a global subduction-related framework. On the European side, the oldest Tertiary magmatism dated at ca. 35 Ma was mainly calc-alkaline. It included the emplacement of plutonic bodies of adakitic affinity, such as the quartz microdiorite laccolith locally referred to as "esterellite". Younger magmatic events on-land within the whole Ligurian domain were mostly medium-K or K-rich calc-alkaline. Miocene volcanic activity was important in Sardinia, where andesites and ignimbrites were erupted during several magmatic cycles. In Corsica, it was minor although it emplaced lamprophyres near Sisco at 15 Ma.

Dredging and diving cruises conducted in the Ligurian Sea during the last thirty years allowed us to collect a number of submarine samples. We discuss here their geochemistry (major and trace elements) and their whole-rock K-Ar ages and mineral <sup>40</sup>Ar-<sup>39</sup>Ar plateau ages. Around 15 Ma, minor amounts of adakitic lavas were emplaced off southwestern Corsica, in the deepest part of the Liguria-Corsica Basin. They rested over the thinnest southwestern Corsica Hercynian continental crust. Closer to the coast, contemporaneous calc-alkaline rocks erupted

on a less thinned crust. The adakitic events could be indicative of either the final stages of active subduction, or alternatively of a slab tearing linked to the southeastern retreat and steepening of the slab. The latter event could be connected with the end of the Corsica-Sardinia block drifting and its correlative eastern collision.

Younger volcanic effusions, dated at 14-6 Ma, occurred mostly northwest and north of Corsica. K-rich calc-alkaline basalts, shoshonites and K-rich trachytes were emplaced during this period, and alkali basalts erupted as early as 12 Ma in Sardinia. In the Toulon area, alkali basalts dated at 7-6 Ma represent the last onshore activity just before the Messinian crisis, and the Pliocene alkali basaltic outpouring in Sardinia. We propose to link these latter volcanic events to the development of a slab window in a post-collisional tectonic framework.

*This work is dedicated to the memory of our colleague Henriette Lapierre, Professor at Grenoble University, who died in January 2006. She was an important contributor to our initial project.*

**Key-Words:** Mediterranean, Ligurian margins and Basin, Offshore Corsica, Miocene (K-Ar and  $^{40}\text{Ar}$ - $^{39}\text{Ar}$  ages), Normal and K-rich calc-alkaline lavas, Adakites, Shoshonites, Alkali basalts, Slab breakoff, Slab tearing, Slab window, Subduction.

\* Corresponding author. Tel: 02 98 21 95 94, 02 98 01 60 90

E-mail addresses: [jprehault@wanadoo.fr](mailto:jprehault@wanadoo.fr) (J-P. Réhault), [christian.honthaas@upmc.fr](mailto:christian.honthaas@upmc.fr) (C. Honthaas), [p.guennoc@brgm.fr](mailto:p.guennoc@brgm.fr) (P. Guennoc), [herve.bellon@univ-brest.fr](mailto:herve.bellon@univ-brest.fr) (H. Bellon), [gilles.ruffet@univ-rennes1.fr](mailto:gilles.ruffet@univ-rennes1.fr) (G. Ruffet), [sosson@geoazur.unice.fr](mailto:sosson@geoazur.unice.fr) (M. Sosson), [rene.maury@univ-brest.fr](mailto:rene.maury@univ-brest.fr) (R. C. Maury)

## 1. Introduction

The Mediterranean domain represents a wide, geodynamically active area where the Cenozoic convergence between the African and Eurasian plates resulted in a complex spatial and temporal tectonic pattern. Between Alps-Provence and Corsica, a highly thinned continental crust on the deep part of the margins underlies the Ligurian Sea, while an oceanic-type crust is present in its narrow central part. Corsica and Sardinia islands are underlain by a "typically" Variscan bowl-shaped continental crust (Galson and Mueller, 1986).

During the Neogene, the western Mediterranean domain and its margins evolved through a complex succession of NW-directed subductions, back-arc openings and collisions, involving

slab tearings and detachments (Réhault et al., 1984; von Blanckenburg and Davies, 1995; Gueguen et al., 1998; Carminati et al., 1998a, 1998b; Faccenna et al., 2004; Lucente et al., 2006; Carminati et al., 2010; Lustrino et al., 2011).

The magmatic activity linked to these complex geodynamic patterns led to the emplacement, both onshore and offshore, of geochemically diverse volcanic and plutonic associations. These include MORB-type and back-arc oceanic basalts (Beccaluva et al., 1990), from calc-alkaline to ultrapotassic lavas (Peccerillo, 2005), plutonic and volcanic rocks of crustal anatectic origin (Zeck et al., 1998) and alkali basalt series (Oyarzun et al., 1997; Lustrino and Wilson, 2007). These complex rock associations occur throughout the whole Mediterranean domain, e.g. in the Betic Cordilleras (Zeck et al., 1996; Benito et al., 1999), the Maghreb alpine chain (Maury et al., 2000), the Apennines-Calabrian-Sicilian domain and the Eolian arc and Tuscany (Hawkesworth and Vollmer, 1979; Savelli, 1988; Lustrino et al., 2011).

Within the Liguro-Provençal Sea and its margins as well as on the Sardinia-Corsica block, a Neogene magmatic evolution from medium-K calc-alkaline towards K-rich calc-alkaline lavas was followed by the emplacement of alkali basaltic lavas in the Toulon area (France) and in Sardinia (Coulon, 1977; Montigny et al., 1981; Dostal et al., 1982; Aguilar et al., 1996; Morra et al., 1997; Gattacceca, 2001; Gattacceca et al., 2007; Lustrino et al., 2007a, b). In Corsica, the only evidences are the Sisco lamprophyre at Cap Corse and the ignimbritic tuffs of Balistra (Bellon, 1976) and the Tre Paduli, Francolu, and Maore (Ottaviani-Spella et al., 1996, 2001; Ferrandini et al., 2003). The geochronology and geochemistry of this onshore magmatic activity, which has been related to the drifting of the Sardinia-Corsica block, are relatively well documented (Bellon and Brousse, 1977; Wilson and Bianchini, 1999; Savelli, 1979, 1988, 2002; Oudet et al., 2010; Lustrino et al., 2011).

In comparison with onshore igneous rocks, the literature data on the offshore volcanics from the Ligurian Sea are nearly completely missing. The present paper is based on the study of the dredging and diving cruises carried out by French scientific institutions that sampled a large number of volcanic rocks during the three last decades in the Corsica-Liguria Basin. Our new data highlight the tectono-magmatic processes, which controlled the Tertiary evolution of the northwestern Mediterranean domain.

## **2. Northwestern Mediterranean magmatic events**

### *2.1. Onland magmatism in SE France, Corsica and Sardinia*

Tertiary magmatic rocks are present mainly in the emerged part of the northern Ligurian

margin. They are well-known since the XIXth century, especially the “porphyre bleu de l’Estérel” or “estérellite” (Michel-Lévy, 1898), a quartz-bearing microdiorite forming a thick laccolithic complex near Le Drammont. Basaltic to andesitic pyroclastic deposits cropping out around Villeneuve-Loubet were described by Brousse and Lefèvre (1990). Finally, andesitic and dacitic pebbles occur in volcanogenic breccias interbedded within the Eocene sedimentary rocks in the Saint-Antonin syncline, located to the north of Nice (Féraud et al., 1995; Boyet et al., 2001).

The first published K-Ar age at  $26.2 \pm 1.2$  Ma (Bellon and Brousse, 1971) concerned the andesites exposed between Biot and Grasse. Complementary ages carried on lavas collected at Tourettes sur Loup, Juan-les-Pins and La Vanade, are bracketed between 32.5 and 30.8 Ma (Bellon, 1981). More recently, two pyroclastic levels sampled during the Monaco railway tunnel engineering works were dated at respectively  $27 \pm 0.8$  and  $18.7 \pm 0.8$  Ma (Ivaldi et al., 2003).  $^{40}\text{Ar}$ - $^{39}\text{Ar}$  ages for Le Drammont microdiorites and for the Saint-Antonin andesites range from 33 to 31 Ma (Féraud et al., 1995). Similar plateau ages (31-30 Ma) have been measured on Alpine plutons such as Traversella and Biella (Ruffet, unpublished data) and nearby bodies of similar ages (32-29 Ma; Buergi and Klotzli, 1990; Romer et al., 1996). Andesitic to dacitic pebbles from a volcanoclastic unit interbedded within an Early Oligocene (Priabonian-Rupelian) marine formation at the Baratus pass, in the vicinity of St Auban, have been dated at  $29.6 \pm 0.5$  and  $29.0 \pm 0.5$  Ma (Montenat et al., 1999).

Northwest of Aix en Provence, at Beaulieu, two Miocene volcanic events emplaced a calc-alkaline lava flow and an alkali basaltic flow, respectively (Gueirard, 1964), which have been considered later as transitional to alkaline by Dautria and Liotard (1990). The Formation de Beaulieu, which includes coastal deposits overlain by lacustrine limestones, is subcontemporaneous of this volcanic complex.  $^{40}\text{Ar}$ - $^{39}\text{Ar}$  dating of a basaltic sample taken in the quarry site, previously studied by Baubron et al. (1975), yielded a plateau age of  $17.5 \pm 0.3$  Ma, which can be correlated with N6 + N7 biozones dated in the neighbouring marine sediments and the paleomagnetic chron C5Dn (Aguilar et al., 2003). It is consistent with the previous K-Ar age of ca.  $18.2 \pm 0.5$  Ma (Baubron et al., 1975). North of Toulon, alkali basaltic flows dated at  $6.97 \pm 0.24$  and  $6.30 \pm 0.22$  Ma (Bellon, unpublished data) represent the last volcanic event known in Provence (Coulon, 1967; Gouvernet et al., 1997).

The important Neogene magmatic activity documented in Sardinia may be divided in two main periods. The first one occurred between 32 and 15 Ma with a peak between 22 and 18 Ma, and the second one emplaced alkali basalts between 12 and 0.1 Ma (Lustrino et al., 2007). In Northeast Corsica, lamproitic dykes intruding the “Schistes lustrés” unit yielded a whole rock K-Ar age of 13.75 Ma (Bellon, 1976, age corrected according to constants in Steiger and Jäger,

1978) and a Rb-Sr age of 15 Ma (Féraud et al., 1977). Their emplacement is related to that of K-rich and shoshonitic lavas in Sardinia.

## 2. 2. Offshore Corsica-Liguria Basin volcanism

Offshore volcanism appears relatively scattered within the Corsica-Liguria basin, which comprises the Ligurian Sea and its submarine margins. However, two main volcanic fields are distinguished in Fig. 1. The first one, the southwestern Corsica volcanic field, is located in the prolongation of the central Sardinia rift, while the second one, the northwestern Corsica volcanic field, is located south of Genoa Gulf and along the Central Ligurian Sea. This latter field underlines the N10°-20° trending foot of the Corsica continental margin and Liguria Central Basin.

A large set of pre-existing data and studies have been considered in our study. It includes previous geological samplings, bathymetric and geophysical data, large transverse magnetic anomalies southwest of Corsica (Bayer, 1974), dredged samples in the Ligurian basin (Réhault et al., 1974), identification of reflectors of the Ligurian margins (Bellaiche et al., 1974), and studies of the relationships between tectonics, volcanism and sedimentation (Gennessieux et al., 1989). A first synthetic map (Sartori et al., 1982) was based on data obtained on cored samples during drillings and on lavas dredged or sampled *in situ* in the western Mediterranean. Additional data include (i) the first K-Ar dating of dredged lavas from the "Tristanite Ridge" (Réhault, 1981; Réhault et al., 1985), (ii) K-Ar and  $^{40}\text{Ar}$ - $^{39}\text{Ar}$  ages of columnar-jointed lavas in SW Corsica (Bellon et al., 1985), (iii) dating of submarine volcanoes (Monte Doria complex and Genoa Gulf central volcano), south of Genoa Gulf (Fanucci et al., 1993), and finally (iv) the trace element geochemistry and  $^{40}\text{Ar}$ - $^{39}\text{Ar}$  ages of calc-alkaline volcanism in southwest Corsica (Rossi et al., 1998).

New multi-beam bathymetric coverage of the Ligurian Sea resulted in a better mapping of the northwestern and southwestern Corsica volcanic fields (Réhault et al., 1998; Guennoc et al., 1998). These data were gathered and partly reinterpreted by Gattacceca (2001) and Rollet et al. (2002). The present paper is based on 25 new ages (whole rock K-Ar conventional ones and mineral  $^{40}\text{Ar}$ - $^{39}\text{Ar}$  ages), 22 geochemical analyses of major and trace elements by ICP-AES, and microprobe analyses of primary clinopyroxenes from 26 lavas. The data obtained on offshore sites and samples collected during five main cruises, Geomed IV and Marsili in 1974, Cyaligure in 1977, Marco in 1995 and Cylice in 1997, are shown in Table 1 and Fig. 2.

### 3 – Geochronology, petrology and geochemistry of the offshore volcanism

#### 3.1. Alteration effects

Many submarine rocks display typical alteration features including the development of iron oxides and hydroxides, ferromagnesian or carbonated coatings. Black Mn oxyhydroxide-coated carbonates and thin ferromagnesian films, with later organic carbonate coatings, have been observed on the Asinara Gulf lavas (Castelsardo Canyon). Rocks dredged on the "Tristanite Ridge" (e.g. GIV DR 10, Geomed IV cruise) contain frequent "serpulid polychaete" among a diversified fauna of Pleistocene corals, sponges and gorgonarians (Zibrowius, 1980). Hydrothermal carbonate vesicles are common in Cyl 22-04 and Cyl 22-03 lavas from Monte Doria (-1588 m; Fig. 2).

Alteration processes led to important changes of major and trace elements as discussed in section 3.3. Such a strong alteration is a major problem for obtaining significant K-Ar and  $^{40}\text{Ar}$ - $^{39}\text{Ar}$  ages. Many of the dated samples display obvious features of a well developed low-temperature alteration, with iron oxides and hydroxides, clays and carbonates invading the cores of samples. Numerous occurrences of celadonite, zeolites and clay-type minerals suggest that the secondary development of these minerals was favoured either by processes, which took place just after magma emplacement or by gradual alteration by seawater over a large time span.

#### 3.2. Dating the volcanic rocks

##### 3.2.1 K-Ar dating procedures

Twenty five lavas have been considered for dating purposes. Among these, 14 samples display a loss on ignition (LOI) lower than 6 wt. % while 8 of them have a higher LOI. Nevertheless, we attempted to date the latter samples because of their interesting geological position.

Potassium-argon ages were measured in Brest (UBO, Université de Bretagne Occidentale) on whole-rock lavas. Grains of rocks 0.3 to 0.15 mm in size were prepared after crushing and subsequent sieving of the solid samples. One aliquot of grains was powdered in an agate grinder for chemical attack of around 0.1 g of powder by 4 cc of hydrofluoric acid, before its analysis of K content by AAS (Atomic Absorption Spectrometry). A second aliquot of grains was reserved for argon analysis. About 0.3 g to 1 g of grains were heated and fused under vacuum in a molybdenum crucible, using a high frequency generator. Released gases during this step of the process were cleaned successively on three quartz traps containing titanium sponge during their decreasing temperature during 10 minutes, from 800°C to the ambient one, and at the final step

the remaining gas fraction was ultra-purified with an Al-Zr SAES getter. Isotopic composition of argon and concentration of  $^{40}\text{Ar}_R$  were measured in a stainless steel mass spectrometer with a  $180^\circ$  geometry. Isotopic dilution was realized with the fusion step, using for this process precisely concentrations of  $^{38}\text{Ar}$  buried as ions in aluminium targets (Bellon et al., 1981).

Resulting ages, listed in Tables 1 and 2, are calculated using Steiger and Jäger's (1977) constants and errors, following the equation of Mahood and Drake (1982). Results for the 8 samples, which have a high LOI are underlined in Tables 1 and 2, and must be interpreted with caution. We have crosschecked some of these whole-rock K-Ar conventional ages with  $^{40}\text{Ar}$ - $^{39}\text{Ar}$  data carried on carefully separated grain minerals (plagioclase, amphibole and biotite) from these lavas. The irradiation technique of grains has led to  $^{40}\text{Ar}$ - $^{39}\text{Ar}$  results, which are presented in Tables 1 and 3 and in Fig. 3.

### 3.2.2 $^{40}\text{Ar}$ - $^{39}\text{Ar}$ analytical procedures

Single grains of amphibole and biotite used for the experiments were carefully handpicked under a binocular microscope from the 0.5-1mm fraction of the crushed rock sample Cyl 02-1. The plagioclase crystals (Cyl 03-1 and Cyl 07-3) were separated by the classical methods (magnetic separator and heavy liquids) and the two final mineral separates (in the range 125-160  $\mu\text{m}$ ) were obtained by handpicking under a binocular microscope. The samples were wrapped in Al or Cu foils to form small packets (11x11mm.). These packets were stacked up to compose a pile in which packets of flux monitors were inserted every 8 to 10 samples. The stack, put in an irradiation can, was irradiated for 5 hours at the McMaster reactor (Hamilton, Canada) with a total flux of  $6.4 \times 10^{17} \text{ n.cm}^{-2}$ . The irradiation standard was the sanidine Fish-Canyon with an age of  $28.02 \pm 0.28 \text{ Ma}$  (Renne et al., 1998). This sample arrangement allows monitoring the flux gradient with a precision as low as  $\pm 0.2\%$ .

The step-heating experiment procedure was described in details by Ruffet et al. (1991, 1995). The single grains were heated for analyses with a continuous argon-ion laser. Analyses were performed with a VG3600 Mass Spectrometer. Blanks were performed routinely each first or third run, and then subtracted from the subsequent sample gas fractions. Typical blank values were in the range  $3.7 \times 10^{-13} < \text{M}/\text{e}_{40} < 7.8 \times 10^{-13}$ ,  $2.0 \times 10^{-14} < \text{M}/\text{e}_{39} < 1.6 \times 10^{-13}$ ,  $1.1 \times 10^{-13} < \text{M}/\text{e}_{37} < 1.23 \times 10^{-13}$  and  $3.9 \times 10^{-14} < \text{M}/\text{e}_{36} < 6.8 \times 10^{-14} \text{ cm}^{-3} \text{ STP}$ .

Argon gas was extracted from bulk samples in a double vacuum HF furnace and purified in a line including two SAES GP 50W getters with St101<sup>®</sup> zirconium-aluminium alloy operating at  $400^\circ\text{C}$  and a  $-95^\circ\text{C}$  cold trap. Corresponding analyses were performed with a mass spectrometer which consists of a  $120^\circ$  M.A.S.S.E.<sup>®</sup> tube, a Baur Signer<sup>®</sup> source and an SEV 217<sup>®</sup> electron-multiplier (total gain:  $5 \times 10^{12}$ ).

To define a plateau age (Fig. 3), a minimum of three consecutive steps was considered,



corresponding to a minimum of 70% of the total  $^{39}\text{Ar}_K$  released, and the individual fraction ages should agree within 2 sigma with the integrated age of the plateau segment.

### 3.2.3. Age results (Tables 1, 2 and 3)

For a better comparison of the results obtained by whole-rock K-Ar dating and by  $^{40}\text{Ar}$ - $^{39}\text{Ar}$  dating on separated minerals, they are presented in the text and the figures with one decimal and  $\pm$  two sigma error, while they are listed in Tables 1, 2 and 3 with two decimals and  $\pm$  one sigma error.

Offshore volcanics in southwestern Corsica display ages ranging between 21 and 7 Ma. This cluster is further split into four groups, 21 to 18 Ma, 16 to 14 Ma, ca 12 Ma, and finally ca 8 Ma. The volcanic complex is located at sites 3, 1 and 2 (Fig. 2a) in the Canyon des Moines, the Castelsardo Canyon and at Monte Paoli, west of the N20°W trending fault bordering the Bonifacio straits. These represent at least four volcanic events, at  $20.7 \pm 1.0$  Ma to  $19.2 \pm 0.9$  Ma (Canyon des Moines), at  $18.5 \pm 2$  Ma to  $16.5 \pm 1.0$  Ma (Canyon des Moines and Monte Paoli) and finally at  $14 \pm 0.8$  Ma (Castelsardo) and  $11.7 \pm 2.2$  Ma (Canyon des Moines).

Valinco Canyon, Ajaccio and Propriano Highs were loci of volcanic events at  $20.6 \pm 1.0$  Ma ( $^{40}\text{Ar}$ - $^{39}\text{Ar}$  age on plagioclase), and between  $16.1 \pm 0.80$  Ma ( $^{40}\text{Ar}$ - $^{39}\text{Ar}$  age on amphibole) and  $14.6 \pm 0.7$  Ma (whole rock K-Ar age). These data are in agreement with intermediate  $^{40}\text{Ar}$ - $^{39}\text{Ar}$  plateau ages of  $15.8 \pm 0.2$  Ma and  $15.6 \pm 0.1$  Ma measured on separated biotites and amphiboles. A more recent event is documented by two whole rock ages of  $12.8 \pm 3.7$  Ma and  $11.9 \pm 0.6$  Ma, respectively. Volcanics sampled in northwestern Corsica on the slope of Cap Corse yielded an age of  $19.6 \pm 3.0$  Ma.

Surprisingly, the “Tristanite Ridge” samples gave three different results for similar K-rich compositions: the “tristanite” (potassic benmoreite) lava first dated at  $18.0 \pm 1.0$  Ma (Réhault et al., 1984) is in fact a trachyte. K-Ar dating of two related lavas (this study) sampled by diving on the same volcano yielded  $12.8 \pm 0.6$  and  $12.4 \pm 0.6$  Ma, respectively. An older age of  $43 \pm 2.3$  Ma was also measured on a lava collected on the neighbouring volcano.

Monte Doria seamounts yielded ages ranging from  $11.4 \pm 1.4$  Ma (shoshonitic lava; Fanucci et al., 1993) to  $7.3 \pm 1.4$  Ma, with intermediate ages between 9.2 and 7.5 Ma within the error bars ( $8.6 \pm 0.6$  Ma yielded by a Cylice basalt and  $8.4 \pm 0.6$  Ma by a Marco basalt). Finally, a lava from Genoa Gulf Central Volcano was dated at  $14.8 \pm 2.8$  Ma.

### 3.3. Main geochemical features of the studied lavas

Major and trace element analyses are listed in Tables 4a (SW Corsica lavas) and 4b (NW Corsica lavas and references for geochemical comparisons). Results were obtained at Brest by

Inductively Coupled Plasma - Atomic Emission Spectrometry (ICP-AES) on solutions of agate-grinded powders. AC-E, BE-N, JB-2 and PM-S standards were used for calibration tests. Relative standard deviations are 2% for major oxides except for MnO and P<sub>2</sub>O<sub>5</sub>, and less than 5% for trace elements. Details of the analytical techniques are given by Cotten et al., (1995).

Reference onshore samples listed in Table 4 are two K-rich basaltic andesites collected near Nice (Tourettes and Villa Maure) and two quartz-bearing microdiorites or “esterellites” (Le Drammont quarry) and a basalt collected north of Toulon (Coulon, 1977; Dautria and Liotard, 1990). Quartz-bearing microdiorites display the high silica and alumina contents, high Na<sub>2</sub>O/K<sub>2</sub>O ratios and very low heavy rare earth element (HREE) and Y contents considered typical of adakites (Defant and Drummond, 1990; Defant et al., 1991, 1992; Martin, 1999; Martin et al., 2005; Richards and Kerrich, 2007; Moyen, 2009). However, their Sr/Y and La/Yb ratios (43 and 26-32, respectively), although higher than those of “regular” calc-alkaline lavas, are lower than those of calculated or experimental slab melts (>80 and >30, respectively; see Jégo et al., 2005; Moyen, 2009 and references therein) and their Sr contents are also lower than those of the former. Therefore, they can be termed “intermediate” adakites (Sajona et al., 2000; Jégo et al., 2005; Calmus et al., 2008, 2011).

Some offshore lavas have LOI contents reaching up to 22 wt.%. These high LOI are mainly due to the presence of carbonates filling up vesicles or developed as veinlets resulting from the circulation of hydrothermal fluids. These samples usually display low SiO<sub>2</sub> contents together with high Al<sub>2</sub>O<sub>3</sub> (e.g. 41 and 22 wt.%, respectively, for an altered basaltic andesite). The variation of silica contents versus LOI in the lavas is shown in Fig. 4. Silica contents decrease drastically when LOI increases, as illustrated by lavas from Propriano High (site 6) or by those of the trachytes from the “Tristanite Ridge” (site 7). Such a negative correlation is characteristic of low-temperature and hydrothermal alteration by seawater (Cann, 1979; Alt, 1995).

The compositions of the less altered offshore lavas range from basaltic to intermediate and acidic (60 to 70 wt. % SiO<sub>2</sub>). Most basalts, basaltic andesites and andesites display relatively low TiO<sub>2</sub> and P<sub>2</sub>O<sub>5</sub> contents (< 1.3 wt.% and < 0.36 wt.%, respectively) consistent with a calc-alkaline signature. A rather fresh adakite depleted in HREE and Y (Propriano High, sample Cyl 02-02, Table 4) was also analysed.

Multielement patterns normalised to the primitive mantle of Sun and McDonough, 1989 are shown for lavas collected within the southwestern Corsica volcanic field (Figs. 5a and 5b), and from the northwestern field: Cap Corse and reference samples (Fig. 5c), Doria seamounts lavas (Fig. 5d) and Tristanite Ridge lavas (Fig. 5e). A comparison of patterns for offshore lavas with patterns of selected onshore lavas, taken as references (Figs. 5c and 5d) because of their low LOI, leads us to the conclusion that the REE and the high field strength elements (HFSE: Nb, Zr, Ti) were relatively immobile during the

alteration processes (Cann, 1979; Alt, 1995). On the other hand, the large ion lithophile elements (LILE: Rb, Ba, Sr) show large variations and erratic behaviour in Fig. 5 plots, related to their mobility during alteration.

The multielement patterns of 6 lavas from Castelsardo, Monte Paoli, Valinco, Ajaccio and Propriano sites are shown in Fig. 5a. All of them display a significant negative Nb anomaly typical of subduction-related magmas. Their patterns are variably enriched, as La/Yb normalised ratios range from 4 to 25.

Two different types of patterns of subduction-related lavas (negative Nb anomaly) are shown in Fig. 5b. Canyon des Moines lavas display medium-K calc-alkaline patterns while the two Propriano samples have very steep REE and multielement patterns, with very high Sr contents (945 and 795 ppm) and La/Yb and Sr/Y ratios (68-72 and 31-36, respectively) which plot within the range of adakites. The latter patterns are similar to those of onshore adakites from Le Drammont (77S4F and Est 96-2), shown in Fig. 5c together with that of calc-alkaline lava from the Cap Corse. However, the two Propriano samples are more K-rich than most adakites (Table 4a; Moyen, 2009), a feature, which could be due to post-magmatic processes.

In Fig. 5d, the patterns of Doria seamounts and of Genoa Gulf Central Volcano lavas are very similar to each other. By comparison with diagrams 5a, 5b and 5c, they display a less pronounced negative Nb anomaly. These K-rich “shoshonitic” lavas differ, however, from the Toulon alkali basalt, which shows a positive Nb anomaly and lower potassium content. Finally, the patterns of andesitic and trachytic lavas collected from the “Tristanite Ridge” (site 7) are shown in Fig. 5e. All these samples are K-rich and display a negative Sr anomaly, possibly indicative of plagioclase fractionation.

### 3. 4. Clinopyroxene compositions

Chemical compositions (Table 5) of primary clinopyroxene phenocrysts and microphenocrysts from 26 mafic and intermediate lavas have been analysed using the Cameca SX 100 microprobe in BRGM (Orléans, France) and the Cameca SX 50 and Cameca SX 100 microprobes in Brest. They have been plotted in the Leterrier et al., (1982) Ti *versus* Ca+Na discrimination diagram (Fig. 6) and compositions are given in Table 5. The pyroxenes from most southwestern Corsica studied lavas (Fig. 6d) plot in the sub-alkalic field, while some are clearly located in the alkalic field pyroxenes from Cap Corse lavas (Fig. 6b) are clustered in the sub-alkalic field. The pyroxenes of lavas sampled from the Tristanite Ridge (Fig. 6c) plot in both fields. Finally, most analyses of Monte Doria clinopyroxenes plot within the alkalic field (Fig. 6d).

### 3.5. Minerals compositions

Microprobe analyses of clinopyroxenes, feldspars, amphiboles, biotites, and oxides are detailed in Appendix 1 (Data repository), where can be successively found: (1) selected analyses of clinopyroxenes and feldspars in basaltic andesites collected at sites 1, 3 and 12; (2) selected analyses of clinopyroxenes and feldspars in shoshonitic and alkaline lavas collected at sites 9 and 10; and (3) selected analyses of feldspars, biotites, amphiboles, and oxides in adakitic andesites collected at site 6.

## 4- Integrated presentation of offshore Corsica volcanic fields: geology, K-Ar ages and geochemistry

### 4.1. The southwestern Corsica volcanic field

Sites of sampling (Table 1 and Fig 2a) are located on a thinned continental crust (Morelli, 1974; Gennesseaux et al., 1989; Gueguen, 1995; Rollet et al., 2002). Previous surveys (Bayer et al., 1973) predicted volcanic occurrences along two main linear ridges well displayed on magnetic anomalies maps of Galdeano and Rossignol (1977). More recent seismic lines and sampling informations suggest the lack of continuous magmatism (Guennoc et al., 1998; Réhault et al., 1998). The linear trends of volcanic centres probably mark the locations of tear faults. Offshore, the southwest Corsica area presents northwest-southeast elongated transverse anomalies. Although some reliefs of the acoustic basement can be associated with magnetic anomalies, there is rarely a direct relationship between these two features. Indeed, (i) most of the magnetic sources are located at depth within the crust, and (ii) shallow basement reliefs and exposed submarine volcanic units appear to be non-magnetic, as confirmed by the very low or non-magnetic susceptibility of the collected samples.

Further to the north, up to 42°N, several isolated volcanic seamounts oriented N10° to N20°E have recently been identified (Fig. 2a). The eastern limit of this volcanic field is located along the northern to northwestern – southern to southeastern fault bordering the Bonifacio continental shelf (Guennoc et al., 2004). There, volcanic intrusions within the whole Miocene series have been detected on seismic profiles and shallow volcanic seamounts are visible at the western edge of the shelf.

During Marco and Cylice cruises, additional samplings and observations were performed on reliefs located along the three main north-west - south-east axes (Fig. 2a), on the northern edge of the area, and on isolated seamounts more easily accessible along the flanks of major canyons: Castelsardo, Moines, Propriano, Valinco and Ajaccio canyons (Table 1, Fig. 2a). Magmatic

units observed during divers are made up of massive rocks, often fractured. They were somewhat difficult to sample because of cementation by oxides coating and/or thick carbonate crust and organic crust. In a few areas, on some seamounts and on the flanks of the Canyon des Moines, the layered volcanic structures evidenced on seismic lines resulted from submarine emissions as shown byropy lavas or pillow lavas and columnar-jointed structures observed during dives Cya 77-35 (Bellon et al., 1985) and Cyl 07. Pyroclastic deposits interbedded within Miocene sediments have been observed in the upper part of the margin area. From seismic profiles, widely extended and thick volcano-detritic deposits are thought to occur around volcanic seamounts. All these observations point out to a significant magmatic event, which occurred during a relatively short period of time within the Lower Miocene on the southwestern Corsica margin. The Balistra and Tre Paduli ignimbritic tuffs located in southern Corsica (Fig. 2) (Ottaviani-Spella et al., 2001) can be reasonably considered as remnants of this event.

#### *4.1.1 Site 1 - Castelsardo Canyon*

Most of the lavas collected at -1859 and -1785 m from the sharp northern flank of this canyon are porphyritic basalts, which contain plagioclase (An<sub>72-52</sub>) and augite phenocrysts, with or without altered olivine. Some lavas show a large amount of secondary calcite and quartz (Cyl 01-03) and their vesicles are filled by smectites, zeolites and celadonite. The multielement pattern of MA 74 DR 05 (Fig. 5a) show a negative Nb anomaly typical of calc-alkaline lavas and a moderate enrichment in the most incompatible elements, with a La/Yb normalized ratio of 4.

These lavas, dated on two different fractions at  $14 \pm 0.8$  and  $13.7 \pm 1.8$  Ma respectively, are nearly contemporaneous basaltic andesite flows overlaying the granitic basement (supposed of Variscan age), as attested by the seven samples of monzodiorite, monzogranite and leucomonzogranite collected in the course of Cylice cruise. In their vicinity, pelagic calcareous sediments were collected on the flanks of the canyon using a Kullenberg-type piston corer. These sediments contain no volcanic ashes nor detrital fragments. Planctonic foraminiferas (*Globorotalia acostaensis*) and others from Miozea group (Genesseeux et al., 1974) indicate a Lower Tortonian age for this sub-horizontal level. Therefore, these onlapping sediments were deposited about 3 My after these volcanic emissions.

#### *4.1.2 Site 2 - Monte Paoli*

Monte Paoli, a large sub-circular relief uprising to -1600 m (about 20 km in basal diameter and 8 km near its top), was visited during the Cyaligure Cruise in 1977. Because the flanks were highly coated by thick (ca 10 to 20 cm) Fe-Mn crusts, no volcanic sample was collected during submarine operations despite two dives. However, volcanic samples (Cya 77 DR02-a2 and a)

were dredged at -1980 and -1950 m on its southern and western flanks. These basaltic andesites show typical negative Nb anomalies, and relatively flat multielement patterns (Fig. 5a). They yielded two different K-Ar ages of respectively  $18.3 \pm 1.0$  and  $15.9 \pm 0.8$  Ma. The older age is tentatively preferred to the younger one because of the lower alteration of the sample. Nevertheless this age might be slightly rejuvenated.

#### 4.1.3 Site 3 - *Canyon des Moines*

Samples Cyl 07-11, 07-10, (coarse-grained doleritic basalts), Cyl 07-07 (highly porphyritic basalt) and Cyl 07-03 (porphyritic basaltic andesite) were collected by the Cyana submersible along the northern side of Canyon des Moines incision, at depths ranging from -1200 and -1000 m. They complete a previous sampling made during Cyana dive in 1977, during which a columnar-jointed lava (Cya 77-35-03) was collected at -1682 m (Bellon et al, 1985). They contain plagioclase ( $An_{72-52}$ ) and augite phenocrysts, with generally altered olivine. Their trace elements patterns (Fig. 5b) show a typical negative Nb anomaly,  $(La/Yb)_N$  ratios of 4 to 5, and Rb, Ba and K abundances about 30 times higher than the primitive mantle estimates. These features are consistent with a medium-K calc-alkaline signature (Gill, 1981). Four whole-rock ages and two  $^{40}Ar$ - $^{39}Ar$  ages for separated plagioclases have been performed on collected lavas. Two whole-rock ages of respectively  $19.4 \pm 0.9$  Ma (Cyl 07-11) and  $19.2 \pm 0.9$  Ma (Cyl 07-10) were measured on lavas located at -980-983 m. They have LOI < 2.3 wt.% and contain respectively 2.58 and 2.39 wt.% of  $K_2O$ . A plateau age of  $20.7 \pm 0.1$  Ma has been defined for separated plagioclases from Cyl 07-03, a porphyritic basalt collected at -1104 m. Fig. 3 shows its spectrum shape with a slight and regular increase of apparent ages from the low to the intermediate temperature steps. The sizeable error bars calculated for this sample are directly related to its high measured  $^{37}Ar_{Ca}/^{39}Ar_K$  ratios. A significantly younger whole-rock age of  $11.7 \pm 2.2$  Ma has been obtained for Cyl 07-07, located slightly deeper at -1137 m. The columnar-jointed Cya 77-35 03 basalt (Bellon et al., 1985), collected at -1682 m, yielded a whole rock age of  $18.5 \pm 2.0$  Ma.  $^{40}Ar$ - $^{39}Ar$  dating on plagioclase separates from this latter sample, gave a plateau age of  $16.5 \pm 0.5$  Ma for 80 % of extracted  $^{39}Ar$ . As a consequence, a preferred crystallization age of 16.5 Ma is proposed for sample Cya 77-35 03 after evaluation and subtracting excess argon.

The interpretation of seismic lines indicates that all these volcanic samples are from the main volcanic unit interfingering within a sedimentary sequence older than Messinian. According to our results, this volcanic pile resulted from successive emissions, including at least one possible subaerial event attested by the occurrence of columnar-jointed basaltic flows. We conclude that three different events occurred at ca. 20-19 Ma, 16.5 Ma, and finally around 12 Ma. The depths of the studied lavas are not correlated with their respective ages. Indeed, sample Cyl 07-07

dated at  $11.7 \pm 2.2$  Ma at -1137 m is deeper than basalt (Cyl 07-03) at -1104 m dated at  $20.7 \pm 0.1$  Ma, a nearly common rule in the building of volcanic edifices.

#### 4.1.4 Site 4 - Valinco Canyon

The basaltic andesite sample Cyl 03-01 was collected from the south flank of the canyon at the edge of a linear N130°E trending ridge. Its relatively smooth multielement pattern (Fig. 5a) and its primary pyroxenes plotting in the sub-alkalic field (Fig. 6a) are consistent with a medium-K calc-alkaline signature. Plagioclase separated from this sample yielded a "plateau" age of  $20.6 \pm 1.0$  Ma. Its spectra shape (Fig. 3) shows a slight and regular increase of apparent ages from the low to the intermediate temperature steps. The flat segments defined by apparent ages in the high temperature steps are correlated with rather constant  $^{37}\text{Ar}_{\text{Ca}}/^{39}\text{Ar}_{\text{K}}$  ratios (# Ca/K ratio). This fact suggests a degassing of pure plagioclase phases. This age overlaps with that determined for plagioclases from the porphyritic basalt from Canyon des Moines (Cyl 07-03 at 20.7 Ma).

#### 4.1.5 Site 5 - Ajaccio High

Basaltic andesite Marco DR06-08 (LOI = 11.85 wt.%;  $\text{K}_2\text{O}$  = 0.47 wt.%) yielded a whole rock age of  $12.8 \pm 3.6$  Ma. It was sampled at -1700 m from a large volcano with numerous lava flows and volcanoclastics interlayered within sediments. A nearly similar age (12.4 Ma) has been measured for the last medium K-volcanism (Cyl 07-07;  $\text{K}_2\text{O}$  = 0.79 %) in Canyon des Moines. This edifice is presently isolated by several canyon incisions.

#### 4.1.6 Site 6 - Propriano High

This volcano rises from the abyssal plain, merging out from a very thick pile of sediments at -2700 to -2000 m on the southern flank of Propriano Canyon, at the crossing of Valinco, Propriano and Canyon des Moines. Three lavas taken from this edifice have been analyzed: two basaltic andesites, Cyl 02-01 (this study) and Marco Dr 02 by Rossi et al. (1998), and an andesite, Cyl 02-02 (this study). These lavas are characterized by low HREE and Y contents together with high Sr/Y and La/Yb ratios (Fig. 5a, b). While the two basaltic andesites have high LOI, sample Cyl 02-02 is rather fresh (LOI = 1.36 wt.%, Table 4a). This sample has preserved the characteristic mineralogical and geochemical (major and trace elements) signature of silica-rich adakites (Defant and Drummond, 1990; Maury et al., 1996; Martin, 1999), although it is more potassic and less rich in Cr and Ni than most of them. The two others might be classified as low-silica adakites (Martin et al., 2005; Moyen, 2009) but alteration effects largely overprint their geochemical signature. This is the first occurrence of adakitic lavas reported for the Corsica margin

The K-Ar whole-rock age of Cyl 02-02 is  $14.6 \pm 0.7$  Ma, while those of two amphiboles and

one biotite from Cyl 02-01 are  $15.6 \pm 0.2$  and  $15.8 \pm 0.5$  Ma, respectively (Fig. 3). Cyl 02-02 is a porphyritic lava containing zoned plagioclases ( $An_{62-42}$ ), biotite ( $X_{Mg} = 64-60$ ), magnesiohornblende ( $X_{Mg} = 78-70$ ) (see appendix), rare quartz, apatite and zircon. It is similar, although less altered, to the andesite Dr 02-1a, dredged during the Marco cruise from this edifice, dated at  $16.1 \pm 0.4$  Ma ( $^{40}Ar-^{39}Ar$  plateau age for amphiboles, Rossi et al., 1998). A nearly similar plateau age of 16.5 Ma had been obtained for Cya 77-35 03 lava, dredged in the Canyon des Moines (Bellon et al., 1985). The concordance between low temperature apparent ages displayed by plagioclase Cyl 03-1 and biotite and amphibole "plateau" ages from sample Cyl 02-1 is worth noting. This cluster of similar ages strongly suggests the presence of a new volcanic event at ca. 16 Ma, i.e. during the last stages of the Ligurian Basin opening (Gattacceca et al., 2007).

#### *4.2. Northwestern Corsica margin and the Liguria Basin volcanic fields*

A relatively widespread magmatism in the Liguria Basin is assumed on the basis of the observed magnetic anomalies (Galdeano et Rossignol, 1977; Réhault, 1981; Réhault et al., 1985; Rollet et al., 2002). Sites of sampling and investigation are listed in Table 1 and located in Fig. 2a and 2b. Isolated large magnetic anomalies were observed at the foot of the northern Provence margin, south of Antibes and Cap d'Ail. To the north, in the Ligurian Basin, an elongated transverse anomaly is stretching the Liguria Basin from Cap Mele to north of Cap Corse.

##### *4.2.1. Site 7 - The "Tristanite Ridge"*

Direct evidence of Tertiary magmatism within the central basin has been so far restricted to a linear relief, the so-called "Tristanite Ridge", merging up to about -1900 m from the deep sea-bottom at -2550 m in the northern part of the Liguria Basin. This large elongated magnetic structure, sampled at sites 7 a, b, c and d, (Fig. 2a and 2b), is prolonged south-westwards by buried seamounts (median relief, Fig 2a). Lateral erosional surfaces pointed on seismic lines suggest that it was an archipelago during Messinian times (Réhault, 1981; Gennesseaux et al., 1989; Réhault et al., 1998; Gueguen et al., 1998; Rollet et al., 2002). Structurally, this ridge is lying along the external border of the Corsica deep thinned margin, towards the central part of the Basin.

Three separate culminating reliefs from this ridge were sampled (Fig. 2a and 2b). The most south western relief rises from -2550 m in the central deep Liguria Basin. Dredging at site 7a yielded a volcanic white tuff MA 74 DR 01 near its base (-2470 m). At site 7b, a porphyritic



andesitic lava was collected near its base (Cyl 20-01), and a volcanic white tuff was sampled near its top (Cyl 20-02 at -2440 m and Cyl 20-04 at -2285 m). At site 7c, a light green lava, G IV DR 11a, was dredged on the western flank of the intermediate relief. At site 7d, the northeasternmost relief only yielded a brownish microgranular carbonate (MA 74 DR02), thinly coated with Fe-Mn oxides. Submarine photographic surveys evidence numerous solitary corals fixed on the outcrops.

Lava MA 74 DR 01 shows an irregular shape coated by a thin Fe-Mg carbonated crust, associated with solitary corals; its fresher broken face presented a white and laminated “tuff” that was named at that time “tristanite” according to its high potassium andesitic to trachytic composition (Table 1). We carefully separated this sample in two parts, the central part (core) and the outer one (rim) to check the potential effects of alteration. Very high concentrations of  $K_2O$  (up to 7 wt.%) together with those of Rb (up to 300 ppm) are characteristic of these rocks. However, microprobe data suggest that they are partly due to K-rich post-magmatic minerals. The K-Ar ages measured for the rim (15.7 Ma) and the core (18.0 Ma) of this sample differ significantly, the younger age being yielded by the most altered analysed fraction (i.e. the rim). Thus, the core age of 18 Ma is considered as the most realistic.

The porphyritic andesite Cyl 20-01 collected at site 7 b contains phenocrysts of plagioclase ( $An_{53-33}$ ), diopside, rare amphibole and microlites of potassic feldspar ( $Or_{65}$ ) set in a variably altered groundmass. Its high  $K_2O$  content (5.14 wt.%) is considered as a primary characteristic of the magma. The whole rock fraction yielded an age of  $12.8 \pm 0.3$  Ma.

The K-rich Cyl 20-02 ( $K_2O = 7.55$  wt.%) and rather fresh (LOI = 2.81 wt.%) acidic tuff ( $SiO_2 = 63.6$  wt.%) bears plagioclases ( $An_{54-41}$ ), potassic feldspar ( $Or_{74-65}$ ), biotite ( $X_{Mg} = 38$ ) and quartz. It plots within the trachytic field in the total-alkali-silica diagram of Le Bas et al. (1986) (not shown). Its whole-rock K-Ar age,  $12.4 \pm 0.3$  Ma, is very similar to the age of the K-rich andesite Cyl 20-01.

The well-rounded block, GIV DR 11a, showing a fluidal texture, dredged at site 7c, is composed of plagioclase phenocrysts up to 2 mm in size and ghosts of ferromagnesian minerals up to 0.2 to 0.5 mm, set in crypto-crystalline matrix containing post-magmatic minerals. A much older age of  $43 \pm 2.3$  Ma was measured on this lava. This result can be compared with the age of the Calabona microdiorite in Sardinia dated at 38.3 Ma (plateau age; Lustrino et al., 2009). This age can be also compared with the  $^{40}Ar-^{39}Ar$  plateau age of  $40 \pm 2$  Ma (Maluski, 1977) obtained on phengites from the “Schistes lustrés” unit located in the Cap Corse region. Another explanation would be a possible thermal rejuvenation. All these interpretations are consistent with the hypothesis that the basement of the “Tristanite Ridge” might be similar to that of the Corsican ophiolitic series.

#### 4.2.2. Sites 8, 9 and 10: Monte Doria volcanic complex

Monte Doria volcanic complex (Fig. 2a), approximately 40 km in length and 25 km in width, consists of a huge seamount (site 9) and parasitic volcanoes located either east of the main centre (site 8) or on it (site 10).

At site 9, eight samples were collected from 2500 to 780 m, along the sharp most southern NW-SE trending scarp. The base was sampled by dredging, the medium part by diving and the highest lavas have been piston-cored near the summit. A pile of pillow-shaped lava flows, the individual thickness of which decreases upwards, was observed during divers Cyl 21 and 22. No direct observation was made at site 10, near the centre of the complex, but highly vesicular lavas dredged nearby attest the submarine outpouring of magma at low to moderate depths.

At site 8, submarine flows were sampled by Fanucci et al., (1993) along the western flank of La Spezia canyon, from the Monte Doria eastern flank. A K-Ar age of  $11.4 \pm 1.4$  Ma has been measured for a separated biotite from this shoshonitic lava (Fanucci et al., 1993).

At site 9, most of the sampled lavas are porphyritic olivine basalts with phenocrysts of plagioclase ( $An_{65-53}$ ) and diopside such as in Cyl 22 basalts (see appendix). An age of  $8.6 \pm 0.6$  Ma, rather close to the ages of  $7 \pm 0.5$  and  $6.3 \pm 0.4$  Ma of the Toulon alkali basalts, was measured on the K-rich basalt Cyl 22-05, collected from the Monte Doria southern flank. This sample displays a positive Nb anomaly (Table 4b and Fig. 5e) consistent with an alkali basaltic affinity. Finally, in Monte Doria centre, at site 10, whole-rock ages obtained on untreated and treated grains of a basaltic sample (Marco DR52-06) were  $8.4 \pm 0.6$  Ma and  $7.3 \pm 1.4$  Ma, respectively.

#### 4.2.3. Site 11: Genoa Gulf Central Volcano

North of Monte Doria centre, another large edifice located in the centre of the Genoa Gulf and culminating at nearly - 450 m was dredged during the Marco Cruise. A basalt (Marco Dr 49-03) dredged near the top of this volcano yielded a whole-rock age of  $14.8 \pm 2.8$  Ma.

#### 4.2.4. Site 12 - Cap Corse western steep margin

On the steep northwestern steep Corsica margin, a new volcanic occurrence has been discovered and sampled during the Marco and Cylice cruises (dive Cyl 15). It is located at the tip of an east-west trending promontory, west of the northern edge of Cap Corse (site 12, Fig. 2). The outcrops, observed from -1730 to - 720 m, are made of altered pillowed basalts. Sample Cyl 15-10 yielded an age of  $19.6 \pm 3.0$  Ma, for a  $K_2O$  content of 1.57 wt.%. This age fits the climax of volcanic activity in the southwest Corsica margin, particularly in the Canyon des Moines and the bulk of the Sardinia magmatism, around 22-18 Ma (Lustrino et al., 2009, and references therein).

## 5. Discussion

### 5.1. Structural reinterpretation of the Corsica-Liguria Basin magmatism

The Ligurian margins and the western and northern Corsica margins were considered for a long time as having a relatively simple and rather homogeneous structure, because of their steepness and narrowness. This area was poorly investigated because of the presence of a thick cover of Upper Miocene evaporites that blankets the deepest external areas, preventing a detailed investigation of the continent-oceanic transition. Geophysical and geological studies (Gennesseaux et Réhault, 1989; Rollet et al., 2002) confirmed the occurrence of two large magmatic areas. They allowed us to define precisely the morphology and the nature of the volcanic basement and revealed the presence of volcanoclastic units beneath the pelagic sediments.

The West Corsica margin segment presents a narrow and rectilinear trend, which parallels the ocean-continent transition (Figs. 1 and 2a). No evidence of magmatism was recognized offshore on this margin between the southwestern Corsica and northwestern Corsica-Liguria volcanic fields (Fig. 2). However, a mafic dike swarm within the Hercynian basement onshore north of Porto (Aghia Campana) has been dated at ca 25-20 Ma from combined fission track and K-Ar, Rb-Sr and Sm-Nd methods (Van Tellingen et al., 1996).

#### 5.1.1. The southwest Corsican magmatic field

The southwest Corsican field represents the northward extension and termination of the Sardinian rift magmatic area (Fig. 1). Most of the isotopic ages (ca. 16-18 Ma) post-date the 21-18 Ma main oceanic spreading period of the Ligurian basin (Gattacceca et al., 2007), and the peak of igneous activity in Sardinia (Lustrino et al., 2009). This late magmatism, as well as the occurrence of faulted Miocene series in the offshore basins, the Sardinia and southwestern Corsica volcanic events, has been related to a second aborted-rifting stage (Réhault et al., 1984a; Thomas et Gennesseaux, 1986; Gattacceca, 2001; Monaghan, 2001; Ferrandini et al., 2003; Oudet et al., 2010).

The southwestern Corsica volcanic field is bounded eastwards by a N-S fault, in the prolongation of the Sardinian rift faults. It is characterised by isolated volcanic seamounts scattered over the rifted and more or less thinned continental crust, as demonstrated by the granite sampled at the foot of large relief in the Castelsardo canyon. Sills and lava flows are also observed beneath the recent sedimentary cover. Around the volcanic centres, extensive dipping

reflectors are interpreted as volcanoclastic series, with possible interbedded lava flows. The specific character of this field is the occurrence of well-expressed northwestern-southeastern trending linear volcanic ridges, which have been detected for a long time because of the associated strong magnetic anomalies. These magmatic and magnetic transverse features most likely represent previous deep transverse/transform faults intersecting the Sardinian-Corsican margin, which would have been reactivated during the Middle Miocene volcanic event.

#### *5.1.2. The Sardinia rift*

The Sardinian rift underwent a long calc-alkaline volcanic history beginning around 38 Ma, with a climax around 22-18 Ma during the tensional rifting phase (Lustrino et al., 2009, and references therein). It was followed by a marine transgression and a second episode of fracturation and volcanic emissions during Langhian times (16-15 Ma; Monaghan, 2001). The latter was linked to a restricted prolongation of the Corsica-Sardinia block rotation until ca. 15 Ma (Ferrandini et al., 2003).

#### *5.1.3. The northwestern Corsica volcanic field*

Several hypotheses and interpretations of magnetic anomaly patterns have been proposed to account for the extension of oceanic-type crust within the Northern Ligurian sea. Previous studies (R  hault, 1981, Genesseaux et R  hault, 1989; Gueguen, 1995; Contrucci, 1998; Rollet et al., 2002) proposed that the area extending from the huge Monte Doria composite volcano to the Median massif, hidden by a large sedimentary blanket, and passing through the central "Tristanite Ridge" (Fig. 7), is located at the edge of the thinned continental margins and nearby transverse/transform zones. Especially, Monte Doria is located on the northern - continental side - of the Capo delle Mele - Cap Corse transform fault zone, a major crustal feature linked to a sharp down faulting of Moho. Indeed, an abrupt deepening of 6 kilometres was registered between two shots distant of 3 kilometres during the Geotraverse Project (Galson and Mueller, 1986).

The two major magmatic areas of the Ligurian sea margins are located on the thinned continental crust edges cut by the major Capo delle Mele-Cap Corse transform fault zone. We assume that the emplacement of important volumes of magma emitted here by comparison with other areas (Fig. 7) even after the end of the oceanic spreading, was favoured by such deep faulted and weakened zones of thinned crust. Therefore, the southwestern Corsica-margin's Miocene magmatism lies at the northern edge of an aborted rift, which disrupted the Sardinian block, while the Northern Ligurian margin volcanism is located at the NNE edge of the Ligurian oceanic area. These volcanic events occurred during the last steps of the "oceanisation" of the Ligurian Sea before its transfer to the Tyrrhenian Sea.

## 5.2. *Oligo-Miocene magma types and their tectonic settings*

The magmatic rocks investigated in this study can be classified into three main groups, i.e. (i) K-depleted and K-rich calc-alkaline basaltic andesites and andesites, which are the most abundant, (ii) adakite-related lavas such as Cyl 02-02 (site 6), and (iii) alkali basalts and related intermediate and felsic lavas, e.g. trachytes Cyl 20-02 and MA 74 DR 01.

### 5.2.1. *Calc-alkaline magmas*

Calc-alkaline lavas erupted in the southwest Liguro-Provençal basin and its margins display the usual mineralogical and geochemical features of subduction-related magmas. Most of these rocks are rich in potassium and plot either in the K-rich calc-alkaline or shoshonitic fields in Peccerillo and Taylor's (1976) diagram (not shown). This relatively K-rich character is a typical feature of circum-Mediterranean magmatism (Wilson et Bianchini, 1999; Lustrino et al., 2011), usually linked to an isotopic signature strongly inherited from continental crust. Although the altered character of most of our submarine K-rich calc-alkaline samples precludes any detailed radiogenic isotope studies, Sr and Nd isotopic data are available for the Ligurian margin calc-alkaline andesites (Galassi, 1995a, b) and the K-rich calc-alkaline lavas from Sardinia (Cioni et al., 1982; Lustrino et al., 2004). They are rather radiogenic in Sr ( $^{87}\text{Sr}/^{86}\text{Sr} = 0.7045\text{--}0.707$ ) and unradiogenic in Nd ( $^{143}\text{Nd}/^{144}\text{Nd} = 0.51235\text{--}0.51265$ ). Such a continental crust imprint is usually explained by the chemical contribution of continentally derived subducted sediments combined with shallow-level crustal contamination (Wilson and Bianchini, 1999). The petrogenetic modelling of Sardinia calc-alkaline lavas concludes to their primary derivation from melting of mantle wedge peridotites previously metasomatized by hydrous fluids carrying a sedimentary crustal component (Dostal et al., 1982; Lustrino et al., 2004, 2011).

### 5.2.2. *Adakites*

The origin of adakitic magmas is still a matter of hot debate. It has been attributed to the partial melting of thickened continental crust or to moderate- or high-pressure fractionation of andesitic liquids (see Jégo et al., 2005; Richards and Kerrich, 2007; Moyen, 2009 and references therein). Many authors (Martin et al., 2005; Maury et al., 2009; Moyen, 2009) consider that typical (silica-rich) adakites derive from 10-35 % melting of MORB-type basalts converted into garnet amphibolites or eclogites (Defant and Drummond, 1990). Such a melting requires temperatures higher than 800 °C, even in the presence of hydrous fluid, at pressures of ca. 2 GPa (Prouteau et al., 1999). This set of pressure-temperature conditions is usually attained

in cases of subduction of either active oceanic ridges or very young oceanic crust (Defant and Drummond, 1990; Peacock et al., 1994; Martin, 1999; Lagabrielle et al., 2000).

Obviously, this is not a realistic situation for the oceanic lithosphere subducting below the studied area, which is thought to have been either of Alpine Tethysian (Handy et al., 2010, Oudet et al., 2010) or Mesogean (Carminati et al., 2010) origin, even if we inclined to favour the last one. However, adakites are also known to occur in transient tectonic settings corresponding either to the initiation of subduction of relatively old oceanic crust (Sajona et al., 1993), to the end of its subduction (Sajona et al., 1994; Maury et al., 1996), or to the development of a slab tear or slab window during collision (Pallares et al., 2007; Gasparon et al., 2009; Lustrino et al., 2009; Maury et al., 2009; Calmus et al., 2011).

In such transient P-T regimes, melting of the subducted MORB crust may occur (Peacock et al., 1994) because of the additional heat provided either by the sinking of the edge of the downgoing crust into the hot asthenospheric arc mantle (initiation of subduction), or by the thermal rebound affecting the slab at the end of subduction (Sajona et al., 1994), or near the edges of the slab tear or window (Thorkelson and Breitsprecher, 2005). These situations can apply to Le Drammont adakitic “esterellites” and Propriano High adakites. The emplacement of the “esterellites” could mark the onset of subduction-related magmatic activity in the Ligurian margin. The Propriano High adakites could either mark the end of subduction-related magmatic activity of southwest Corsica margin, or they could be linked to a slab tearing or even slab detachment process.

### 5.2.3. *Alkali basalts and related rocks*

The third group, i.e. the alkali basalts and related rocks, is difficult to document because of the highly altered character of the corresponding mafic lavas from the three dredged sites (Monte Doria seamount, South Doria area and northwestern Corsica margin), the alkaline affinity of which is only deduced from their clinopyroxene compositions. The only relatively fresh alkali-rich rock recovered is the trachyte Cyl 20-02, the composition of which is too evolved to allow chemical characterisation of its initial mantle source. Its alkaline affinity, however, is dubious because of its Nb and Zr contents clearly lower than those of “anorogenic trachytes” found, for instance, in Isola del Toro (Lustrino et al., 2007b). The fact that the emplacement of these sodic alkali basalts during the Langhian times seems to immediately post-date the end of the subduction event is not easy to explain in an area where there is no specific indication of the occurrence of a mantle plume. However, similar very rapid transitions from K-rich calc-alkaline toward alkaline basaltic activity has been documented in other parts of the Mediterranean domain e.g. in Tunisia (Halloul, 1989), northern Morocco (El Azzouzi et al., 1999), Oranie (Coulon et al., 2002) and Sardinia (Lustrino et al., 2004, 2007b). Maury et al.

(2000) have interpreted this rapid transition as indicating a slab break-off. Such a process was documented from other lines of evidence by Carminati et al., (1998a, b) and de Boorder et al., (1998) for the Langhian geological evolution of the Maghreb. However, these authors do not mention the possibility of a Langhian breakoff beneath the Liguro-Provençal Basin, originally proposed by Serri et al. (1993). During the breaking-off of the subducted slab, the calc-alkaline magmatism, which derives from the melting of the metasomatized mantle wedge overlying the slab, is progressively replaced by a sodic alkali basaltic magmatism originating from adiabatic partial melting of the hot asthenosphere uprising through the slab window (Davies and von Blanckenburg, 1995; Pallares et al., 2007; Thorkelson et al., 2011).

### *5.3. Incidences on the geodynamic evolution of the western Mediterranean domains*

#### *5.3.1. Regional tectonic framework*

It is largely admitted that the Tertiary convergence between Europe and Africa led to north-dipping and northwestern-dipping subductions of the African lithosphere and its precursors beneath the European plate (Cohen, 1980; Réhault, 1981; Réhault et al., 1985; Carminati et al., 2010). Especially, an Oligocene to Early Miocene northwestern- to west-dipping subduction of the Apulia-Adriatic-African lithosphere beneath the Corsica-Sardinia block is considered in most geodynamic reconstructions (Dercourt et al., 1986; Beccaluva et al., 1987, 1994, 2005; Faccenna et al., 1997; Gueguen et al., 1998; Jolivet et al., 1998; Carminati et al., 1998, Gattacceca, 2001; Ferrandini et al., 2003. Lustrino et al., 2009; Carminati et al., 2010, Oudet et al., 2010). During the Middle to Late Miocene, the rollback of the oceanic slab resulted in a passive asthenospheric upwelling in the back-arc domain. It led to the subsequent opening of the Liguro-Provençal Basin and the counter-clockwise rotation of Corsica and Sardinia (Malinverno et al., 1986; Serri et al., 1993; Faccenna et al., 1996; Jolivet et al., 1998; Doglioni et al., 1999; Séranne, 1999; Gattacceca et al., 2007; Lustrino et al., 2009). Some authors, e.g. Serri et al. (1993), proposed that a slab detachment of the oceanic part of the Apulia-Adriatic lithosphere occurred during the Early Miocene. Then, during the Upper Miocene and the Plio-Quaternary, the dominant tectonic regime in the northern part of the Tyrrhenian basin and the northwestern part of the Ligurian basin was extensional (Jolivet et al., 1998 and references therein). It led to the emplacement of numerous magmatic bodies (Serri et al., 1993) and to a high thermal flux in this area (Jemsek et al., 1985, della Vedova et al., 1995). The tomographic images obtained by Carminati et al. (1998) and de Boorder et al. (1998) are consistent with such an evolution. Indeed, they show below the Liguro-Provençal basin negative anomalies at shallow depths, which are consistent with the occurrence of a hot thermal regime (Jemsek, 1988). Our geochemical and chronological data on the magmatic rocks from the Corsica

margin, Algero-Provençal basin and the Ligurian basin allow us to put relatively precise temporal constraints on this tectonic evolution.

### 5.3.2. *Volcanic types and main periods of volcanism off Corsica*

Figure 8 shows the plot on four kinematic positions of our age data completed by the mineral ages carried on Corsica-Sardinia lavas (Savelli et al., 1977; Deino et al., 2001; Speranza et al., 2002; Gattacceca et al., 2007; Lustrino et al., 2009; Oudet et al., 2010; Carminati et al., 2010). These kinematic positions are reconstructed at 33.7 to 26 Ma (pre-rotation fit in Rupelian-Early Chattian times), 23 to 20 Ma (end of rifting and incipient rotation period), 19-18 Ma (time of fast rotation), and 15-14 Ma (present-day position after final rotation of the Sardinia-Corsica block, according to timing proposed by Gattacceca et al., (2007) and Oudet et al., (2010). The space and time distribution of magmatic affinities is presented in Fig. 9, where ages are indicated with error bars at the level of two sigma, owing to comparisons with other data from literature.

The Ligurian domain experienced a succession of volcanic events during the Oligo-Miocene. Rather than a more or less continuous activity, ages of magmatic activity cluster in several groups and geochemical affinities of magmas evolve from normal calc-alkaline with episodic adakitic lavas and K-rich lavas until shoshonitic magmas: onshore between 33 and 26 Ma, Le Drammont adakitic “esterellites” and calc-alkaline lavas in Tourette, Saint Antonin and la Vanade, Monaco and Biot), and offshore, calc-alkaline occurrences are dated between 21 and 18 Ma (ie 20.6 Ma for minerals and slightly younger, 19.4 - 19.2 Ma, for whole rocks; calc-alkaline lavas and adakites dated at 16 to 14 Ma are more or less contemporaneous with K-rich lavas and shoshonites (Genoa Gulf) and Sisco lamproites in northern Corsica.

Finally, between 14 and 6 Ma, K-rich and shoshonitic lavas erupted in southwestern Corsica and on the “Tristanite Ridge”, accompanied and/or followed onshore by alkali basalts, since 12 Ma in Sardinia and later, 7 to 6 Ma, in Toulonnais.

### 5.3.3. *Proposed geodynamical and tectono-magmatic model for the Corsica-Liguria Basin*

After examining the age and the nature of magmatism versus the four kinematic reconstructions, we suggest to distinguish five main geodynamical and tectono-magmatic stages in the evolution of the Ligurian Sea and its margins from Oligocene to Tortonian. The variations in these proposed periods, as well for their number (five instead of four) as their respective durations, are mainly coming from the delay between main geodynamical events and the linked tectono-magmatic effects.

*Stage I (33–31 Ma)*, early beginning of rifting, corresponds to the initiation of the subduction of an oceanic plate of either Alpine Tethysian (Handy et al., 2010, Oudet et al., 2010) or



Mesogean (Carminati et al., 2010) origin beneath the European margin, which includes both the present-day Ligurian margin and the Corsica-Sardinia block (Lustrino et al., 2011). Melting of the down-going edge of this oceanic crust in the transient thermal regime linked to subduction initiation (Peacock et al., 1994; Sajona et al., 1993) could have resulted in the emplacement of adakitic magmas (Le Drammont “esterellites”). In the Alps, Saint-Antonin andesites were most likely derived from the melting of the metasomatized mantle overlying the slab.

An alternative tectonic framework to the onset of the oceanic lithosphere subduction would be to consider the former stage of the evolution of the Alps domain during Late Eocene and Oligocene times. It marked the end of the European lithosphere subduction relayed by collisional processes. Geodynamic consequences would have involved the steepening, tearing and finally break-off of the down-going lithosphere, which might have been responsible for the widespread Paleocene magmatism in the western Alps (Boyet et al., 2001), including Corsica at that time.

It continued up to 26 Ma with the main initial phase of rifting of the incipient Liguria back arc basin and the linked calc-alkaline emissions.

*Stage II (25-23 Ma)* was marked by a following intensive emission of calc-alkaline magmas in the Ligurian margin, whereas calc-alkaline activity continued in Sardinia. The onset of an intra-arc rifting process led to the crustal thinning between the Ligurian margin and the Corsica-Sardinia block and the initiation of the Corsica-Liguria Basin.

*Stage III (21-18 Ma)* was influenced by a slab roll-back process which led to the steepening of the subducted lithosphere. An asthenospheric upwelling was associated with the fast opening of the whole Liguro-Provençal back-arc basin. Calc-alkaline magmatism occurred both in the northwestern and southwestern Corsica volcanic fields, as well as in the Sardinia rift where large magma volumes were emplaced (Coulon, 1977; Lustrino et al., 2004, 2007a, 2009, 2011), during the rotation of the Corsica-Sardinia block (Gattacceca, 2001; Speranza et al., 2002; Gattacceca et al., 2007). In southern Corsica, paleomagnetic data indicate that the rotation was not completely achieved at 19 Ma (Ferrandini et al., 2003, Oudet et al., 2010).

*Stage IV (16-14 Ma)*. During the Langhian, medium-K and K-rich calc-alkaline magmas (2003) were again emplaced in the southwestern Corsica volcanic field and in Sardinia (Fig. 2). We relate the adakitic lavas collected at site 6 (Propriano High) to the partial melting of subducted oceanic crust at the end of the Corsica Sardinia rotation. We suggest that these emissions were linked either to the end of subduction or to tearings in the slab which allowed a subsequent asthenospheric uprise through the slab windows (Thorkelson and Breitsprecher, 2005; Pallares et al., 2007; Thorkelson et al., 2011). This hypothesis is consistent with the high heat flow regime measured east of the deep basin, near the base of the Corsica margin.

*Stage V (14-6 Ma)*. Calc-alkaline lavas were replaced by K-rich calc-alkaline and shoshonitic

lavas, as commonly observed during the evolution of collision zones involving the opening of slab windows (Davies and von Blanckenburg, 1995). Calc-alkaline and shoshonitic lavas (Fannucci et al., 1993) and sodic alkali olivine basalts were emplaced in the Monte Doria seamounts complex. During the final period of this stage, sodic alkali basaltic volcanism occurred first onshore, with the emission of basalts dated at 12 Ma in Isola del Toro, SW Sardinia (Lustrino et al., 2007b) and 7-6 Ma in the vicinity of Toulon. Then, after the main Messinian crisis, voluminous alkali basalts were emplaced in Sardinia and alkaline seamounts in the Tyrrhenian Sea (Savelli et al., 1986; Beccaluva et al., 1990; Mascle et al., 2004; Lustrino et al., 2007a; Lustrino and Wilson, 2007). Melting of the deep asthenosphere uprising through the slab window below the northwestern Corsica margin might account for this alkali basaltic (OIB-type) volcanism (Thorkelson et al., 2011).

## 6. Conclusions

From Early Oligocene to late Miocene times, geochemically diverse lavas were emplaced in the Corsica-Liguria Basin and its margins (Fig. 8 and Fig.9). This diversity includes K-depleted calc-alkaline and K-rich calc-alkaline basalts, basaltic andesites and andesites, adakites, shoshonitic basalts and related intermediate/evolved rocks (trachytes), and finally sodic alkali basalts.

We propose that the emplacement of Le Drammont adakites (“esterellites”) at 33-31 Ma marked the onset of the subduction of an old oceanic lithosphere beneath the southern European margin. It was followed until 18 Ma by the emplacement of medium-K and K-rich calc-alkaline lavas in the Ligurian margin (Villeneuve-Loubet), and in the southwestern Corsica margin as well as in Sardinia. This subduction-related volcanic activity ended near 16-15 Ma in the southwestern Corsica margin with the emission of adakite-related lavas (Marco Dr 02, Cyl 02), while K-rich calc-alkaline activity ended in Sardinia at 14 Ma. K-rich calc-alkaline and shoshonitic lavas were, however, emplaced until 8 Ma in the Tristanite Ridge and Monte Doria Complex (Fig.9).

These changes in the subduction-related magmatism may be attributed to the slab rollback process which led to the break-off and sinking of the oceanic lithosphere during the Langhian times. This slab rollback was also responsible for the intra-arc rifting of the European margin, followed by the Burdigalian “oceanic-type” accretion in the back-arc Liguro-Provençal basin. Finally, during the Late Miocene, the deep asthenosphere uprising through the slab window experienced decompression melting, which led to the emplacement of alkali basaltic edifices in the northwestern Corsica margin and the Tyrrhenian Sea as well as onland (Toulon and Sardinia).

**Acknowledgments:** The authors thank Monique Tegye (BRGM microprobe, Orléans), Marcel Bohn (Microsonde Ouest, Brest) for their contribution to the study of clinopyroxenes and Jean-Claude Philippet (UMR Domaines océaniques, Brest) for K-Ar dating during the first steps of this study. The manuscript was greatly improved according to the very detailed and pertinent comments of two anonymous reviewers. The authors warmly thank Virginia and Roger Hekinian for having improved the English language.

### References

- Aguilar, J.P., Clauzon, G., de Goër de Herve, A., Maluski, H., Michaux, J., Welcomme, J.L., 1996. The MN3 fossil mammal-bearing locality of Beaulieu (France): biochronology, radiometric dating, and lower age limit of the early Neogene renewal of the mammalian fauna in Europe. *News letters of stratigraphy* 34, 3, 177-191.
- Alt, J.C., 1995. Sub-seafloor processes in mid-oceanic ridge hydrothermal systems. In: Humphris, S., Lupton, J., Mullineaux, L., Zierenberg, R. (eds.) *Seafloor hydrothermal systems: physical, chemical, biological and geological interactions*. Geophys. Monogr. 91, AGU, Washington D.C., 85-114.
- Arculus, R. J., 1994. Aspects of magma genesis in arcs, *Lithos* 33, 189-208.
- Arnaud, N.O., Vidal, Ph., Taponnier, P., Matte, Ph., Deng, W.M., 1992. The high K<sub>2</sub>O volcanism of northwestern Tibet: geochemistry and tectonic implications. *Earth Planetary Science Letters* 111, 351-367.
- Barruol, G., Granet, M., 2002. A tertiary asthenospheric flow beneath the southern French Massif central indicated by upper mantle seismic anisotropy and related to the west Mediterranean extension, *Earth Planetary Science Letters* 202, 31-47.
- Barruol, G., Deschamps, A., Coutant, O. 2004. Mapping upper mantle anisotropy beneath SE France by SKS splitting indicates a Neogene asthenospheric flow induced by the Apenninic slab rollback and deflected by the deep Alpine roots, *Tectonophysics* 394, 125-138.
- Baubron, J.-C., Donville, B., Magné, J., Wallez, M.-J., 1975. Datation absolue du volcanisme de Beaulieu (Bouches-du-Rhône, France). Conséquences stratigraphiques. *Bulletin de la Société Géologique de France*. (7), XVII, 5, 773-776.
- Bayer, R., Le Mouel, J.L., Le Pichon, X., 1973. Magnetic anomaly pattern in the western Mediterranean. *Earth and Planetary Science Letters* 19, 168-176.
- Beccaluva, L., Brotzu, P., Macciotta, G., Morbidelli, L., Serri, G. Traversa, G., 1987. Cainozoic tectono-magmatic evolution and inferred mantle sources in the Sardo-Tyrrhenian area, In

- Boriani, A., Bonafede, M., Piccardo, G.B., Vai, G.B., (Eds), The lithosphere in Italy, *Advances in Earth Science Research, Atti dei Convegni Lincei*, 80, 229-248.
- Beccaluva, L., Bonatti, E., Dupuy, C., Ferrara, G., Innocenti, F., Lucchini, F., Macera, P., Petrini, R., Rossi, P.L., Serri, G., Seyler, M. Siena, F., 1990. Geochemistry and mineralogy of volcanic rocks from ODP sites 650, 651, 655 and 654 in the Tyrrhenian Sea. In: Kasten K.A., Mascle J. et al. (eds). *Proc. ODP, Scientific Results*, 107, 49-74.
- Beccaluva, L., Di Girolamo, P. Serri, G., 1991. Petrogenesis and tectonic setting of the Roman Volcanic Province, Italy, *Lithos*, 26, 191-221.
- Beccaluva, L., Coltorti, M., Galassi, R., Macciotta, G., Siena, F., 1994. The Cainozoic calc-alkaline magmatism of the western Mediterranean and its geodynamic significance. *Bolletino Geofisica Teorica Applicata.*, 36, 141-144, 293-309.
- Beccaluva, L., Bianchini, G., Coltorti, M., Siena, F., Verde, M., 2005. Cenozoic tectono-magmatic evolution of the central-western Mediterranean: migration of an arc-interarc basin system and variations in the mode of subduction. In: I.R. Finetti (Ed.) *CROP Project: Deep seismic exploration of the central Mediterranean and Italy*. Elsevier, 623-639.
- Bellaiche, G., Gennesseaux, M., Mauffret, A., Réhault, J.P., 1974. Prélèvements systématiques et caractérisation des réflecteurs acoustiques: nouvelle étape dans la compréhension de la géologie de la Méditerranée occidentale. *Marine Geology* 16: M47-M56.
- Bellon, H., 1976. Séries magmatiques néogènes et quaternaires du pourtour méditerranéen occidental, comparées dans leur cadre géochronométriques. Implications géodynamiques. Thèse de Doctorat d'Etat, Université Paris sud Orsay, 367 p.
- Bellon, H., 1981. Chronologie radiométrique K-Ar des manifestations magmatiques autour de la Méditerranée occidentale entre 33 et 1 Ma. In: Wezel, F.C. (Ed.), *Sedimentary basins of Mediterranean margins*, Tecnoprint Bologna, pp. 341-360.
- Bellon, H., Brousse, R., 1971. L'âge oligo-miocène du volcanisme ligure. *Comptes Rendus de l'Académie des Sciences de Paris* 272, 3109-3111.
- Bellon, H., Brousse, R., 1977. Le magmatisme périméditerranéen occidental. Essai de synthèse, *Bulletin de la Société géologique de France* 7, XIX, 469-480.
- Bellon, H., Quoc Buu, N., Chaumont, J., Philippet, J.C., 1981. Implantation ionique d'argon dans une cible support: application au traçage isotopique de l'argon contenu dans les minéraux et les roches. *Comptes Rendus de l'Académie des Sciences de Paris II*, 292, 977-980.
- Bellon, H., Maury, R.C., Bellaiche, G., Mermet, J.F., Réhault, J-P., Auzende, J.M., 1985. Age et nature des formations volcaniques prismées observées et prélevées dans le Canyon des Moines (sud-ouest Corse) pendant la campagne Cyaligure. *Marine Geology* 67, 163-176.
- Benito, R., Lopez-Ruiz, J., Cebrià, J.M., Hertogen, J., Doblas, M., Oyarzun, R., Demaiffe, D.,

1999. Sr and O isotopic constraints on source and crustal contamination in the high-K calc-alkaline and shoshonitic neogene volcanic rocks of SE Spain, *Lithos*, 46, 773-802.
- Bianchini, G., Beccaluva, L., Siena, F., 2008. Post-collisional and intraplate Cenozoic volcanism in the rifted Appenines/Adriatic domain, *Lithos* 101,125-140.
- Boyet, M., Lapierre, H., Tardy, M., Bosch, D., Maury, R.C., 2001. Nature des sources des composants andésitiques des grès du Champsaur et des grès de Taveyannaz. Implications dans l'évolution des Alpes occidentales au Paléogène. *Bulletin de la Société géologique de France* 172, 487-501.
- Brousse, R., Lefèvre, C., 1990. Le volcanisme en France et en Europe limitrophe. Guides géologiques régionaux, Masson (eds), 263 p.
- Buerger, A., Klotzli, U., 1990. New data on the evolutionary history of the Ivrea Zone (Northern Italy). *Bulletin der Vereinigung Schweizerischer Petroleum - Geologen und - Ingenieure* 56, 130, 49-70.
- Calmus, T., Pallares, C., Maury, R.C., Bellon, H., Pérez-Segura, E., Aguillón-Robles, A., Carreno, A.-L., Bourgois, J., Cotten, J., Benoit, M., 2008. Petrologic diversity of Plio-Quaternary post-subduction volcanism in Baja California: an example from Isla San Esteban (Gulf of California, México). *Bulletin de la Société géologique de France* 179, 465-481.
- Calmus, T., Pallares, C., Maury, R.C., Aguillón-Robles, A., Bellon, H., Benoit, M., Michaud, F., 2011. Volcanic markers of the post-subduction evolution of Baja California and Sonora, Mexico: slab tearing versus lithospheric rupture of the Gulf of California. *Pure and Applied Geophysics* 168, 1303-1330.
- Cann, J.R., 1979. Metamorphism of the oceanic crust. In: *Deep drilling results in the Atlantic ocean: oceanic crust*, Talwani, M., Harrison, C.G., Hayes, D.E. (eds.) Maurice Ewing Symposium Series, 2, AGU, Washington D.C., 48, 230-238.
- Carminati, E., Wortel, M. J. R., Spakman, W., Sabadini, R., 1998a. The role of slab detachment processes in the opening of the western-central Mediterranean basins: some geological and geophysical evidence. *Earth Planetary Science Letters* 160, 651-665.
- Carminati, E., Wortel, M. J. R., Meijer, P.Th., Sabadini, R., 1998b. The two-stage opening of the western-central Mediterranean basins: a forward modeling test to a new evolutionary model. *Earth Planetary Science Letters* 160, 667-679.
- Carminati, E., Lustrino, M., Cuffaro, M., Doglioni, C., 2010. Tectonics, magmatism and geodynamics of Italy : what we know and what we imagine. *Journal of the Virtual Explorer* 36, paper 9, DOI: 10.3809/jvirtex.2010.00226.
- Cioni, R., Clocchiatti R., Di Paola G.M., Santacroce, R., Tonarini, M., 1982. Miocene calc-alkaline heritage in the Pliocene volcanism of Monte Arci (Sardinia Italy). *Journal of Volcanology and Geothermal Research* 14, 133-167.

- Cohen, C.R., 1980. Plate tectonic model for the Oligo-Miocene evolution of the Western Mediterranean. *Tectonophysics*, 68, 283-311.
- Contrucci, I., 1998. Structure profonde du bassin Nord Ligure et structures du bassin Nord Tyrrhénien. Thèse de doctorat, Université de Corte, Corse, 217p.
- Cotten, J., Le Dez, A., Bau, M., Caroff, M., Maury, R. C., Dulski, P., Fourcade, S., Bohn, M., Brousse, R., 1995. Origin of anomalous rare-earth element and yttrium enrichments in subaerially exposed basalts: evidence from French Polynesia. *Chemical Geology* 119, 115-138.
- Coulon, C., 1967. Le volcanisme tertiaire de la région toulonnaise (Var). *Bulletin de la Société géologique de France*, 7, IX, 691-700.
- Coulon, C., 1977. Le volcanisme calco-alkalin cénozoïque de Sardaigne (Italie). *Pétrographie, géochimie et genèse des laves andésitiques et des ignimbrites*. Signification géodynamique. Thèse de Doctorat d'Etat, Université de Marseille, 385 p.
- Coulon, C., Demant, A., Bellon, H., 1974. Premières datations par la méthode K/Ar de quelques laves cénozoïques et quaternaires de Sardaigne Nord-Occidentale. *Tectonophysics* 22, 41-57.
- Coulon, C., Megartsi, M., Fourcade, S., Maury, R.-C., Bellon, H., Louni-Hacini, A., Cotten, J., Coutelle A., Hermitte D., 2002. Post-collisional transition from calc-alkaline to alkaline volcanism during the Neogene in Oranie (Algeria): magmatic expression of slab-breakoff. *Lithos* 62, 87-110.
- Dautria, J.-M., Liotard, J.-M., 1990. Les basaltes d'affinité tholéiitique de la marge méditerranéenne française. *Comptes Rendus de l'Académie des Sciences, Paris*, 311, II, 821-827.
- Davies, J. H., von Blanckenburg, F., 1995. Slab breakoff: a model of lithosphere detachment and its test in the magmatism and deformation of collisional orogens, *Earth and Planetary Science Letters* 129, 85-102
- de Boorder, H., Spakman, W., White, S.H., Wortel, M.J.R., 1998. Late Cenozoic mineralization, orogenic collapse and slab detachment in the European Alpine Belt, *Earth Planetary Science Letters* 164, 569-575.
- Defant, M.J., Drummond, M.S., 1990. Derivation of some modern arc magmas by melting of young subducted lithosphere. *Nature* 347, 662-665.
- Defant, M.J., Richerson, M., de Boer, J.Z., Stewart, R.H., Maury, R.C., Bellon, H., Drummond, M.S., Feigenson, M.D., Jackson, T.E., 1991. Dacite genesis via both slab melting and differentiation: petrogenesis of La Yeguada volcanic complex, Panama. *Journal of Petrology* 32, 1101-1142.
- Defant, M.J., Jackson, T.E., Drummond, M.S., de Boer, J.Z., Bellon, H., Feigenson, M.D., Maury, R.C., Stewart, R.H., 1992. The geochemistry of young volcanism throughout western

- Panama and southeastern Costa Rica: an overview. *Journal of the Geological Society of London* 149, 569-679.
- De Jong, M.R., Wortel, M.J.R., Spakman, W., 1994. Regional scale tectonic evolution and the seismic velocity structure of the lithosphere and upper mantle: the Mediterranean region, *Journal of Geophysical Research* 99, 12091-12108.
- Deino, A.L., Gattacceca, J., Rizzo, Montanuri, L. 2001.  $^{40}\text{Ar}/^{39}\text{Ar}$  dating and paleomagnetism of the Miocene volcanic succession of Monte Furru (western Sardinia): Implications for the rotation history of the Corsica-Sardinia microplate. *Geophysical research Letters* 28, 17, 3373-3376.
- Della Vedova, B., Pellis, G., 1981. Misure di flusso di calore nel Mar Ligure e nel Tirreno settentrionale: risultati preliminari, Istituto di Miniere e geofisica Applicata dell'Università di Trieste, 42 pp.
- Della Vedova, B., Lucazeau, F., Pasquale, V., Pellis, G., Verdoya, M., 1995. Heat flow in the tectonic provinces crossed by the southern segment of the European Geotraverse. *Tectonophysics*, 244, 1-3, 57-74.
- Dercourt, J., Zonenshain, L.P., Ricou, L.E., Kazmin, V.G., Le Pichon, X., Knipper, A.L., Grandjacquet, C., Sbertshikov, I.M., Geyssant, J., Lepvrier, C., Pechersky, D.H., Boulin, J., Sibuet, J.C., Savostin, L.A., Sorokhtin, O., Westphal, M., Bazhenov, M.L., Lauer, J.P., Biju-Duval, B., 1986. Geological evolution of the Tethys belt from the Atlantic to the Pamirs since the Lias. *Tectonophysics* 123, 241-315.
- Doglioni, C., Gueguen, E., Harabaglia, P., Mongelli, F., 1999. On the origin of west-directed subduction zones and applications to the western Mediterranean. In: Durand B., Jolivet L., Horvath F. and Séranne M., (eds) *The Mediterranean basins: Tertiary Extension within the Alpine orogen*. *Journal of the Geological Society of London*, Special Publication 156, 541-561.
- Dostal, J., Coulon, C., Dupuy, C., 1982. Cenozoic andesitic rocks of Sardinia (Italy), In "Orogenic andesites and related rocks" R.S. Thorpe (Ed.), John Wiley, 353-370.
- Duggen, S., Hoernle, K.A., Hauff, F., Klügel, A., Bouabdellah, M., Thirlwall, M.F., 2009. Flow of Canary mantle plume material through a subcontinental lithospheric corridor beneath Africa to the Mediterranean. *Geology* 37, 3, 283 - 286.
- El Azzouzi, M., Bernard-Griffiths, J., Bellon, H., Maury, R.C., Piqué, A., Fourcade, S., Cotten, J., Hernandez, J., 1999. Evolution des sources du volcanisme marocain au cours du Néogène. *Comptes Rendus de l'Académie des Sciences de Paris* 329, 95-102.
- Faccenna, C., Mattei, M., Funiciello, R., Jolivet L., 1997. Styles of back-arc extension in the Central Mediterranean. *Terra Nova* 9, 126-130.
- Faccenna, C., Davy, P., Brun, J.P., Funiciello, R., Giardini, D., Mattei, M., Nalpas T., 1996. The

- dynamics of back-arc extension: an experimental approach to the opening of the Tyrrhenian Sea. *Geophysical Journal International* 126, 781-795.
- Faccenna, C., 2002. Extensional tectonics on Sardinia Italy: insights into the back arc transitional regime. *Tectonophysics* 356, 213-232.
- Faccenna, C., Piromallo, C., Crespo-Blanc, A., Jolivet, F., Rossetti, F., 2004. Lateral slab deformation and the origin of the western Mediterranean arcs. *Tectonics* 23, TC1012, 21 p. doi:10.1029/2002TC001488.
- Fanucci, F., Firpo, M., Piccardo, G.B., Piccazzo, M., Vetuschi Zuccolini, M., 1993. Attività magmatica Neogenica in Mar Ligure. Atti 12° convegno annuale del gruppo nazionale di geofisica della Terra solida, Roma, 24-26 Nov. 1993, 1003-1007.
- Ferrandini, J., Gattacceca, J., Ferrandini, M., Deino, A., Janin, M.C., 2003. Chronostratigraphie et paléomagnétisme des dépôts oligo-miocènes de Corse: implications géodynamiques pour l'ouverture du bassin liguro-provençal. *Bulletin de la Société géologique de France* 174, 4, 357-371.
- Féraud, J., Fornari, M., Geffroy, J., Lenck P.P., 1977. Minéralisations arséniées et ophiolites: le filon à réalgar et stibine de Matra et sa place dans le district à Sb-As-Hg de la Corse alpine. *Bulletin du BRGM II*, 2, 91-112.
- Féraud, G., Ruffet, G., Stéphan, J.F., Lapierre, H., Delgado, E., Popoff, M., 1995. Nouvelles données géochronologiques sur le volcanisme paléogène des Alpes occidentales: existence d'un événement magmatique bref généralisé. Séance Spéciale de la Société géologique de France et de l'Association des Géologues du SE "Magmatismes dans le sud-est de la France", Nice, 25-26 Octobre 1995, abstracts, 38.
- Galassi, B., 1995a. Evoluzione magmatologica delle associazioni orogeniche cenozoiche del Mediterraneo Centro-Occidentale. Ph D thesis, Università di Ferrara, Italy.
- Galassi, B., 1995b. Magmatological evolution of the Cainozoic orogenic associations of the Central-Western Mediterranean. *Plinius. European Journal of Mineralogy, Italian Supplement* 13, 86-91.
- Galdeano, A., Rossignol J.C., 1977. Assemblage à altitude constante de cartes d'anomalies magnétiques couvrant l'ensemble du bassin occidental de la Méditerranée. *Bulletin de la société géologique de France*, 7, 461-468.
- Galson, D.A., Mueller, St., 1986. An introduction to the European Geotraverse "Project: first results and present plans. *Tectonophysics* 126, 1-30.
- Gasparon, M., Rosenbaum, G., Wijbrans, J., Manetti, P., 2009. The transition from subduction arc to slab tearing: Evidence from Capraia Island, northern Tyrrhenian Sea. *Journal of Geodynamics* 47, 30-38.
- Gattacceca, J., 2001. Cinématique du bassin liguro-provençal entre 30 et 12 Ma. Implications



- géodynamiques, Thèse de Doctorat, Ecole des mines de Paris, 299 p.
- Gattacceca, J., Deino, A., Rizzo, R., Jones, D.S., Henry, B., Beaudoin, B., Vadeboin, F., 2007. Miocene rotation of Sardinia: New paleomagnetic and geochronological constraints and geodynamic implications. *Earth and Planetary Science Letters* 258, 359-377.
- Gennesseaux, M., Glaçon, G., Réhault, J.P., Fierro, G., 1974. Les affleurements sédimentaires néogènes dans la vallée sous-marine d'Asinara (Sardaigne septentrionale). XXIV<sup>e</sup> Congrès-Assemblée Générale Plénière de Monaco, 6-14 décembre 1974, CIESM, géologie et géophysique marines.
- Gennesseaux, M., Réhault, J.P., Thomas, B., 1989. La marge continentale de la Corse, *Bulletin de la Société géologique de France* 5, 2, 339-351.
- Gill, J., 1981. *Orogenic andesites and plate tectonics*. Springer-Verlag, Berlin, 390 p.
- Giraud, J.D., Bellon, H., Turco, G., 1979. L'intrusion microdioritique tertiaire d'Alghero (Sardaigne). Age K/Ar et relation avec le magmatisme calco-alcalin sarde. Analogies avec les estrellites de l'Estérel (Var). *Comptes Rendus de l'Académie des Sciences Paris*, 288, série D, 9-12.
- Gouvernet, C., Guieu, C., Rousset, C., 1997. *Guide géologique de Provence*, Masson Ed.
- Gueguen, E., 1995. Le bassin liguro-provençal: un véritable océan. Exemple de segmentation des marges et de hiatus océaniques. Implications sur les processus d'amincissement crustal. Thèse Doctorat Université de Brest, 310 p.
- Gueguen, E., Doglioni, C. and Fernandez, M., 1998. On the post-25 Ma geodynamic evolution of the western Mediterranean. *Tectonophysics*, 298, 259-269.
- Gueirard, S., 1964. Le « volcan » de Beaulieu, près Rognes (Bouches-du-Rhône), *Bulletin de la Société géologique de France* 7, VI, 443-455.
- Guennoc, P., Réhault, J.P., Gilg-Capar, L., Deverchère, J., Rollet, N., Le Suavé, R., 1998. Les marges Ouest et Nord de la Corse; Nouvelle cartographie à 1/250 000°. Réunion annuelle des sciences de la terre, Brest, France, March 31 to April 3, 1998.
- Guennoc, P., Ferrandini, J., Réhault, J.P., Thinon, I., 2004. Evolution of the Corsica-Sardinia microplate: consequences of multiple rifting on the margin of the Western Bonifacio straits., in RST 2004 - 20ème Réunion des Sciences de la Terre - Strasbourg - France - 20-25/09/2004.
- Halloul, N., 1989. Géologie, pétrologie et géochimie du bimagmatisme néogène de la Tunisie septentrionale (Nefza et Mogod). Implications pétrogénétiques et interprétation géodynamique, Thèse de Doctorat, Univ. Blaise Pascal, Clermont-Ferrand, 203 p.
- Handy, M.R., Schmid, S., Bousquet, R., Kissling, E., Bernoulli, D., 2010. Reconciling plate-tectonic reconstructions of Alpine Tethys with the geological-geophysical record of spreading and subduction in the Alps. *Earth-Science Reviews* 102, 121-158.

- Hawkesworth, C.J., Vollmer, R., 1979. Crustal contamination versus enriched mantle:  $^{143}\text{Nd}/^{144}\text{Nd}$  and  $^{87}\text{Sr}/^{86}\text{Sr}$  evidence from the Italian volcanics. *Contribution to Mineralogy and Petrology*, 69, 151-165.
- Ivaldi, J.-P., Bellon, H., Guardia, P., Mangan, C., Müller, C., Perez, J.-L., Terramorsi, S., 2003. Contexte lithostructural, âges  $^{40}\text{K}/^{40}\text{Ar}$  et géochimie du volcanisme calco-alkalin tertiaire de Cap-d'Ail dans le tunnel ferroviaire de Monaco. *Comptes Rendus Geoscience* 335, 411-421.
- Jégo, S., Maury, R.C. Polvé, M., Yumul Jr., G.P., Bellon, H., Tamayo Jr., R.A., and Cotten, J., 2005. Geochemistry of adakites from the Philippines: constraints on their origins. *Resource Geology* 55, 163-187.
- Jemsek, J., Von Herzen, R.P., Réhault, J.P., Williams, D.L., Sclater, J.G., 1985. Heat flow and lithospheric thinning in the Ligurian Basin (N.W. Mediterranean). *Geophysical Research Letters* 12, 693-696.
- Jemsek, J.P., 1988. Heat flow and tectonics of the Ligurian Basin and margins. Ph.D. Thesis MIT/WHOI, WHOI 88-25, 488p.
- Jolivet, L., Faccenna, C., d'Agostino, N., Fournier, M., Worrall, D., 1999. The kinematics of back-arc basins, examples from the Tyrrhenian, Aegean and Japan Seas. In: Durand B., Jolivet, L., Horvath, F., Séranne, M., (eds) *The Mediterranean basins: Tertiary Extension within the Alpine orogen*. Geological Society of London Special Publication 156, 21-53.
- Kincaid, C., Griffiths, R.W., 2004. Laboratory models of the thermal evolution of the mantle during rollback subduction. *Nature* 425, 58-62.
- Lagabrielle, Y., Guivel, C., Maury, R.C., Bourgois, J., Fourcade, S., Martin, H., 2000. Magmatic-tectonic effects of high thermal regime at the site of active ridge subduction: the Chile Triple Junction model. *Tectonophysics* 326, 215-228.
- Le Bas, M.J., Le Maitre, R.W., Streckeisen, A., Zanettin, B., 1986. A chemical classification of volcanic rocks based on the total-alkali-silica diagram. *Journal of Petrology* 27, 745-750.
- Leterrier, J., Maury, R.C., Thonon, P., Girard M., Marchal, M., 1982. Clinopyroxene composition as a method of identification of the magmatic affinities of paleo-volcanic series. *Earth Planetary Science Letters* 59, 139-154.
- Lucente, F.P., Margheriti, L., Piromallo, C., Barruol, G., 2006. Seismic anisotropy reveals the long route of slab through the western-central Mediterranean mantle. *Earth Planetary Science Letters* 241, 517-529.
- Lustrino, M., Morra, V., Melluso, L., Brotzu, P., d'Amelio F., Fedele, L., Franciosi, L., Lonis, R., Petheruti Liebercknecht A.M., 2004. The Cenozoic igneous activity of Sardinia. *Periodico di Mineralogia* 73, 105-134.
- Lustrino, M., Wilson, M., 2007. The Circum-Mediterranean Anorogenic Cenozoic Igneous Province. *Earth-Science Reviews* 81, 1-65.

- Lustrino, M., Melluso, L., Morra, V., 2007a. The geochemical peculiarity of “Plio-Quaternary” volcanic rocks of Sardinia in the circum-Mediterranean area. In: L. Beccaluva, G. Bianchini and M. Wilson (Eds.) *Cenozoic Volcanism in the Mediterranean Area: Geological Society of America Special Paper 418*, p. 277–301,
- Lustrino, M., Morra, V., Fedele, L., Serracino, M., 2007b. The transition between ‘orogenic’ and ‘anorogenic’ magmatism in the western Mediterranean area: the middle Miocene volcanic rocks of Isola del Toro (SW Sardinia, Italy). *Terra Nova* 19, 149-159.
- Lustrino, M., Morra, V., Fedele, L., Francosi, L., 2009. Beginning of the Apennine subduction system in the central Western Mediterranean: Constraints from Cenozoic “orogenic” magmatic activity of Sardinia, Italy. *Tectonics*, vol 28, TC 5016, 1-23.
- Lustrino, M., Duggen, S., Rosenberg, C.L., 2011. The central-Western Mediterranean: anomalous igneous activity in an anomalous collisional tectonic setting. *Earth-Science Reviews* 104, 1-40.
- Mahood, G.A., Drake, R.E., 1982. K-Ar dating young rhyolitic rocks: a case study of the Sierra La Primavera, Jalisco, Mexico. *Geological Society of America Bulletin* 93, 1232-1241.
- Malinverno, A., Ryan, W., 1986. Extension in the Tyrrhenian Sea and shortening in the Apennines as result of arc migration driven by sinking of the lithosphere. *Tectonics* 5, 227-246.
- Maluski, H., 1977. Application de la méthode  $^{40}\text{Ar}/^{39}\text{Ar}$  aux minéraux des roches cristallines perturbées par des événements thermiques et tectoniques en Corse, thèse, université de Montpellier (USTL), 113 p.
- Martin, H., 1999. Adakitic magmas: modern analogues of Archaean granitoids. *Lithos* 46, 411-429.
- Martin, H., Smithies, R.H., Rapp, R.P., Moyen, J.-F., Champion, D.C., 2005. An overview of adakite, tonalite-trondhjemite-granodiorite (TTG) and sanukitoid: relationships and some implications for crustal evolution. *Lithos* 79, 1-24.
- Mascle, G., Tricart, P., Torelli, L., Bouillin, J.; -P., Compagnoni, R., Depardon, S., Mascle, J., Pecher, A., Peis, D., Rekhiss, F., Rolfo, F., Bellon, H., Brocard, G., Lapierre, H., Monié, P., Poupeau, G., 2004. Structure of the Sardinia Channel: crustal thinning and tardi-orogenic extension in the Apenninic-Maghrebien orogen; results of the Cyana submersible survey (SARCYA and SARTUCYA) in the western Mediterranean. *Bulletin de la Société géologique de France* 175, 6, 607-627.
- Mauffret, A., Frizon de Lamotte, D., Lallement, S., Gorini, C., Maillard, A., 2004. E-W opening of the Algerian Basin (Western Mediterranean). *Terra Nova*, 16, 257-264.
- Maury, R.C., Sajona, F.G., Pubellier, M., Bellon, H., Defant, M., 1996. Fusion de la croûte océanique dans les zones de subduction/collision récentes: l'exemple de Mindanao,

- Philippines. Bulletin de la Société géologique de France 167, 579-595.
- Maury, R.C., Fourcade, S., Coulon, C., El Azzouzi, M., Bellon, H., Ouabadi, A., Semroud, B., Megartsi, M., Cotten, J., Belanteur, O., Louni-Hacini, A., Coutelle, A., Piqué, A., Capdevila, R., Hernandez, J., 2000. Post-collisional Neogene magmatism of the Mediterranean Maghreb margin: a consequence of slab detachment. *Comptes Rendus de l'Académie des Sciences de Paris* 331, 159-173.
- Maury, R.C., Calmus, T., Pallares, C., Benoit, M., Grégoire, M., Aguillon-Robles, A., Bellon, H., Bohn, M., 2009. Origin of the adakite-high-Nb basalt association and its implications for post-subduction magmatism in Baja California, Mexico: Discussion. *GSA Bulletin*, 121, 1465-1469.
- Michel Lévy, A., 1898. Mémoire sur le porphyre bleu de l'Estérel. Bulletin du Service de la Carte géologique de la France, Topographies souterraines 57, IX, 1897-1898, 47 p.
- Monaghan, A., 2001. Coeval extension, sedimentation and volcanism along the Cenozoic rift system of Sardinia, in: Ziegler, P. A., Cavazza, W., Robertson, A.H.F., Crasquin-Soleau, S., (Eds.), *Peri-Tethys Memoir 6: Peri-Tethyan Rift / Wrench Basins and Passive Margins*. Mémoire. Museum. National d'Histoire Naturelle, 186: 707-734. Paris ISBN/ 2-85653-528-3.
- Montenat, C., Leyrit, H., Gillot, P.Y., Janin, M.C., Barrier, P., 1999. Extension du volcanisme oligocène dans l'Arc de Castellane (Chaînes subalpines de Haute-Provence). *Géologie de la France* 1, 43-48.
- Montigny, R., Edel, J.B., Thuizat, R., 1981. Oligo-Miocene rotation of Sardinia: K-Ar ages and paleomagnetic data of Tertiary volcanics. *Earth Planetary Science Letters* 54, 261-271.
- Morra, V., Secchi, F.A.G., Melluso, L., Franciosi, L., 1997. High-Mg subduction-related Tertiary basalts in Sardinia, Italy. *Lithos* 40, 69-91.
- Morelli, C., 1974. Modello strutturale d'Italia. Carte 2 feuilles, C.N.R. ed.
- Moyen, J.-F., 2009. High Sr/Y and La/Yb ratios: the meaning of the "adakitic signature". *Lithos* 112, 556-574.
- Ottaviani-Spella, M-M., Girard, M., Cheilletz, A., 1996. Les ignimbrites burdigaliennes du Sud de la Corse, pétrologie et datation K-Ar. *Comptes Rendus de l'Académie des Sciences de Paris II a*, 323, 771-778.
- Ottaviani-Spella, M-M., Girard, M., Rochette, P., Cheilletz, A., Thion, I., 2001. Le volcanisme acide burdigalien du Sud de la Corse: pétrologie, datation K-Ar, paléomagnétisme. *Comptes Rendus de l'Académie des Sciences de Paris, IIA*, 333, 2, 113-120.
- Oudet, J., Münch, Ph., Verati, C., Ferrandini, M., Melinte-Dobrinescu, M., Gattacceca, J., Cornée, J.J., Oggiano, G., Quillévéré, F., Borgamano, J., Ferrandini, J., 2010. Integrated chronostratigraphy of an intra-arc basin:  $^{40}\text{Ar}/^{39}\text{Ar}$  datings, micropaleontology and magnetostratigraphy of the early Miocene Castelsardo basin (northern Sardinia, Italy).

- Paleogeography, Paleoclimatology, Paleoecology, 295, 293-306.
- Oyarzun, R., Doblas, M., Lopez-Ruiz, J., Cebria, J.M., 1997. Opening of the Central Atlantic and asymmetric mantle upwelling phenomena: implications for long-lived magmatism in western North Africa and Europe, *Geology*, 25, 727-730.
- Pallares, C., Maury, R. C., Bellon, H., Royer, J.-Y., Calmus, T., Aguilon-Robles, A., Cotten, J., Benoit, M., Michaud, F., Bourgois, J., 2007. Slab-tearing following ridge-trench collision: Evidence from Miocene volcanism in Baja California, Mexico, *Journal of Volcanology and Geothermal Research*, 161, 95-117.
- Peccerillo, A., 2005. Plio-Quaternary volcanism in Italy. *Petrology, geochemistry, geodynamics*. Springer Verlag, Heidelberg, 365p.
- Peccerillo, A, Taylor, S.R., 1976. Geochemistry of Eocene calc-alkaline volcanic rocks from the Kastamonu area, Northern Turkey. *Contrib. Mineral. Petrol.* 58, 63-81.
- Peacock, S.M., Rushmer, T., Thompson, A.B., 1994. Partial melting of subducting oceanic crust. *Earth Planetary Science Letters* 121, 224-227.
- Piqué, A., Brahim, L. A., El Azzouzi, M., Maury, R. C., Bellon, H., Semroud, B., Laville, E, 1998. The Maghreb indenter: structural and chemical data. *Comptes Rendus de l'Académie des Sciences de Paris IIA*, 326, 575-581.
- Piomallo, C., Morelli, A., 2003. P wave tomographic constraints on the geodynamic evolution of the Italian region, *J. Geophys. Res.* 108, doi:10.1029/2002JB001757.
- Platt, J.P., Soto J.-I., Whitehouse, M.J., Hurford, A.J., Kelley, S.P., 1998. Thermal evolution, rate of exhumation, and tectonic significance of metamorphic rocks from the floor of the Alboran extensional basin, western Mediterranean. *Tectonics* 17, 671-689
- Prouteau, G., Scaillet, B., Pichavant, M., Maury, R.C., 1999. Fluid-present melting of ocean crust in subduction zones. *Geology* 27, 1111-1114.
- Réhault, J.-P., Olivet, J.L., Auzende, J.M. 1974. Le bassin nord-occidental méditerranéen: structure et évolution. *Bulletin de la Société géologique de France* 7, XVI, 3, 281-294.
- Réhault, J.P., 1981. Evolution tectonique et sédimentaire du bassin ligure (Méditerranée Occidentale). Thèse d'Etat, Paris VI, 132 p-107 fig.
- Réhault, J.-P., Boillot, G., Mauffret, A., 1984. The Western Mediterranean basin geological evolution. *Marine Geology* 55, 447-477.
- Réhault, J.P., Boillot, G. and Mauffret, A., 1985, The western Mediterranean basins, edited by D.J. Stanley and F.C. Wezel, pp 101-129, Springer-Verlag
- Réhault, J.P., Bellon, H., Maury, R., Rossi, P., Guennoc, P., Sosson, M., Poupeau, G., 1998. Nouveautés sur le volcanisme en mer Ligure, paper presented at Réunion des Sciences de la Terre, Brest, France, March 31 to April 3.
- Renne, P.R., Swisher, C.C., Deino, A.L., Karner, D.B., Owens, T.L., DePaolo, D.J., 1998.

- Intercalibration of standards, absolute ages and uncertainties in  $^{40}\text{Ar}/^{39}\text{Ar}$  dating. *Chemical Geology* 145, 117-152.
- Richards, J.P., Kerrich, R., 2007. Adakites: their diverse origins and questionable role in metallogenesis. *Economic Geology* 102, 537-576.
- Rivière, M., Bellon, H., Bonnot-Courtois, C. 1981. Geochemical and geochronological aspects of a pyroclastic deposit drilled in in the Valencia Trough – Site 123 DSDP, Leg 13 (Spain): geodynamical implications. *Marine Geology* 41, 295-307.
- Rollet, N., Deverchère, J., Beslier, O., Guennoc, P., Réhault, J.-P., Sosson, M., Truffert, C., 2002. Back-arc extension, tectonic inheritance and volcanism in the Ligurian Ocean, Mediterranean Sea. *Tectonics* 21, 3, 6-1 – 6-23.
- Romer, R. L., Scharer, U., Steck, A., 1996. Alpine and pre-Alpine magmatism in the root-zone of the western Central Alps. *Contributions to Mineralogy and Petrology* 123, 138-158.
- Rossi, P., Guennoc, P., Réhault, J.-P., Arnaud, N., Bouchra, J., Poupeau, G., Tegye, M., Ferrandini, J., Sosson, M., Beslier, M.O., Rollet, N., Gloaguen R., 1998. Importance du volcanisme calco-alkalin miocène sur la marge sud-ouest de la Corse (campagne Marco), *Comptes Rendus de l'Académie des Sciences de Paris* 327, 369-376.
- Ruffet, G., Féraud, G., Amouric, M., 1991. Comparison of  $^{40}\text{Ar}/^{39}\text{Ar}$  conventional and laser dating biotites from the North Trégor Batholith: *Geochimica et Cosmochimica Acta* 55, 1675-1688.
- Ruffet, G., Féraud, G., Ballèvre, M., Kiénast, J. R., 1995. Plateau ages and excess argon on phengites: A  $^{40}\text{Ar}/^{39}\text{Ar}$  laser probe study of alpine micas (Sesia zone): *Chemical Geology* 121, 327-343.
- Sajona, F.G., Bellon, H., Maury, R.C., Cotten, J., Defant M.J., Pubellier, M., 1993. Initiation of subduction and the generation of slab melts in western and eastern Mindanao, Philippines. *Geology* 21, 1007-1010.
- Sajona, F.G., Bellon, H., Maury, R.C., Pubellier, M., Cotten, J., Rangin, C., 1994. Magmatic response to abrupt changes in tectonic setting: Pliocene-Quaternary calc-alkaline lavas and Nb-enriched basalts of Leyte and Mindanao (Philippines). *Tectonophysics* 237, 47-72.
- Sajona, F.G., Bellon, H., Maury, R.C., Pubellier, M., Quebral, R.D., Cotten, J., Bayon, F.E., Pagado, E., Pamatian, P., 1997. Tertiary and Quaternary magmatism in Mindanao and Leyte (Philippines): Geochronology, geochemistry and tectonic setting. *Journal of Asian Earth Sciences* 15, 121-153.
- Sajona, F.G., Maury, R.C., Prouteau, G., Cotten, J., Schiano, P., Bellon, H., Fontaine, L., 2000. Slab melt as metasomatic agent in island arc mantle sources, Negros and Batan (Philippines). *Island Arc* 9, 472-486.
- Savelli, C., Beccaluva, L., Deriu, M., Macciotta, G., Maccioni, L., 1979. K/Ar geochronology

- and evolution of the Tertiary "calc-alkalic" volcanism of Sardinia (Italy). *Journal of Volcanology and Geothermal Research* 5, 257-269.
- Savelli, C., 1988. Late Oligocene to recent episodes of magmatism in and around the Tyrrhenian Sea: implication for the processes of opening in a young inter-arc basin of intra orogenic (Mediterranean) type. *Tectonophysics*, 146, 1-4, 163-181.
- Savelli, C., 2002. Time-space distribution of magmatic activity in the western Mediterranean and peripheral orogens during the past 30 Ma (a stimulus to geodynamic considerations). *Journal of Geodynamics* 34, 99-126.
- Séranne, M., 1999. The Gulf of Lion continental margin (NW Mediterranean) revisited by IBS: an overview. In: Durand, B., Jolivet, L., Horvath, F., Séranne M., (eds) *The Mediterranean basins: Tertiary Extension within the Alpine orogen*. Geol. Soc. London, Spec. Pub., 156, 15-36.
- Serri, G., Innocenti, F., Manetti, P., 1993. Geochemical and petrological evidence of the subduction of delaminated Adriatic continental lithosphere in the genesis of the Neogene-Quaternary magmatism of central Italy. *Tectonophysics*, 223, 117-147.
- Speranza, F., Villa, I.M., Sagnotti, L., Florindo, F., Cosentino, D., Cipollari, P., Mattei, M., 2002. Age of the Corsica-Sardinia rotation and Liguro-Provençal Basin spreading: new paleomagnetic and Ar/Ar evidence. *Tectonophysics* 347, 231-251.
- Steiger, R.H., Jäger E., 1977. Subcommittee on geochronology: convention on the use of decay constants in geo- and cosmochemistry. *Earth Planetary Science Letters* 36, 359-362.
- Stern, C.R., Kilian, R., 1996. Role of the subducted slab, mantle wedge and continental crust in the generation of adakites from the Austral Volcanic Zone. *Contribution to Mineralogy and Petrology*, 123, 263-281.
- Sun, S.S., McDonough, W.F., 1989. Chemical and isotopic systematics of oceanic basalts: implications for mantle composition and processes. In Saunders, A.D., and Norry, M.J., (Eds.), *Magmatism in ocean basins*, Geological Society of London Special Publication 42, 313-345.
- Thomas, B., Gennesseaux, M., 1986. A two stage rifting in the basins of the Corsica-Sardinia straits. *Marine Geology* 72, 225-239.
- Thorkelson, D.J., Breitsprecher, K., 2005. Partial melting of slab window margins: genesis of adakitic and non-adakitic magmas. *Lithos*, 79, 25-41.
- Thorkelson, D.J., Madsen, J.K., Slagter, C.L. 2011. Mantle flow through the Northern Cordilleran slab window revealed by volcanic geochemistry. *Geology*, 39, 267-270.
- Van Tellingen, H.W., Verschure R.H., Andriessen, P.A.M., 1996. Indications for an Early Miocene mafic dike swarm in Western Corsica. A combined fission track, Isotopic and geochemical investigation, *Proceedings of the Koninklijke Nederlandse Akademie van*

- Wetenschappen 99 (1-2), 85-104.
- Von Blanckenburg, F., Davies J.H., 1995. Slab breakoff: a model for syncollisional magmatism and tectonics in the Alps, *Tectonics* 14, 120-131.
- Wilson, M., Bianchini, G., 1999. Tertiary-Quaternary magmatism within the Mediterranean and surrounding regions. In: Durand, B., Jolivet, L., Horvath, F. and Séranne, M., (Eds.) *The Mediterranean basins: Tertiary Extension within the Alpine orogen*. Geological Society of London Special Publication 156, 141-168.
- Wortel, M.J.R., Spakman, W., 1992. Structure and dynamics of subducted lithosphere in the Mediterranean region. *Proceedings of the Koninklijke Nederlandse Akademie van Wetenschappen* 95, 325-347.
- Wortel, M.J.R., Spakman, W., 2000. Subduction and slab detachment in the Mediterranean-Carpathian Region, *Science* 290, 1910-1917.
- Zeck, H.P., 1996. Betic-Rif orogeny: subduction of Mesozoic Tethys lithosphere under eastward drifting Iberia, slab detachment shortly before 22 Ma, and subsequent uplift and extensional tectonics. *Tectonophysics* 254, 1-16.
- Zeck, H.P., Kristensen, A.B., Williams, I.S., 1998. Post-collisional volcanism in a sinking slab setting - crustal anatexis origin of pyroxene-andesite magma, Caldear Volcanic Group, Neogene Alboran volcanic province, southeastern Spain. *Lithos* 45, 499-522.
- Zibrowius, H., 1980. Les sclérolithes de la Méditerranée et de l'Atlantique nord occidental. *Mémoire de l'Institut océanographique de Monaco*, 11, 3 volumes.

## Figure captions

Fig. 1.

The Western Mediterranean area: general physiography from ETOPO2 global relief map, showing the distribution of the main volcanic edifices resting on both a transitional crust-type (roughly limited by the 2,500 m isobaths and thinned continental crust. 1- Hercynian basement; 2- Alpine Corsica series; 3- Balearic basement; 4- Thinned to transitional crust; 5- Oceanic – type crust; 6- Volcanic edifices.

Fig. 2. Location maps of the studied submarine samples. a: maps and isotopic ages of magmatic samples collected from southwestern (sites 1 to 4) and northwestern areas (sites 5 to 11) of the western Corsica margin. Conventional  $^{40}\text{K}/^{40}\text{Ar}$  whole-rock ages are shown in italics, and  $^{40}\text{Ar}/^{39}\text{Ar}$  mineral ages are underlined. Site numbers as in Table 1.b: Location map of the



sampling sites **from** the “Tristanite Ridge”.

Fig. 3.

$^{40}\text{Ar}/^{39}\text{Ar}$  spectra of five separated minerals (plagioclase Cyl 07-03, Cyl 03-01; amphibole, biotite Cyl 02-01) from western Corsica margin offshore lavas (sites 3, 4 and 6).

Fig. 4.

$\text{SiO}_2$  vs. LOI (wt.%) plot showing the negative correlation linked to increasing alteration processes. Numbers for analyses refer to that of sites and samples in Table 1.

**1:** MA 74 DR 05a; **2:** Cya 77 DR 02-a; **2a :** Cya 77 DR 02-a2; **3a:** Cya 77-35 03; **3b:** Cyl 07-03; **3c:** Cyl 07-11; **3d:** Cyl 07-10; **3e:** Cyl 07-07; **4:** Cyl 03-01; **5:** Marco DR 06-08; **6a:** Cyl 02-01; **6b:** Cyl 02-02; **6c:** Marco DR02-1a; **7a:** Cyl 20-02; **7b core:** Ma 74 DR 01; **7b rim:** Ma 74 DR 01; **7c:** Cyl 20-01; **9:** Cyl 22-05; **10:** Marco DR 52-06 a; **11:** Marco DR 49-03

Fig. 5.

Primitive mantle-normalised multi-element plots of western Corsica margin offshore magmatism with references to onshore French Ligurian magmatism (diagram 5c). Elements order and normalisation values are from Sun and McDonough (1989). Diagrams 5a and 5b: southwestern Corsica field lavas; diagram 5c: north Corsica volcanic field, Cap Corse and onshore Ligurian magmatism; 5d: northwestern Corsica volcanic field, Tristanite Ridge lavas. diagram 5e: northwestern Liguria volcanic field, Doria seamounts and Genoa Central Volcano lavas and Toulonnais lavas; diagram

Fig. 6.

Ti vs Ca+Na diagrams showing the compositions of primary clinopyroxenes (phenocrysts and microphenocrysts) from offshore mafic and intermediate lavas from the Corsica margin. The separating line between the alkalic field and the sub-alkalic one is from Leterrier et al. (1982). 6a- northwest volcanic field: Monte Doria seamounts.

6b- north Corsica volcanic field: Cap Corse; 6c- northwest Corsica volcanic field: Tristanite Ridge; 6d-southwest Corsica volcanic field;

Fig. 7.

Structural interpretation of retraced from seismic lines Malis 25, crossing the Propriano High (Fig.7a), and Malis 17 (Fig.7b) crossing the “Tristanite Ridge”. They show the locations of the main geological elements, which denote the evolution of the domain in the southwestern part and the northwestern one. Vertical scale in s. twt.(*second, two way travel time*), (for conversion

in m. the measured thickness must be multiplied by the half seismic propagation velocity of each level).

1- Upper Mantle,  $V_m = 7.8-8.0$  km/s. 2- Oceanic-type crust,  $V_m = 6.5-7.0$  km/s. 3- Transitional crust,  $V_m = 6.4-6.8$  km/s. 4- Continental crust,  $V_m = 5.8-6.4$  km/s. 5- Volcanic edifices,  $V_m = 4-6$  km/s.. 6- Lava flows,  $V_m = 3.2-5$  km/s. 7- Miocene marine pelagic sediments, from early Burdigalian up to late Tortonian. 8- Messinian salt layer  $V_m = 4-4.2$  km/s. 9- Messinian upper evaporites,  $V_m = 3.2-3.5$  km/s. 10- reworked volcanic elements, volcanoclastic layers comprising pillows and breccias elements and/or partly interstratified detritals; 11- Plio-Quaternary turbiditic to pelagic series.  $V_m = 1.8-2.5$  km/s. N.B. The dykes framework and alimentation system are hypothetical.

Fig. 8.

Whole rock K-Ar ages (bold italics) and  $^{40}\text{Ar}/^{39}\text{Ar}$  plateau ages of separated minerals (underlined normal characters) from Corsica-Sardinia lavas: plagioclases (this study and Ferrandini et al., 2003; Lustrino et al., 2009;) amphiboles and biotites (this study). All results are plotted in four kinematic reconstructions of Corsica-Sardinia drifting (after Gattacceca et al., 2007 and Oudet et al., 2010). Remark that some ages are prior or after the period of these reconstructions around 33-30 Ma, 23-20 Ma, 19-18 Ma and 15-14 Ma.

Fig. 9.

Spatial and temporal distribution of Oligo-Miocene magmatism within and around the northwestern Mediterranean Sea.

## List of Tables

Table 1. Summary of the main petrologic features and age data for studied volcanics at each site of investigation.

*List of sampling cruises.*

*Geomed IV in 1974, R/V Jean Charcot, recovering of samples by dredging (code sample G IV).*

*Marsili in 1974, R/V Marsili, recovering of samples by dredging (code sample MA74).*

*Cyaligure in 1977, R/V Le Noroit, Cyana, recovering of samples by diving and complementary dredging (code sample Cya 77).*

*Marco cruise in 1995, R/V le Suroit, recovering of samples by dredging (code sample Marco).*

*Cylice cruise in 1997, R/V l'Atalante, Cyana recovering of samples by deep diving (code sample Cyl).*

Table 2. Whole-rock K-Ar ages and analytical parameters for offshore lavas from the southwestern and the northwestern Corsica volcanic fields. Analytical methods detailed in the text.

Table 3.  $^{40}\text{Ar}$ - $^{39}\text{Ar}$  Ar ages of separated amphibole, biotite and plagioclase from lavas collected during dives along the Corsica margin.

Table 4.

Major element oxides (wt.%) and trace element (ppm) concentrations of selected samples of the offshore magmatism from the southwestern and northwestern Corsica margins, with references to onshore French Ligurian magmatism. Analytical methods detailed in the text.  $\text{Fe}_2\text{O}_3^*$ : total iron as  $\text{Fe}_2\text{O}_3$ .

Table 5.

Wo-En-Fs compositions of selected primary clinopyroxenes (phenocrysts and microphenocrysts) from offshore mafic and intermediate lavas, after microprobe analyses. These data were performed using both the BRGM microprobe in Orléans and the Western microprobe in Brest; analytical conditions are detailed in Defant et al. (1991).

## Appendix

Selected microprobe analyses of minerals compositions for the magmatic diversity of Corsica-Liguria lavas. Sheet 1 - clinopyroxenes; sheet 2 - feldspars; sheet 3 - biotites; sheet 4 - amphiboles and, sheet 5 - oxides.

### Clinopyroxenes

Site 1: MA 74 DR05.

Site 3: Cyl 07-10; Cyl 07-11.

Site 7 : Cyl 20-02.

Site 9 : Cyl 22-03 ; Cyl 22-05 ; Cyl 22-7a

Site 10 : Marco Dr 52-03 ; Marco Dr 52-06; Marco Dr 52-07; Marco Dr 52-10.

Site 12 : Cyl 15-10.

### Feldspars

Site 3: Cyl 07-10; Cyl 07-11, Cya 77-35 03.

Site 6: Cyl 02-01; Cyl 02-02.

Site 9 : Cyl 22-03 ; Cyl 22-05 ;Cyl 22-07a ; Cyl 22-08.

Site 12 : Cyl 15-10.

Biotites

Site 6: Cyl 02-01; Cyl 02-02.

Amphiboles

Site 6: Cyl 02-01

Oxides

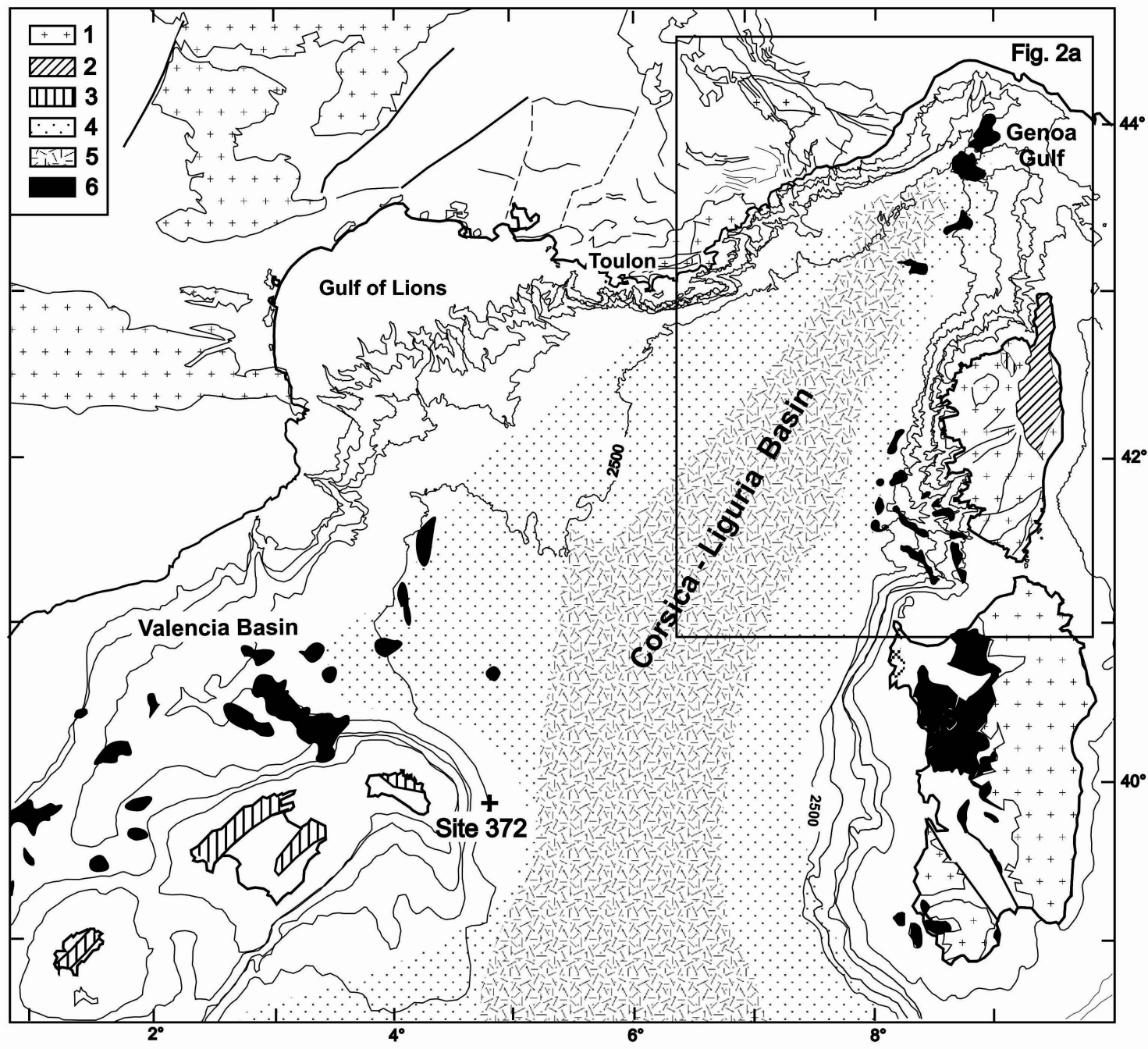
Site 6: Cyl 02-02.

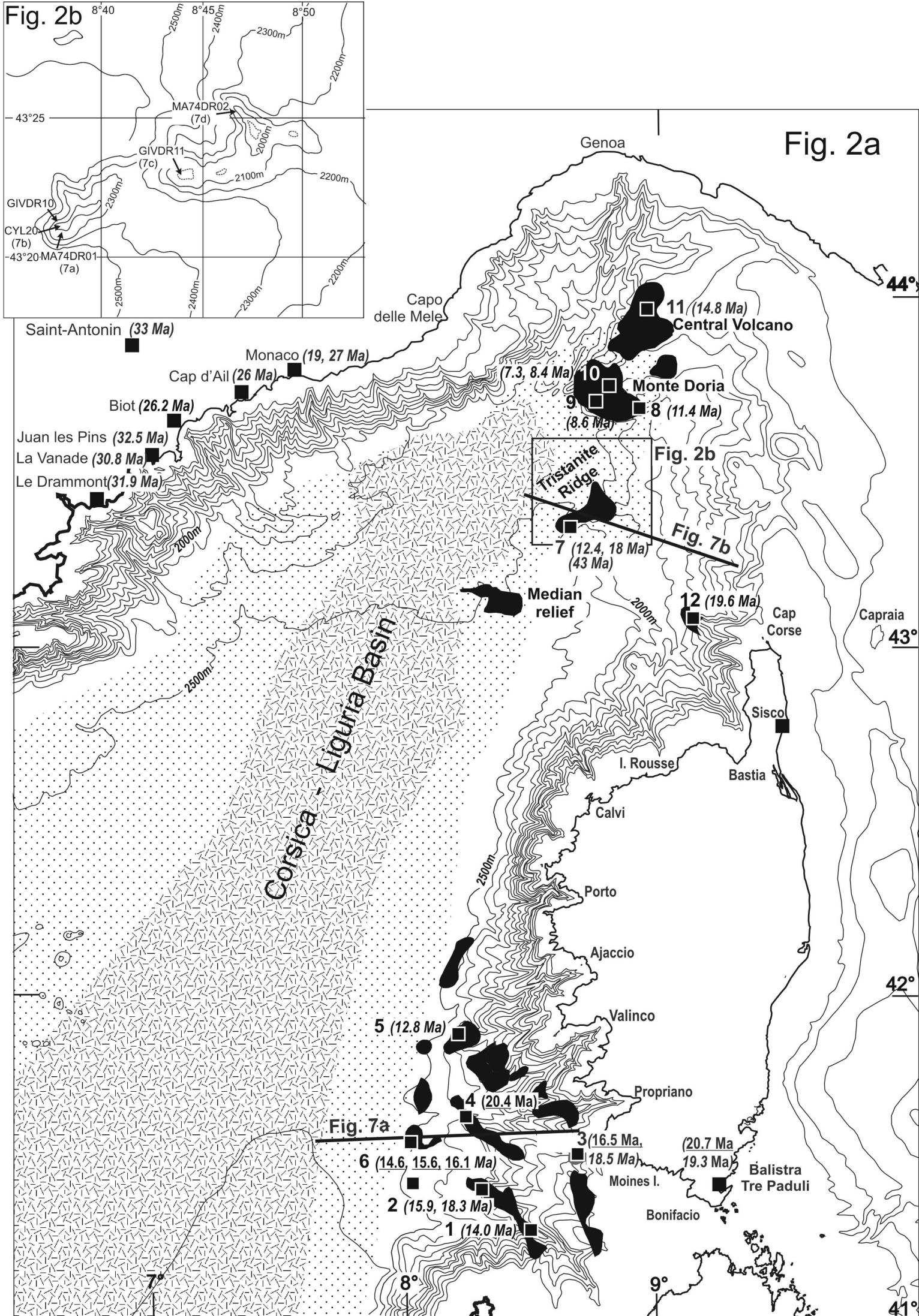
**Offshore Oligo-Miocene volcanic fields within the Corsica-Liguria Basin:  
magmatic diversity and slab evolution in the western Mediterranean Sea**

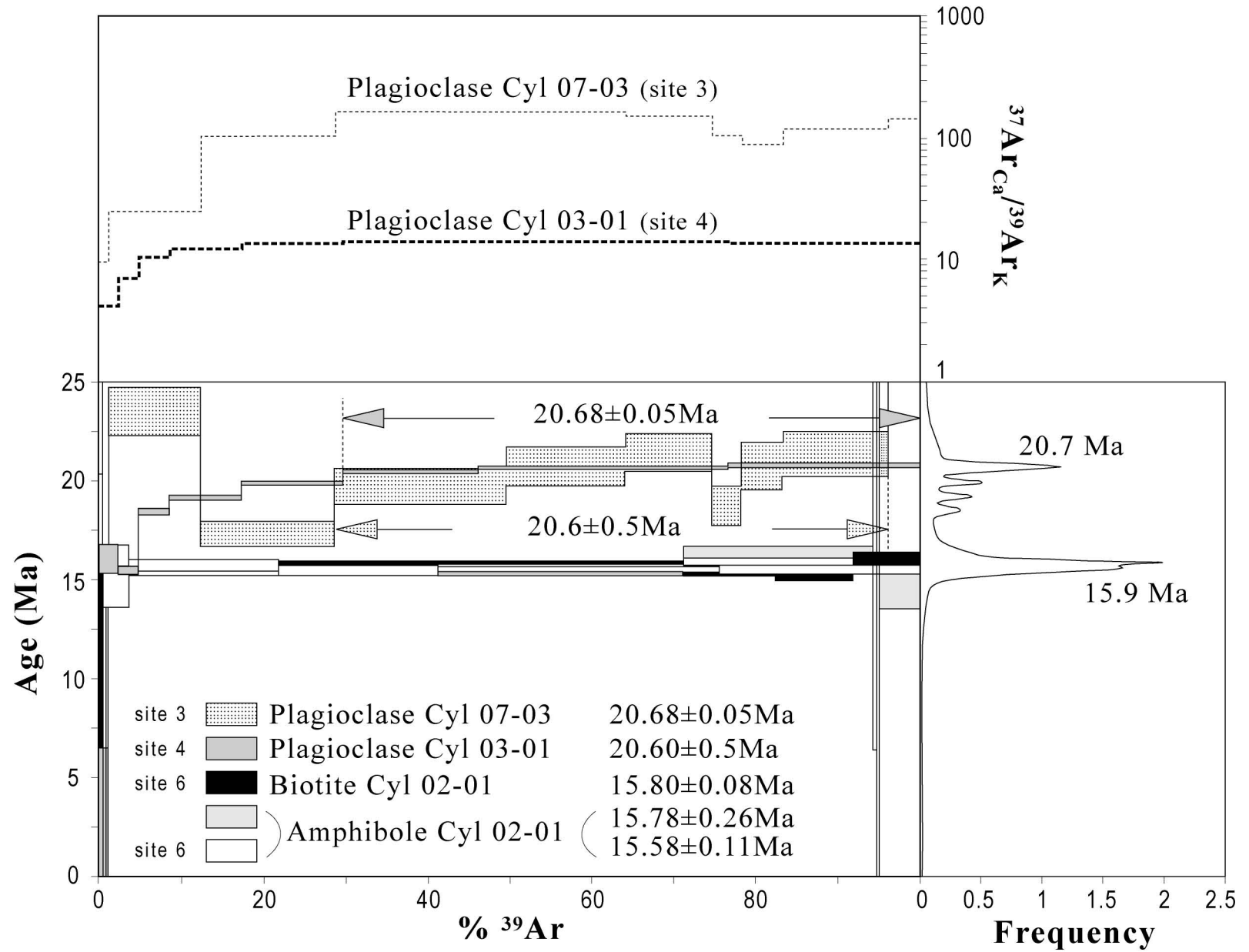
J.-P. Réhault <sup>a\*</sup>, C. Honthaas <sup>b</sup>, P. Guennoc <sup>c</sup>, H. Bellon <sup>a</sup>, G. Ruffet <sup>d</sup>, J. Cotten <sup>a</sup>, M. Sosson <sup>f</sup>, R. C.  
Maury <sup>a</sup>

**Highlights**

- Presentation of an original collection of submarine rocks sampled by dredgings and in situ divers during 25 years within the Liguria-Corsica Basin.
- Geochemical diversity of lavas and K-Ar dating of whole rocks and <sup>39</sup>Ar-<sup>40</sup>Ar of plagioclases and amphiboles between 30 and 6 Ma in several stages.
- West of Corsica, discovery of adakitic emissions K-Ar dated around 16 Ma.
- Transition from calc-alkaline, K-rich calc-alkaline and shoshonitic lavas to alkaline basalts in north Liguria Basin and in Toulonnais.
- Constraints on the kinematic and geodynamic evolution of the northwestern Mediterranean Sea (Liguria-Corsica Basin).









# Malis 17

WNW

10

Site 7

Tristanite ridge

50 km

W Cap Corse

ESE

Cyl 20 12.8 Ma  
MA74-DR01 18 Ma

Ma 17

7b

Ma 25

7a



# Malis 25

w

10

Site 6  
Propriano High

Site 4  
Valinco Canyon

50 km

Site 3  
Canyon des Moines

E

100 km

Cyl 02  
15.8 Ma  
15.6 Ma

Cyl 03 projected  
20.1 Ma

Cyl 07 projected  
20.6 Ma

S.

T.W.T.



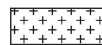
1



2



3



4



5



6



7



8



9



10

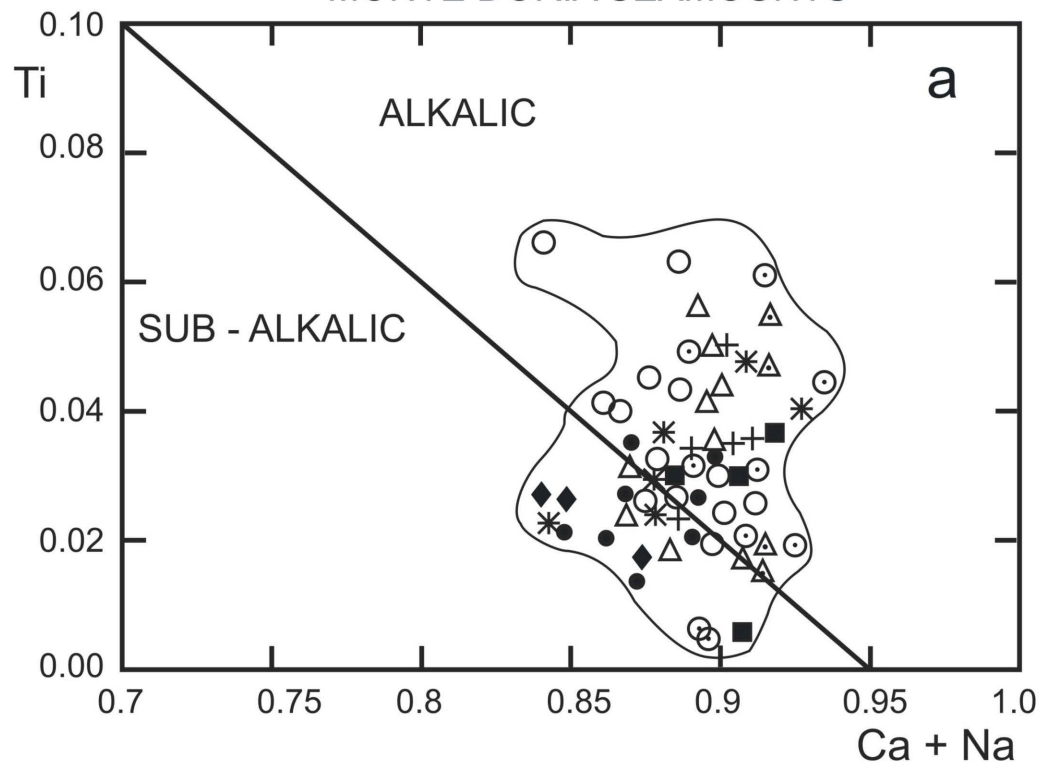


11

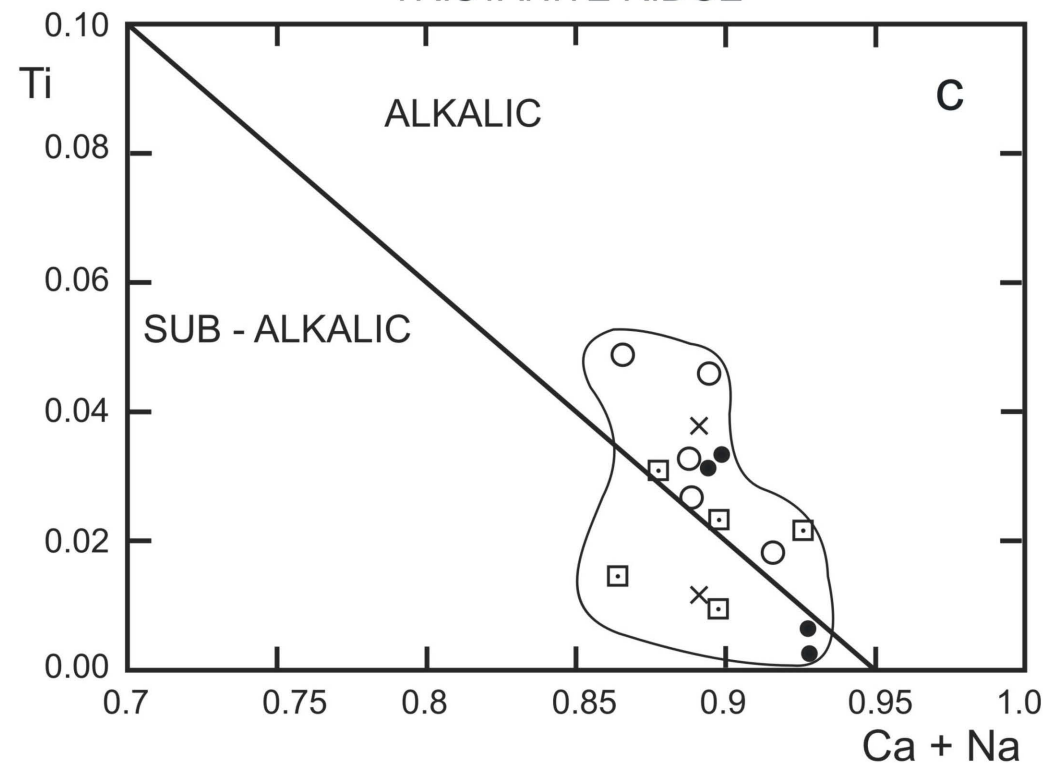


Moho

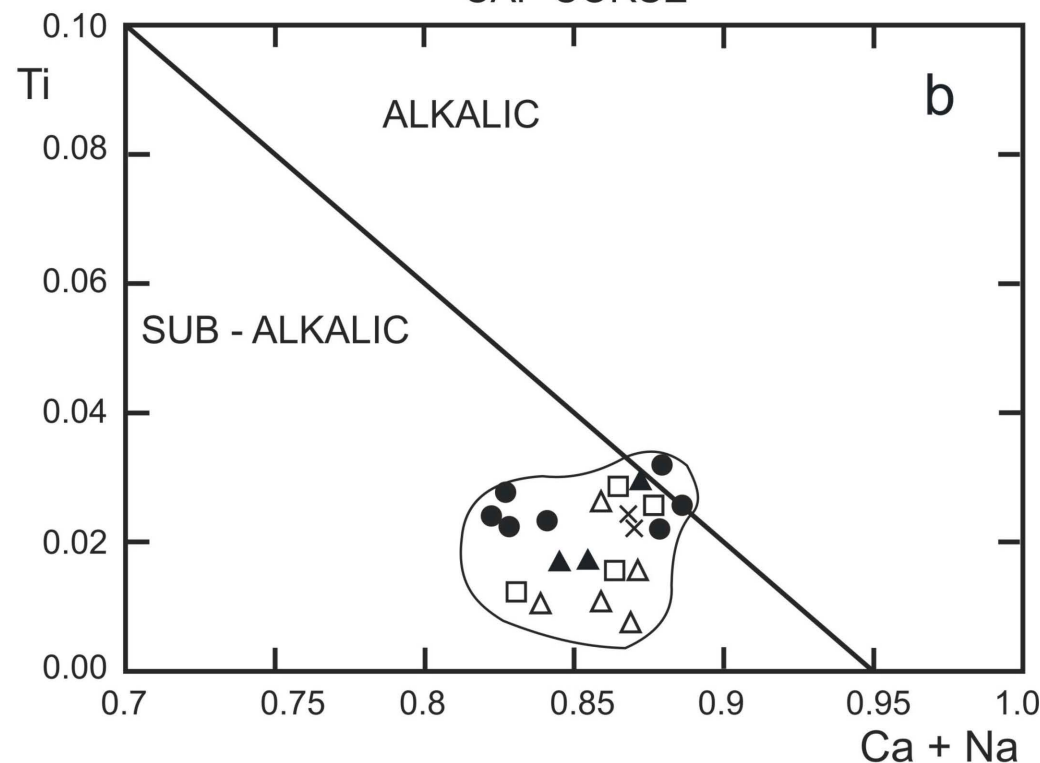
# MONTE DORIA SEAMOUNTS



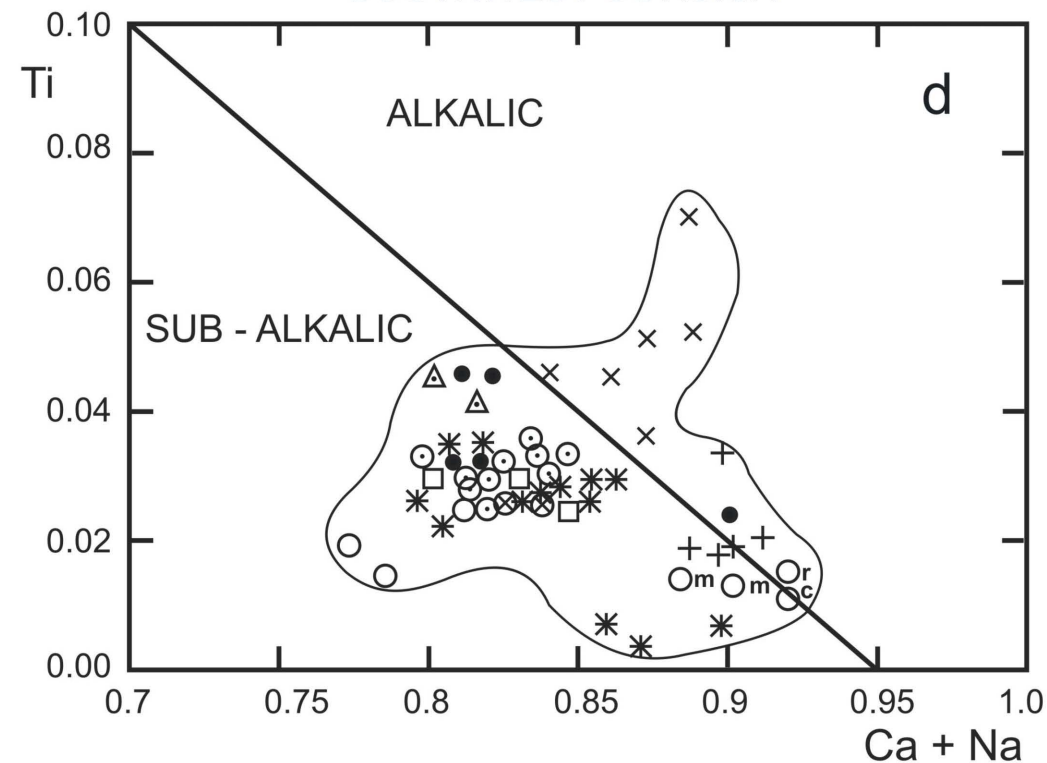
# TRISTANITE RIDGE



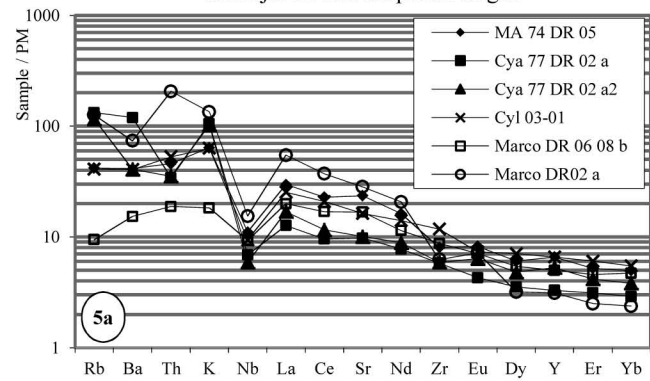
# CAP CORSE



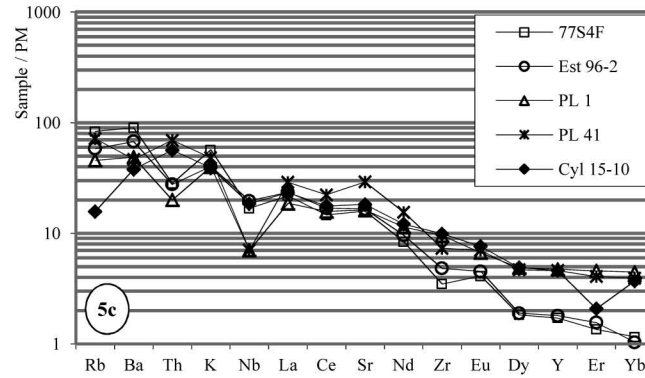
# SOUTHWEST CORSICA



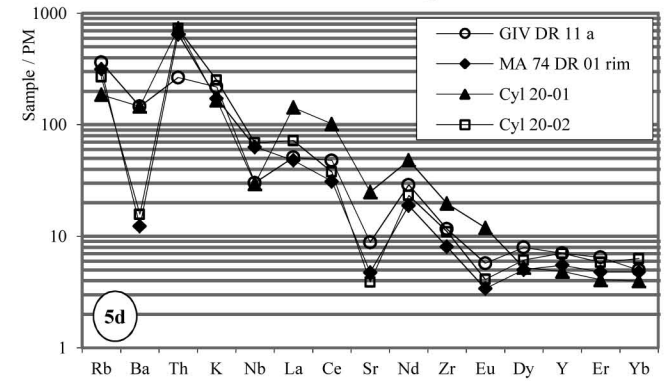
SW Corsica, Monte Paoli, Castelsardo and Valinco Canyons  
and Ajaccio and Propriano Highs



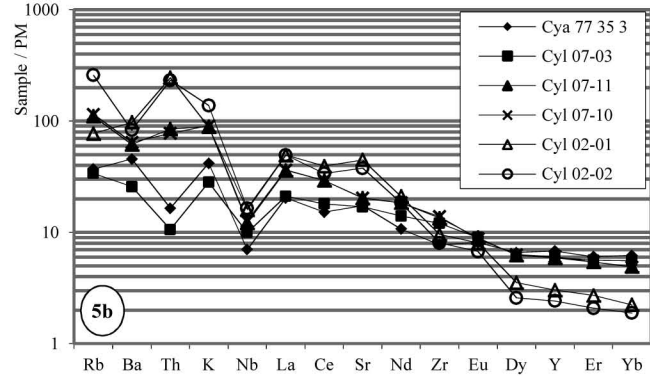
Cap Corse and onshore Ligurian magmatism



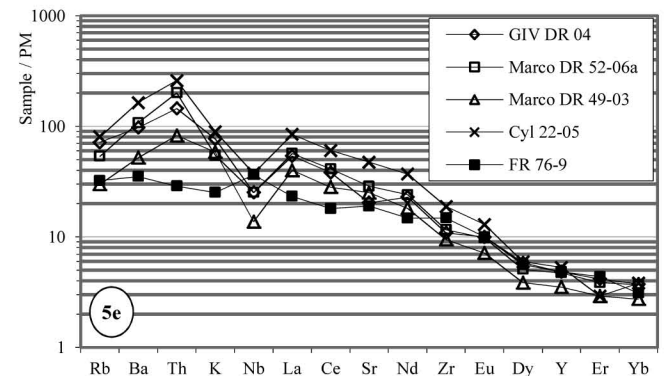
Tristanite Ridge

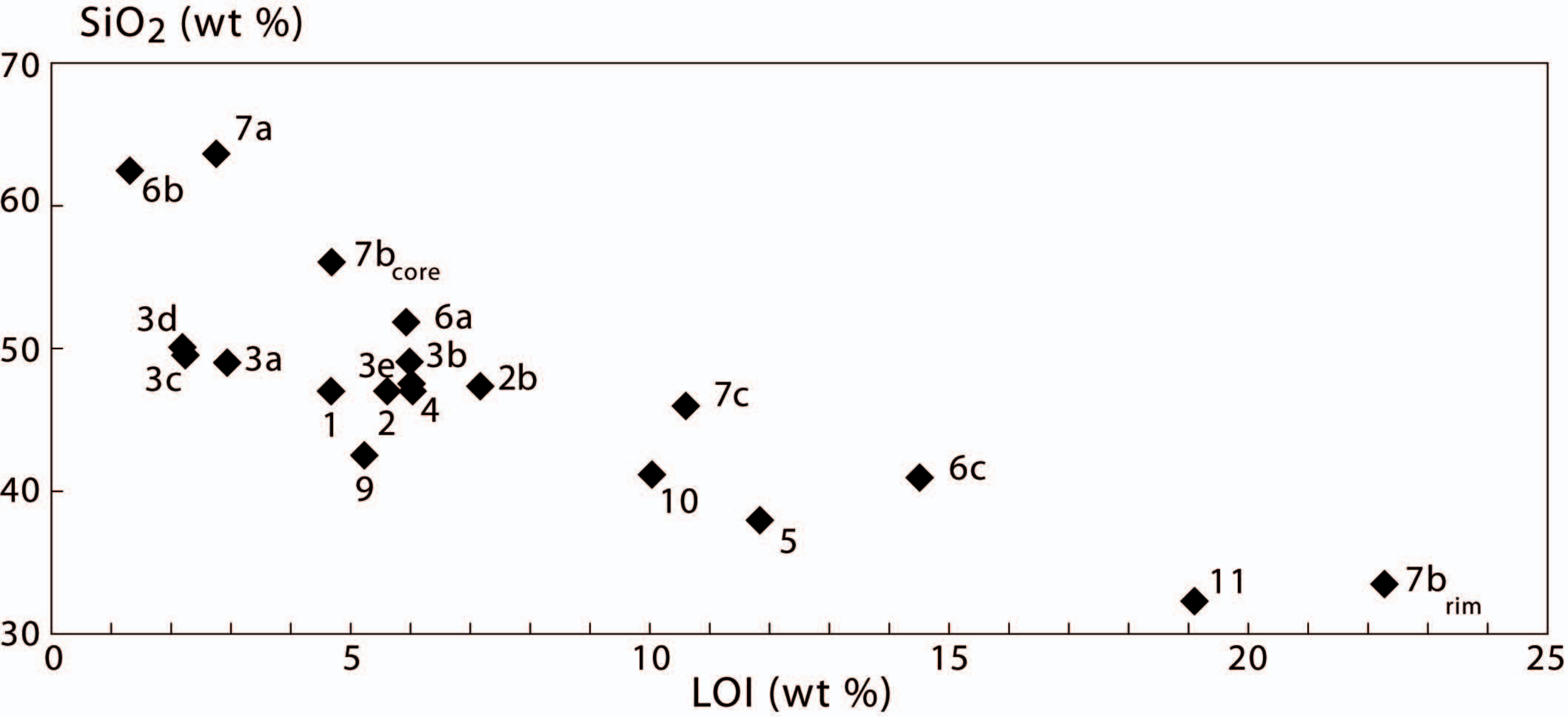


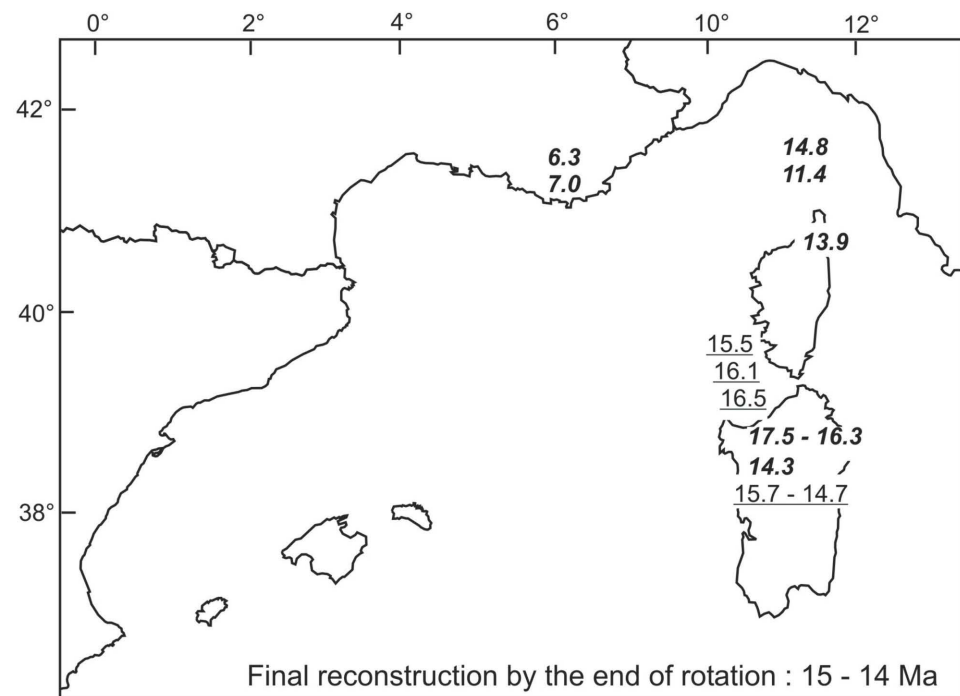
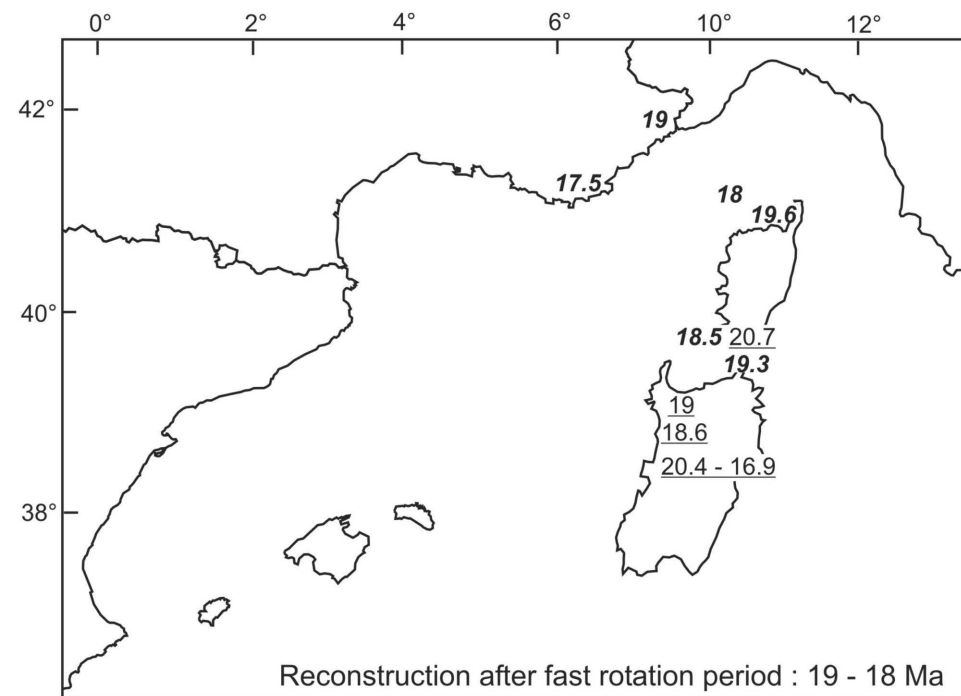
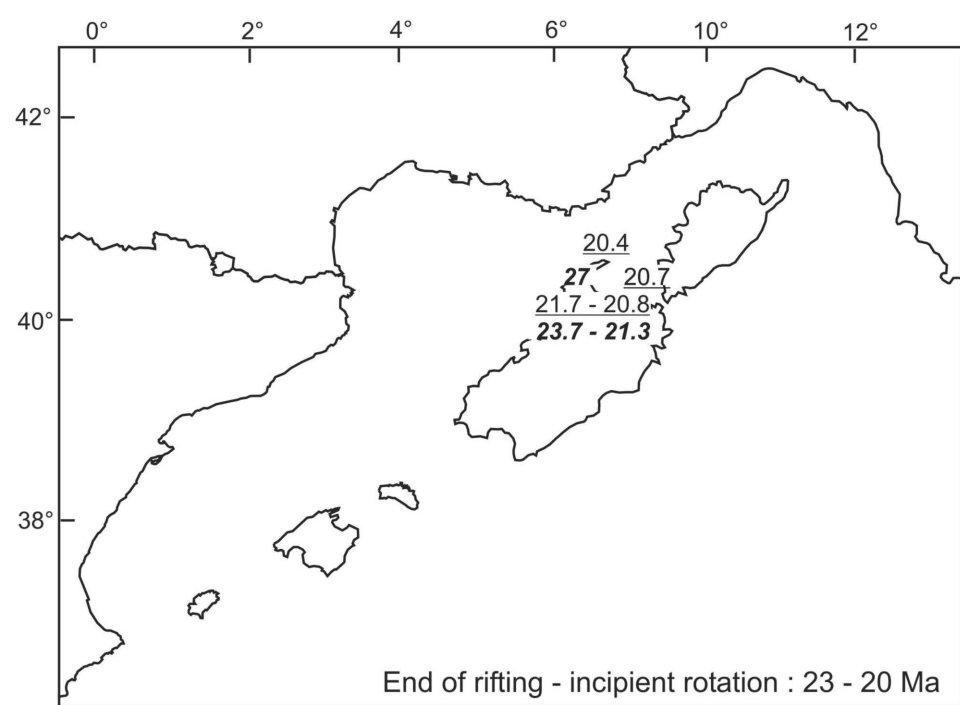
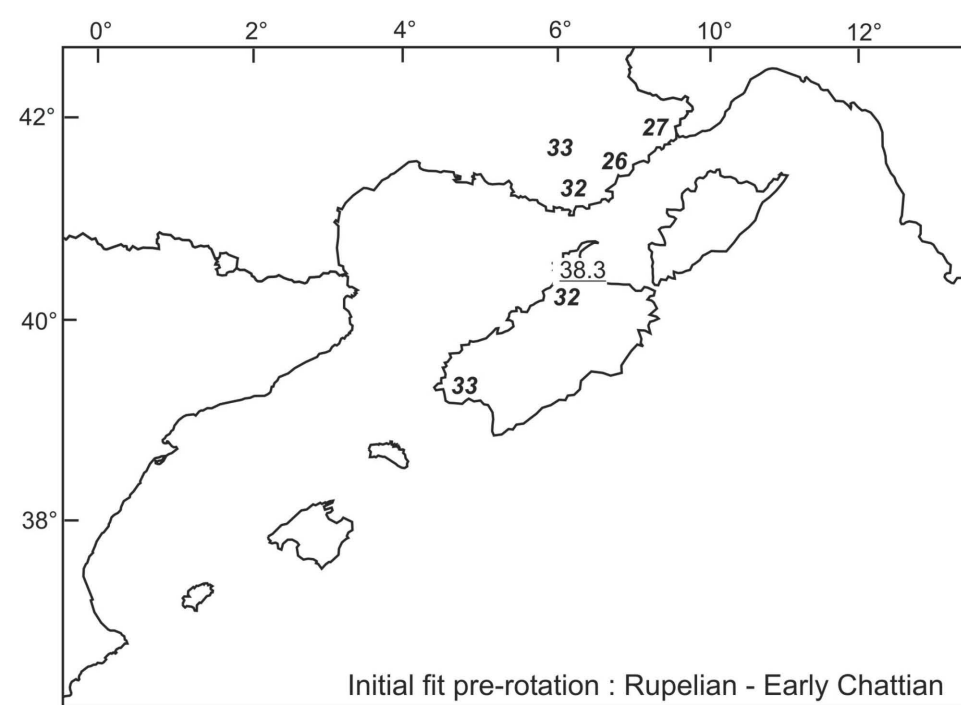
SW Corsica, Canyon des Moines and Propriano High



Doria seamounts complex,  
Genoa Gulf Central Volcano,  
and Toulonnais lavas







|                                  | Castelsardo | Monte Paoli |             |           | Canyon des Moines |                |           |           | Valinco   | Ajaccio High |            | Propriano High |           |           |
|----------------------------------|-------------|-------------|-------------|-----------|-------------------|----------------|-----------|-----------|-----------|--------------|------------|----------------|-----------|-----------|
|                                  | Site 1      | Site 2      |             | Site 3    | Site 3            | Site 3         | Site 3    | Site 3    | Site 4    | Site 5       | Site 5     | Site 6         | Site 6    | Site 6    |
|                                  | MA 74 DR 05 | Cya DR 02a  | Cya DR 02a2 | Cyl 07-07 | Cyl 07-03         | Cyalig 77 35 3 | Cyl 07-11 | Cyl 07-10 | Cyl 03-01 | Marco        | Marco      | Marco          | Cyl 02-01 | Cyl 02-02 |
|                                  |             |             |             |           |                   |                | (a)       |           |           | DR 06 08     | DR 06 08 b | DR 02a         |           |           |
| (wt. %)                          |             |             |             |           |                   |                |           |           |           |              |            |                |           |           |
| SiO <sub>2</sub>                 | 47.00       | 47.00       | 47.30       | 47.00     | 47.50             | 49.00          | 49.50     | 50.00     | 49.00     | 38.50        | 41.00      | 41.00          | 51.80     | 62.40     |
| TiO <sub>2</sub>                 | 1.03        | 1.06        | 1.05        | 1.14      | 1.24              | 0.92           | 1.27      | 1.28      | 1.09      | 0.90         | 0.94       | 0.49           | 0.53      | 0.45      |
| Al <sub>2</sub> O <sub>3</sub>   | 18.55       | 18.00       | 18.40       | 19.8      | 22.00             | 24.85          | 18.60     | 18.60     | 22.10     | 18.10        | 18.20      | 18.45          | 20.20     | 18.10     |
| Fe <sub>2</sub> O <sub>3</sub> * | 11.55       | 12.75       | 11.15       | 8.6       | 7.90              | 4.50           | 10.33     | 9.74      | 6.77      | 8.9          | 3.73       | 3.85           | 4.25      | 2.75      |
| MnO                              | 0.06        | 0.31        | 0.11        | 0.07      | 0.12              | 0.18           | 0.11      | 0.13      | 0.05      | 0.17         | 0.05       | 0.05           | 0.13      | 0.05      |
| MgO                              | 2.65        | 5.30        | 5.08        | 5.42      | 1.54              | 0.79           | 2.98      | 2.96      | 1.20      | 9.35         | 9.90       | 8.68           | 3.75      | 1.75      |
| CaO                              | 9.35        | 3.30        | 3.00        | 7.25      | 9.45              | 12.35          | 8.40      | 8.40      | 8.35      | 9.30         | 3.70       | 4.50           | 5.73      | 4.20      |
| Na <sub>2</sub> O                | 2.79        | 2.15        | 2.50        | 3.10      | 3.20              | 3.13           | 3.20      | 3.25      | 2.95      | 1.95         | 3.40       | 3.36           | 4.46      | 3.70      |
| K <sub>2</sub> O                 | 1.92        | 3.17        | 3.08        | 0.77      | 0.85              | 1.26           | 2.70      | 2.74      | 1.90      | 0.45         | 0.55       | 4.05           | 2.67      | 4.15      |
| P <sub>2</sub> O <sub>5</sub>    | 0.57        | 0.18        | 0.28        | 0.2       | 0.26              | 0.23           | 0.35      | 0.36      | 0.26      | 0.26         | 0.22       | 0.20           | 0.19      | 0.15      |
| LOI                              | 4.7         | 5.64        | 7.2         | 6.06      | 6.04              | 2.97           | 2.29      | 2.23      | 6.01      | 11.85        | 9.89       | 14.54          | 5.96      | 1.36      |
| Total                            | 100.17      | 98.86       | 99.15       | 99.41     | 100.10            | 100.18         | 99.73     | 99.69     | 99.68     | 99.23        | 99.42      | 99.17          | 99.67     | 99.06     |
|                                  |             |             |             |           |                   |                |           |           |           | Marco        | Marco      | Marco          |           |           |
|                                  | MA 74 DR 05 | Cya DR 02a  | Cya DR 02a2 | Cyl 07-07 | Cyl 07-03         | Cyalig 77 35 3 | Cyl 07-11 | Cyl 07-10 | Cyl 03-01 | DR 06 08     | DR 06 08 b | DR02a          | Cyl 02-01 | Cyl 02-02 |
| (ppm)                            |             |             |             |           |                   |                |           |           |           |              |            |                |           |           |
| Rb                               | 26.5        | 84          | 73.5        | 7.3       | 21.5              | 23.5           | 70        | 73        | 26        | 5.5          | 6          | 80             | 49        | 164       |
| Ba                               | 289         | 835         | 285         | 150       | 180               | 319            | 430       | 450       | 284       | 99           | 107        | 515            | 680       | 580       |
| Th                               | 3.9         | 2.9         | 3.0         | 0.9       | 0.9               | 1.4            | 7.2       | 6.6       | 4.5       | 1.8          | 1.6        | 17.5           | 20.8      | 19.7      |
| Nb                               | 7.9         | 4.9         | 4.2         | 5         | 7.1               | 5              | 8.7       | 9         | 6.7       | 6.3          | 6.6        | 11             | 11.4      | 11.7      |
| La                               | 20.4        | 8.7         | 11.6        | 13.1      | 14.5              | 14             | 24.8      | 25        | 17.4      | 15           | 13.7       | 37.5           | 34        | 34        |
| Ce                               | 40.5        | 17          | 20.5        | 28        | 32                | 27             | 52        | 52        | 37        | 31           | 30         | 66             | 70        | 60        |
| Sr                               | 497         | 206         | 212         | 280       | 358               | 365            | 430       | 428       | 343       | 358          | 354        | 596            | 945       | 795       |
| Nd                               | 22          | 10.5        | 12          | 16        | 19                | 14.5           | 25        | 25        | 19        | 16.5         | 15.5       | 28             | 28.5      | 25        |
| Zr                               | 90          | 65          | 66          | 100       | 135               | 87             | 150       | 155       | 132       | 97           | 98         | 70             | 107       | 90        |
| Eu                               | 1.38        | 0.72        | 1.07        | 1.39      | 1.51              | 1.36           | 1.51      | 1.47      | 1.23      | 1.20         | 1.19       | 1.21           | 1.35      | 1.13      |
| Dy                               | 4.45        | 2.6         | 3.55        | 5.1       | 4.6               | 4.85           | 4.6       | 4.65      | 5.2       | 4.15         | 4.0        | 2.35           | 2.6       | 1.9       |
| Y                                | 30          | 15          | 24          | 31.5      | 27                | 31             | 26.8      | 27.5      | 30        | 24.5         | 22.7       | 14.2           | 13.8      | 11        |
| Er                               | 2.5         | 1.5         | 2           | 3         | 2.7               | 2.9            | 2.6       | 2.6       | 2.9       | 2.3          | 2.2        | 1.2            | 1.3       | 1         |
| Yb                               | 2.45        | 1.43        | 1.88        | 2.75      | 2.75              | 3.06           | 2.43      | 2.40      | 2.70      | 2.43         | 2.32       | 1.17           | 1.1       | 0.93      |
| Cr                               | 40          | 26          | 44          | 5         | 11                | 5              | 39        | 37        | 7         | 14           | 15         | 13             | 13        | 11        |
| Ni                               | 16          | 26          | 92          | 7         | 7                 | 4              | 23        | 23        | 12        | 32           | 16         | 36             | 34        | 16        |
| Co                               | 14.5        | 26          | 33          | 22        | 13                | 6              | 24        | 29        | 13        | 30           | 21         | 11             | 15        | 6         |
| Sc                               | 23.5        | 24          | 26          | 32        | 34                | 25             | 24        | 26        | 22        | 24           | 25         | 8.3            | 9.3       | 6         |
| V                                | 252         | 275         | 270         | 275       | 305               | 170            | 260       | 270       | 240       | 165          | 174        | 76             | 80        | 58        |

Analyses - for major elements: in Brest, UBO, except for (a) - Orléans, BRGM; and (b) - Clermont-Ferrand, University; and for trace elements: Brest, UBO.



|                                  | Tristanite Ridge |             |             |           | Doria    | Seamounts |           | Genoa Gulf | Cap Corse | Onshore magmatism |          |           |             |         |
|----------------------------------|------------------|-------------|-------------|-----------|----------|-----------|-----------|------------|-----------|-------------------|----------|-----------|-------------|---------|
|                                  | Site 7           | Site 7      | Site 7      | Site 7    | SW flank |           | Centre    | Volcano    |           | Drammont          |          | Tourettes | Villa Maure | Toulon  |
|                                  | Site 7           | Site 7      | Site 7      | Site 7    | Site 9   | Site 9    | Site 10   | Site 11    | Site 12   | Ref               | Ref      | Ref       | Ref         | Ref     |
|                                  | Cyl 20-01        | G IV DR 11a | MA 74 DR 01 | Cyl 20-02 | GIV DR04 | Cyl 22-05 | Marco     | Marco      | Cyl 15-10 | 77S4F             | Est 96-2 | PL1       | Pl 41       | FR 76-9 |
|                                  |                  |             | core (b)    |           |          |           | DR 52-06a | DR 49-03   |           |                   |          |           |             |         |
| (wt. %)                          |                  |             |             |           |          |           |           |            |           |                   |          |           |             |         |
| SiO <sub>2</sub>                 | 46.00            | 53.00       | 56.04       | 63.00     | 42.50    | 47.00     | 41.20     | 32.25      | 44.00     | 61.60             | 63.00    | 52.90     | 53.85       | 48.60   |
| TiO <sub>2</sub>                 | 0.67             | 0.64        | 0.14        | 0.10      | 1.40     | 1.03      | 1.32      | 0.87       | 1.34      | 0.39              | 0.43     | 0.88      | 0.85        | 2.82    |
| Al <sub>2</sub> O <sub>3</sub>   | 17.20            | 17.72       | 19.32       | 16.90     | 13.30    | 18.55     | 14.80     | 12.80      | 16.00     | 18.20             | 18.00    | 18.10     | 16.43       | 11.5    |
| Fe <sub>2</sub> O <sub>3</sub> * | 4.00             | 4.61        | 5.12        | 1.12      | 14.70    | 11.55     | 6.62      | 6.13       | 11.00     | 4.45              | 4.25     | 9.32      | 9.55        | 14.55   |
| MnO                              | 0.08             | 0.06        | 0.01        | 0.01      | 0.30     | 0.06      | 0.10      | 0.21       | 0.09      | 0.10              | 0.19     | 0.17      | 0.17        | 0.19    |
| MgO                              | 8.00             | 3.90        | 1.65        | 1.64      | 4.76     | 2.65      | 9.24      | 2.38       | 3.76      | 1.70              | 1.69     | 3.8       | 4.55        | 9.55    |
| CaO                              | 3.45             | 3.30        | 0.97        | 1.22      | 8.50     | 9.35      | 11.3      | 20.50      | 10.81     | 4.10              | 5.01     | 9.00      | 9.3         | 8       |
| Na <sub>2</sub> O                | 3.70             | 3.63        | 4.76        | 4.45      | 2.81     | 22.79     | 2.68      | 3.17       | 3.54      | 4.45              | 4.75     | 3.30      | 3.05        | 2.72    |
| K <sub>2</sub> O                 | 5.00             | 6.58        | 7.17        | 7.55      | 2.31     | 1.92      | 1.64      | 1.76       | 1.18      | 1.71              | 1.21     | 1.20      | 1.45        | 0.76    |
| P <sub>2</sub> O <sub>5</sub>    | 0.37             | 0.30        | nd          | 0.01      | 0.70     | 0.57      | 0.47      | 0.59       | 0.67      | 0.17              | 0.19     | 0.22      | 0.25        | 0.3     |
| LOI                              | 10.62            | 5.57        | 4.72        | 2.81      | 5.25     | 4.70      | 10.05     | 19.11      | 7.42      | 2.95              | 1.49     | 1.20      | 0.96        | 0.09    |
| Total                            | 99.09            | 99.39       | 99.90       | 99.41     | 96.53    | 100.17    | 99.445    | 99.77      | 99.81     | 99.82             | 100.2    | 100.09    | 100.41      | 99.08   |
|                                  | Cyl 20-01        | G IV DR 11a | MA 74 DR01  | Cyl 20-02 | GIV DR04 | Cyl 22-05 | Marco     | Marco      | Cyl 15-10 | 77S4F             | Est 96-2 | PL1       | PL 41       | FR 76-9 |
|                                  |                  |             | rim         |           |          |           | DR 52-06a | DR 49-03   |           |                   |          |           |             |         |
| (ppm)                            |                  |             |             |           |          |           |           |            |           |                   |          |           |             |         |
| Rb                               | 118              | 2230        | 200         | 170       | 230      | 26.5      | 34        | 19         | 10        | 53                | 37       | 29        | 45.5        | 20.5    |
| Ba                               | 1020             | 1120        | 86          | 110       | 1120     | 289       | 750       | 363        | 265       | 630               | 472      | 342       | 325         | 246     |
| Th                               | 62               | 3.9         | 55          | 62        | nd       | 3.9       | 17        | 7          | 4.8       | 2.4               | 2.35     | 1.7       | 5.9         | 2.45    |
| Nb                               | 21               | 21.5        | 45          | 49        | 21.5     | 7.9       | 18        | 9.8        | 13.2      | 12                | 14       | 5         | 5           | 34      |
| La                               | 98               | 35          | 33          | 49.5      | 35       | 20.4      | 39        | 27.5       | 16        | 15                | 16.2     | 12.8      | 19.9        | 16      |
| Ce                               | 180              | 85          | 55          | 67        | 85       | 40.5      | 73        | 50         | 31.3      | 26                | 30       | 28        | 39.5        | 32      |
| Sr                               | 525              | 186         | 100         | 82        | 186      | 497       | 605       | 530        | 385       | 335               | 350      | 342       | 615         | 400     |
| Nd                               | 65               | 39          | 25.5        | 31.5      | 39       | 22        | 32.5      | 24.5       | 16.4      | 11.4              | 13       | 15.5      | 21          | 20      |
| Zr                               | 220              | 130         | 90          | 123       | 130      | 90        | 130       | 106        | 111       | 39                | 54       | 107       | 82          | 166     |
| Eu                               | 2.00             | 0.96        | 0.57        | 0.69      | 0.96     | 1.38      | 1.64      | 1.2        | 1.28      | 0.69              | 0.76     | 1.12      | 1.18        | 1.68    |
| Dy                               | 3.85             | 5.85        | 3.7         | 4.5       | 5.85     | 4.45      | 3.75      | 2.85       | 3.6       | 1.35              | 1.4      | 3.6       | 3.45        | 4.15    |
| Y                                | 22               | 32          | 25          | 32        | 32       | 30        | 21.5      | 16         | 21        | 7.8               | 8.2      | 21.5      | 21          | 22      |
| Er                               | 1.95             | 3.10        | 2.30        | 2.80      | 3.10     | 2.50      | 1.85      | 1.40       | 1.00      | 0.65              | 0.75     | 2.20      | 1.95        | 2.1     |
| Yb                               | 1.96             | 2.45        | 2.36        | 3.10      | 2.45     | 2.45      | 1.82      | 1.35       | 1.83      | 0.57              | 0.51     | 2.20      | 1.94        | 1.53    |
| Cr                               | 54               | 91          | 2           | 10        | 172      | 40        | 125       | 72         | 203       | 4                 | 5        | 12        | 40          | 375     |
| Ni                               | 50               | 77          | 183         | 25        | 172      | 16        | 81        | 45         | 121       | 6                 | 2        | 8         | 14          | 220     |
| Co                               | 14               | 18          | 3           | 6         | 50       | 14.5      | 35        | 23         | 36.5      | 8                 | 7        | 22        | 23          | 53      |
| Sc                               | 12               | 10.8        | 1.2         | 0.7       | 22.5     | 23.5      | 23        | 14.2       | 23.5      | 4.0               | 4.2      | 27.0      | 34          | 21      |

|   |    |    |   |   |     |     |     |    |     |    |    |     |     |     |
|---|----|----|---|---|-----|-----|-----|----|-----|----|----|-----|-----|-----|
| V | 86 | 56 | 5 | 3 | 230 | 252 | 195 | 96 | 206 | 60 | 80 | 260 | 320 | 210 |
|---|----|----|---|---|-----|-----|-----|----|-----|----|----|-----|-----|-----|



|   | Temp. °C<br>/ Step n° | <sup>40</sup> Ar <sub>Atm.</sub><br>(%) | <sup>39</sup> Ar <sub>K</sub><br>(%) | <sup>39</sup> Ar <sub>Ca</sub> / <sup>39</sup> Ar <sub>K</sub> | <sup>40</sup> Ar */ <sup>39</sup> Ar <sub>K</sub> | Age<br>(Ma) | ± | error |
|---|-----------------------|---|--------------------------------------|--|---|-------------|---|-------|
| <b>Site 1 Plagioclase Cyl 03-01 Bulk sample J=0,0604228</b>   |                       |   |                                      |  |   |             |   |       |
| Castelsardo<br>Canyon   | 400                   | 100                                     | 0                                    | 7.4  | -   | -           | ± | -     |
|   | 500                   | 100                                     | 0.02                                 | 7.4  | -   | -           | ± | -     |
|   | 600                   | 80.8                                    | 0.04                                 | 2x10 <sup>-3</sup>   | 23.04   | 47.81       | ± | 4.68  |
|   | 700                   | 65.1                                    | 2.29                                 | 4.2  | 7.69  | 16.11       | ± | 0.74  |
|   | 800                   | 32.4                                    | 2.48                                 | 7.1  | 7.42  | 15.54       | ± | 0.21  |
|   | 900                   | 23.2                                    | 3.73                                 | 10.5   | 8.86  | 18.53       | ± | 0.17  |
|   | 1000                  | 18.2                                    | 8.71                                 | 12.3   | 9.19  | 19.22       | ± | 0.13  |
|   | 1100                  | 9.4                                     | 12.31                                | 13.6   | 9.54  | 19.95       | ± | 0.1   |
|   | 1200                  | 6.14                                    | 16.37                                | 13.9   | 9.81  | 20.51       | ± | 0.09  |
|   | 1300                  | 7.86                                    | 30.69                                | 13.9   | 9.89  | 20.68       | ± | 0.09  |
|   | 1400                  | 13.7                                    | 8.99                                 | 13.4   | 9.94  | 20.79       | ± | 0.14  |
|   | 1500                  | 19.7                                    | 14.36                                | 13.4   | 9.95  | 20.8        | ± | 0.12  |
|   |                       |   |                                      |  | Integrated age                                    | 20.15       | ± | 0.05  |
| <b>Site 3 Plagioclase Cyl 07-03 Bulk sample J = 0.0603868</b> |                       |   |                                      |  |   |             |   |       |
| Canyon<br>des Moines  | 400                   | 100                                     | 0                                    | 3x10 <sup>-2</sup>   | -   | -           | ± | -     |
|   | 500                   | 99.3                                    | 1.18                                 | 9.6  | 0.99  | 2.08        | ± | 4.5   |
|   | 600                   | 88.1                                    | 11.14                                | 25.3   | 11.29   | 23.57       | ± | 1.22  |
|   | 700                   | 64.1                                    | 16.28                                | 106.2  | 8.31  | 17.38       | ± | 0.65  |
|   | 800                   | 51.1                                    | 20.96                                | 165.9  | 9.45  | 19.75       | ± | 0.92  |
|   | 900                   | 52.5                                    | 14.53                                | 166.5  | 9.94  | 20.77       | ± | 1     |
|   | 1000                  | 61.5                                    | 10.6                                 | 152.7  | 10.27   | 21.45       | ± | 0.98  |
|   | 1100                  | 78.2                                    | 3.59                                 | 105.9  | 8.97  | 18.76       | ± | 1.04  |
|   | 1200                  | 83.7                                    | 5.03                                 | 88.8   | 9.93  | 20.75       | ± | 1.22  |
|   | 1400                  | 80.2                                    | 12.78                                | 120.2  | 10.23   | 21.37       | ± | 1.15  |
|   | 1550                  | 78.4                                    | 3.91                                 | 145.6  | 12.73   | 26.56       | ± | 1.65  |
|   |                       |   |                                      |  | Integrated age                                    | 20.4        | ± | 0.37  |
| <b>Site 6 Cyl 02-01 Biotite Single grain J=0,0602389</b>      |                       |   |                                      |  |   |             |   |       |
| Propriano<br>High   | 1                     | 91.3                                    | 0                                    | 127  | -   | -           | ± | -     |
|   | 2                     | 99.1                                    | 0.08                                 | -  | 1.24  | 2.61        | ± | 28.46 |
|   | 3                     | 74                                      | 0.33                                 | -  | 5.65  | 11.81       | ± | 9.06  |
|   | 4                     | 29.9                                    | 3.04                                 | -  | 7.67  | 16.01       | ± | 0.54  |
|   | 5                     | 17.3                                    | 5.73                                 | -  | 7.57  | 15.81       | ± | 0.27  |
|   | 6                     | 11                                      | 13.49                                | -  | 7.61  | 15.88       | ± | 0.14  |
|   | 7                     | 6.9                                     | 12.11                                | 1x10 <sup>-3</sup>   | 7.59  | 15.85       | ± | 0.16  |
|   | 8                     | 5.2                                     | 36.63                                | 1.1x10 <sup>-2</sup>   | 7.62  | 15.91       | ± | 0.07  |
|   | 9                     | 7.3                                     | 11.05                                | 3.4x10 <sup>-2</sup>   | 7.43  | 15.5        | ± | 0.3   |
|   | 10                    | 8.5                                     | 9.43                                 | 8.9x10 <sup>-2</sup>   | 7.34  | 15.33       | ± | 0.38  |
|   | Fuse                  | 3.5                                     | 8.13                                 | 8.3x10 <sup>-2</sup>   | 7.65  | 15.97       | ± | 0.45  |
|   |                       |   |                                      |  | Integrated age                                    | 15.8        | ± | 0.09  |
| <b>Cyl 02-01 Amphibole Single grain J = 0.0603150</b>         |                       |   |                                      |  |   |             |   |       |
|   | 1                     | 98.9                                    | 0.16                                 | 7.4x10 <sup>-1</sup>   | 3.44  | 7.2         | ± | 74.09 |
|   | 2                     | 164.3                                   | 0.24                                 | 6.2x10 <sup>-1</sup>   | -   | -           | ± | -     |
|   | 3                     | 76                                      | 0.13                                 | 8.9x10 <sup>-1</sup>   | 1.74  | 3.66        | ± | 70.99 |
|   | 4                     | 193.5                                   | 0.38                                 | 7.6  | -   | -           | ± | -     |
|   | 5                     | 6.4                                     | 70.28                                | 7.2  | 7.46  | 15.59       | ± | 0.31  |
|   | 6                     | 0                                       | 23.02                                | 7  | 7.85  | 16.41       | ± | 0.31  |
|   | 7                     | 16.9                                    | 0.52                                 | 16.1   | 9.03  | 18.86       | ± | 12.41 |
|   | 8                     | 37.2                                    | 0.33                                 | 20.4   | 8.19  | 17.11       | ± | 18.16 |
|   | Fuse                  | 17.3                                    | 4.94                                 | 15.7   | 7.17  | 14.99       | ± | 1.49  |
|   |                       |   |                                      |  | Integrated age                                    | 15.51       | ± | 0.31  |
| <b>Cyl 02-01 Amphibole Single grain J = 0.0603150</b>         |                       |   |                                      |  |   |             |   |       |
|   | 1                     | 86.9                                    | 0.46                                 | 1x10 <sup>-3</sup>   | 14.14   | 29.44       | ± | 9.04  |
|   | 2                     | 21.4                                    | 3.18                                 | -  | 7.28  | 15.23       | ± | 1.58  |
|   | 3                     | 20.4                                    | 18.14                                | 4.7  | 7.55  | 15.79       | ± | 0.3   |
|   | 4                     | 14.2                                    | 19.39                                | 5.8  | 7.42  | 15.52       | ± | 0.25  |
|   | 5                     | 7.3                                     | 34.45                                | 5.9  | 7.43  | 15.54       | ± | 0.13  |
|   | Fuse                  | 6.2                                     | 24.38                                | 4.8  | 7.43  | 15.52       | ± | 0.22  |
|   |                       |   |                                      |  | Integrated age                                    | 15.63       | ± | 0.12  |

|            |                            | Depth<br>of sampling | Sample          | Analysed<br>fraction | Analytical<br>reference | Age<br>Ma | ±<br>at ±1 σ | error<br>wt.% | K <sub>2</sub> O | <sup>40</sup> Ar <sub>R</sub><br>% | <sup>40</sup> Ar <sub>R</sub><br>10 <sup>-7</sup> cm <sup>3</sup> /g | <sup>36</sup> Ar<br>10 <sup>-9</sup> cm <sup>3</sup> /g | Mass<br>fused (g) |
|------------|----------------------------|----------------------|-----------------|----------------------|-------------------------|-----------|--------------|---------------|------------------|------------------------------------|--|---|-------------------|
| SW CORSICA |                            |                      |                 |                      |                         |           |              |               |                  |                                    |  |   |                   |
| Site 1     | Castelsardo Canyon         | -1785 m              | MA 74DR 05      | WR                   | B 4184                  | 14.00     | ±            | 0.40          | 1.91             | 41.2                               | 8.68   | 4.20  | 0.5049            |
|            |                            |                      |                 | WR                   | B 7144                  | 13.70     | ±            | 0.56          | 2.00             | 24.3                               | 8.89   | 2.56  | 0.2732            |
| Site 2     | Monte Paoli                | -1980 m              | Cya 77DR02-a2   | WR                   | B 4487                  | 15.90     | ±            | 0.40          | 3.07             | 48                                 | 15.82  | 5.80  | 0.7056            |
|            |                            |                      | Cya 77DR02-a    | WR                   | B 4486                  | 18.00     | ±            | 0.50          | 3.28             | 36.4                               | 19.13  | 0.11  | 0.7060            |
|            |                            |                      | "               | B 4492               | 18.50                   | ±         | 0.50         | "             | 39.6             | 19.68                              | 0.10   | 0.7065  |                   |
| Site 3     | Canyon des Moines          | -1137 m              | Cyl 07-07       | WR                   | B 5029                  | 10.98     | ±            | 0.80          | 0.79             | 14.6                               | 2.80   | 5.54  | 0.5070            |
|            |                            |                      |                 | "                    | B 5024                  | 12.38     | ±            | 1.10          | "                | 13                                 | 3.16   | 7.17  | 0.4033            |
|            |                            | - 983 m              | Cyl 07-10       | WR                   | B 5023                  | 19.35     | ±            | 0.46          | 2.58             | 91.5                               | 16.18  | 0.51  | 0.6535            |
|            |                            |                      |                 | "                    | B 5030                  | 19.07     | ±            | 0.44          | "                | 92.8                               | 15.95  | 0.42  | 0.6510            |
|            |                            | - 980 m              | Cyl 07-11       | WR                   | B 5022                  | 19.16     | ±            | 0.45          | 2.39             | 90.3                               | 14.84  | 0.54  | 0.6506            |
| Site 5     | Ajaccio high               | -1700 m              | Marco DR06-08   | WR                   | B 7143                  | 12.83     | ±            | 1.83          | 0.47             | 6.7                                | 1.95   | 2.61  | 0.2852            |
| Site 6     | Propriano high             | -2681 m              | Cyl 02-02       | WR                   | B 5021                  | 14.52     | ±            | 0.34          | 4.33             | 89.3                               | 20.34  | 0.83  | 0.6021            |
|            |                            |                      |                 |                      | B 5025                  | 14.68     | ±            | 0.34          | "                | 89.1                               | 20.58  | 0.85  | 0.6640            |
|            |                            |                      | -2250 m         | Marco DR02           | WR                      | B 4183    | 11.90        | ±             | 0.30             | 3.89                               | 75.2   | 14.96   | 1.67              |
| NW CORSICA |                            |                      |                 |                      |                         |           |              |               |                  |                                    |  |   |                   |
| Site 7a    | Tristanite Ridge           | -2470 m              | MA 74DR 01 rim  | WR                   | B 4124                  | 15.70     | ±            | 0.40          | 4.59             | 53.9                               | 23.33  | 6.74  | 0.3535            |
| Site 7b    | Tristanite Ridge           | -2531 m              | Cyl 20-01       | WR                   | B 4599                  | 12.80     | ±            | 0.30          | 5.14             | 77.9                               | 21.40  | 2.05  | 0.7013            |
|            |                            | -2440 m              | Cyl 20-02       | WR                   | B 4598                  | 12.40     | ±            | 0.30          | 8.40             | 81.6                               | 33.72  | 2.57  | 0.6021            |
| Site 7c    | Tristanite Ridge           | -2280 m              | GIV DR 11a      | WR                   | B 5286                  | 42.77     | ±            | 2.30          | 6.20             | 84.6                               | 86.53  | 3.22  | 0.6038            |
|            |                            |                      |                 | "                    | B 7134                  | 43.26     | ±            | 2.34          | "                | 76.9                               | 87.52  | 1.81  | 0.2036            |
| Site 9     | Monte Doria, SW flank      | -1574 m              | Cyl 22-05       | WR                   | B 7290                  | 8.57      | ±            | 0.31          | 2.74             | 28.6                               | 7.58   | 3.20  | 0.2604            |
| Site 10    | Monte Doria, centre        | - 904 m              | Marco DR52-06 a | WR                   | B 7145                  | 7.35      | ±            | 0.32          | 1.79             | 22.5                               | 4.25   | 1.29  | 0.2604            |
|            |                            |                      | Marco DR52-06 b | WR                   | B4240                   | 8.37      | ±            | 0.33          | 1.63             | 43.7                               | 4.41   | 1.35  | 0.7020            |
| Site 11    | Genoa Gulf Central Volcano | - 470 m              | Marco DR49-03   | WR                   | B 7138                  | 14.83     | ±            | 1.40          | 1.18             | 24.2                               | 5.66   | 1.13  | 0.1886            |
| Site 12    | Cap Corse                  | -1290 m              | Cyl 15-10       | WR                   | B 7142                  | 19.59     | ±            | 1.32          | 1.57             | 14.0                               | 9.97   | 5.39  | 0.2601            |

|            |                    | Depth<br>of sampling |        | Sample         | Petrographical and<br>geochemical type | Dated fraction<br>method / technics                                     | Age<br>Ma      | ±     | error<br>1 sigma | K <sub>2</sub> O<br>wt. %<br>(AAS) | Geochemical analyses    |            |             |                         |
|------------|--------------------|----------------------|--------|----------------|--|---|----------------|-------|------------------|------------------------------------|-------------------------|------------|-------------|-------------------------|
|            |                    |                      |        |                |  |   |                |       |                  |                                    | Analytical<br>reference | LOI<br>wt% | SiO2<br>wt% | K <sub>2</sub> O<br>wt% |
| SW CORSICA |                    |                      |        |                |  |   |                |       |                  |                                    |                         |            |             |                         |
| Site 1     | Castelsardo Canyon | -                    | 1785 m | MA 74 DR 05a   | Basaltic flow                          | WR K-Ar age   | 14.0           | ±     | 0.40             | 1.91                               | JC 12571                | 4.70       | 47.0        | 1.92                    |
|            |                    |                      |        | MA 74 DR 05b   |  |   | 13.7           | ±     | 0.90             | 2.00                               |                         |            |             |                         |
| Site 2     | Monte Paoli        | -                    | 1859 m | Cyl 01-03      | Basaltic flow                          |   |                |       |                  |                                    |                         |            |             |                         |
|            |                    | -                    | 1980 m | Cya 77 DR02-a2 | HK basaltic andesite                   | WR K-Ar age   | <u>15.90</u>   | ±     | <u>0.40</u>      | 3.07                               | AC 13996                | 7.20       | 47.3        | 3.08                    |
|            |                    | -                    | 1980 m | Cya 77 DR02-a  |  |   | WR K-Ar age    | 18.25 | ±                | 0.50                               | 3.28                    | AC 13995   | 5.64        | 47.0                    |
| Site 3     | Canyon des Moines  | -                    | 983 m  | Cyl 07-10      | Doleritic diabase                      | WR K-Ar age   | 19.21          | ±     | 0.46             | 2.58                               | AC 14657                | 2.23       | 50.0        | 2.74                    |
|            |                    | -                    | 980 m  | Cyl 07-11      | Doleritic diabase                      | WR K-Ar age   | 19.36          | ±     | 0.45             | 2.39                               | AC 14657                | 2.29       | 49.5        | 2.70                    |
|            |                    | -                    | 1104 m | Cyl 07-03      | Porphyritic basalt                     | Plag. <sup>40</sup> Ar- <sup>39</sup> Ar plateau age                    | 20.68          | ±     | 0.05             |                                    | AC 14655                | 6.04       | 47.5        | 0.85                    |
|            |                    | -                    | 1137 m | Cyl 07-07      | Porphyritic basalt                     | WR K-Ar age   | 11.70          | ±     | 1.10             | 0.79                               | AC 14656                | 6.06       | 47.0        | 0.77                    |
|            |                    | -                    | 1177 m | Cyl 07-01      |  |   |                |       |                  |                                    |                         |            |             |                         |
|            |                    | -                    | 1682 m | Cya 77-35 03   | Jointed basaltic flow                  | Plag. <sup>40</sup> Ar- <sup>39</sup> Ar plateau age<br>WR K-Ar age (a) | 16.50<br>18.50 | ±     | 0.50<br>1.00     | 1.25                               |                         |            |             |                         |
| Site 4     | Valinco Canyon     | -                    | 2383 m | Cyl 03-01      | Basaltic andesite                      | Plag. <sup>40</sup> Ar- <sup>39</sup> Ar plateau age<br>(seeTable 3)    | 20.6           | ±     | 0.50             |                                    | AC 14654                | 6.01       | 49.0        | 1.90                    |
| Site 5     | Ajaccio High       | -                    | 1700 m | Marco DR06-08  | Basalt                                 | WR K-Ar age   | <u>12.83</u>   | ±     | <u>1.83</u>      | 0.46                               | AC 12572                | 11.85      | 38.0        | 0.45                    |
| Site 6     | Propriano High     | -                    | 1020 m | Cyl 06-08      | Andesite                               |   |                |       |                  |                                    |                         |            |             |                         |
|            |                    | -                    | 2000 m | Marco DR02-1a  | K-rich basaltic andesite               | Plag. <sup>40</sup> Ar- <sup>39</sup> Ar plateau age                    | 16.10          | ±     | 0.40             |                                    |                         |            |             |                         |
|            |                    | -                    | 2250 m | Marco DR02     | K-rich basaltic andesite               | WR  | <u>11.90</u>   | ±     | <u>0.30</u>      | 3.89                               | AC 12569                | 14.54      | 41.0        | 4.05                    |
|            |                    | -                    | 2681 m | Cyl 02-02      | Andesite (adakite)                     | WR K-Ar age   | 14.60          | ±     | 0.34             | 4.33                               | AC 14653                | 1.36       | 62.4        | 4.15                    |
|            |                    | -                    | 2690 m | Cyl 02-01      | Basaltic andesite (adakitic)           | Biot. <sup>40</sup> Ar- <sup>39</sup> Ar plateau age                    | 15.80          | ±     | 0.08             |                                    | AC 14652                | 5.96       | 51.8        | 2.67                    |
|            |                    |                      |        |                |  | Amp. <sup>40</sup> Ar- <sup>39</sup> Ar plateau age<br>(seeTable 3)     | 15.51<br>15.63 | ±     | 0.31<br>0.12     |                                    |                         |            |             |                         |

#### Foot notes

Age results in normal characters correspond to lavas having a loss on ignition between 4 and 6 wt.%. They are to be considered with caution.

Underlined age results remain ambiguous as linked to a loss on ignition, upper than 6%. These ages have been possibly rejuvenated.

|   | Depth<br>of sampling | Sample           | Petrographical and<br>geochemical type | Dated fraction<br>method / technics | Age<br>Ma    | ±<br>1 sigma | error<br>wt. %<br>(AAS) | K <sub>2</sub> O<br>wt. %<br>(AAS) | Geochemical analyses<br>Analytical<br>reference | LOI<br>wt% | SiO <sub>2</sub><br>wt% | K <sub>2</sub> O<br>wt% |
|---|----------------------|------------------|--|-------------------------------------|--------------|--------------|-------------------------|------------------------------------|---|------------|-------------------------|-------------------------|
| NW CORSICA                                |                      |                  |  |                                     |              |              |                         |                                    |   |            |                         |                         |
| Site 7a Tristanite Ridge                  | - 2470 m             | MA 74 DR 01 rim  | White welded ignimbritic tuf           | WR K-Ar age                         | <u>15.70</u> | ±            | <u>0.40</u>             | 4.59                               | JC 12568  | 22.29      | 33.5                    | 5.18                    |
|   | - 2470 m             | MA 74 DR 01 core | " "                                    | WR K-Ar age                         | 18.00        | ±            | 0.50                    | 7.40                               | Cantagrel                                       | 4.72       | 56.04                   | 7.17                    |
| Site 7b Tristanite Ridge                  | - 2440 m             | Cyl 20-02        | White welded ignimbritic tuf           | WR K-Ar age                         | 12.40        | ±            | 0.30                    | 8.40                               | JC 13998  | 2.81       | 63.6                    | 7.55                    |
|   | - 2531 m             | Cyl 20-01        | Andesite                               | WR K-Ar age                         | <u>12.80</u> | ±            | <u>0.30</u>             | 5.14                               | JC 13997  | 10.62      | 46.0                    | 5.00                    |
| Site 7c Tristanite Ridge                  | - 2285 m             | Cyl 20-04        | Andesite, top of the massif            |                                     |              |              |                         |                                    |   |            |                         |                         |
|   | - 2280 m             | G IV DR 11a      | Pillowed andesite                      | WR K-Ar age                         | 43.00        | ±            | 2.34                    | 6.20                               | JC 12576  | 5.57       | 53.0                    | 6.58                    |
| Site 8 Monte Doria,<br>eastern flank      | - 1780 m             | MFCB             | Shoshonitic basalt flow (d)            | WR and biot. K-Ar age (d)           | 11.40        | ±            | 0.70                    | 3.3                                |   |            |                         |                         |
| Site 9 Monte Doria,<br>southwestern flank | - 780 m              | F 81             | Olivine basalt                         |                                     |              |              |                         |                                    |   |            |                         |                         |
|   | - 1438 m             | Cyl 22-07        | Porphyritic basalt                     |                                     |              |              |                         |                                    |   |            |                         |                         |
|   | - 1574 m             | Cyl 22-05        | Vesicular olivine basalt               | WR K-Ar age                         | 8.57         | ±            | 0.31                    | 2.74                               | CL 2010   | 5.40       | 44.00                   | 1.18                    |
|   | - 1588 m             | Cyl 22-04        | Vesicular olivine basalt               |                                     |              |              |                         |                                    |   |            |                         |                         |
|   | - 1627 m             | Cyl 22-03        | Porphyritic basalt                     |                                     |              |              |                         |                                    |   |            |                         |                         |
|   | - 2400 m             | Cyl 21-04        | Micro lithic basalt                    |                                     |              |              |                         |                                    |   |            |                         |                         |
|   | - 2450 m             | Cyl 21-02        | Vesicular olivine basalt               |                                     |              |              |                         |                                    |   |            |                         |                         |
|   | - 2490 m             | GIV DR 04        | Olivine basalt                         |                                     |              |              |                         |                                    | JC 12570  | 5.25       | 42.50                   | 2.31                    |
| Site 10 Monte Doria, centre               | - 904 m              | Marco DR52-06 b  | Vesicular basalt                       | WR K-Ar age                         | <u>7.30</u>  | ±            | <u>0.70</u>             | 1.79                               |   |            |                         |                         |
|   |                      | Marco DR52-06 a  | Basalt                                 | WR K-Ar age                         | <u>8.37</u>  | ±            | <u>0.33</u>             | 1.63                               | JC 12575  | 10.05      | 41.2                    | 1.64                    |
|   | - 1000 m             | Marco DR52-03    | Basalt                                 |                                     |              |              |                         |                                    |   |            |                         |                         |
| Site 11 Genoa Gulf,<br>Central Volcano    | - 470 m              | Marco DR49-03    | Olivine basalt                         | WR K-Ar age                         | <u>14.80</u> | ±            | <u>1.40</u>             | 1.18                               | JC 12574  | 19.11      | 32.25                   | 1.76                    |
| Site 12 Cap Corse                         | - 1290 m             | Cyl 15-10        | Micro lithic basalt                    | WR K-Ar age                         | 19.60        | ±            | 1.52                    | 1.57                               | CL 2010   | 7.42       | 44.00                   | 1.18                    |
|   | - 1330 m             | Cyl 15-08        |  |                                     |              |              |                         |                                    |   |            |                         |                         |
|   | - 1450 m             | Cyl 15-06a       |  |                                     |              |              |                         |                                    |   |            |                         |                         |
|   | - 1495 m             | Cyl 15-04a       |  |                                     |              |              |                         |                                    |   |            |                         |                         |

Ages from literature and references below

a- Bellon et al., 1984

b- Rossi et al., 1998

c- Cantagrel in Réhault, 1984

d- Fanucci et al., 1993

|         |                       | Sample         | WO              | EN              | FS            |                  |
|---------|-----------------------|----------------|-----------------|-----------------|---------------|------------------|
|         | SW CORSICA            |                |                 |                 |               |                  |
| Site 1  | Castelsardo Canyon    | MA74 DR 05     | 45.8 / 49.4     | 41.9 / 45.5     | 5.9 / 8.6     |                  |
| Site 3  | Canyon des Moines     | Cyl 07-10      | 41.8 / 46.2     | 41.4 / 50       | 6 / 14.6      |                  |
|         |                       | Cyl 07-11      | 41.1 / 44.9     | 41 / 42.6       | 12.4 / 14.9   |                  |
|         |                       | Cya 77-35      | 38.9 / 41.4     | 43.6            | 15.3 / 17.3   |                  |
| Site 4  | Valinco Canyon        | Cyl 03-01      | 42.5 / 43.2     | 36.7 / 38.2     | 18.6 / 20.7   |                  |
|         | NW CORSICA            |                |                 |                 |               |                  |
| Site 7  | Tristanite Ridge      | Cyl 20-01      | 47.2 / 45.5     | 41.1 / 32.8     | 11.7 / 11     |                  |
|         |                       | Cyl 20-02      | 46.1 / 48.6     | 47.2 / 51       | 3.0 / 5.8     |                  |
|         |                       | Cyl 20-04      | 46.9 C / 47.8 R | 46.8 C / 45.3 R | 6.2 C / 6.9 R | Macrophenocrysts |
| Site 9  | Monte Doria, SW flank | F 81           | 57.3            | 5               | 37.6          |                  |
|         |                       | Cyl 22-05      | 47.1 / 49.6     | 44.4 / 47.1     | 5.8 / 7.1     |                  |
|         |                       | Cyl 22-04      | 46.7            | 40.9            | 12.4          |                  |
|         |                       | Cyl 22-03      | 47.9 C / 48.9 R | 45.9 C / 46.8 R | 6.1 C / 4.2 R | Phenocrysts      |
|         |                       | "              | 48.2 / 48.8     | 43.7 / 44.8     | 6.4 / 8.1     | Microphenocrysts |
|         |                       | G IV DR 04     | 45.3 / 47.6     | 41.7 / 43.7     | 10.6 / 11     |                  |
| Site 10 | Monte Doria, centre   | Marco DR 52-03 | 46.6            | 47              | 6.4           | Phenocryst       |
|         |                       | "              | 44 / 51         | 45 / 48         | 3.8 / 6.4     | Microphenocrysts |
|         |                       | Marco DR 52-06 | 44.7 / 47.6     | 45.2 / 47.7     | 7.2 / 7.6     | Phenocrysts      |
|         |                       | "              | 47 / 47.7       | 46 / 46.8       | 6.1           | Macrophenocrysts |
|         |                       | Marco DR 52-07 | 42 / 45         | 43.8 / 46.4     | 10.4 / 13.1   |                  |
| Site 12 | Cap Corse             | Cyl 15-10      | 43.7 / 46.5     | 46.5 / 48.9     | 6.3 / 7.3     |                  |

#### Abbreviations

"C" core and "R" rim of macrophenocrysts and phenocrysts

WO - wollastonite, EN - enstatite, FS - ferrosilite

## Feldspars

### Site 1: Castelsardo Canyon

### Site 3: Canyon des

| Sample Shape                   | MA74 Dr05 lath | Ma74DR05 microlith | Ma74DR05 lath | Ma74DR05 macrophenocryst core | Ma74DR05 rim | Cyl 07-10 autom phen rim | Cyl 07-10 core |
|--------------------------------|----------------|--------------------|---------------|-------------------------------|--------------|--------------------------|----------------|
| SiO <sub>2</sub>               | 51,19          | 51,24              | 46,31         | 44,57                         | 45,81        | 50,89                    | 49,84          |
| TiO <sub>2</sub>               | 0,06           | 0,05               | 0,03          | 0,00                          | 0,01         | 0,04                     | 0,05           |
| Al <sub>2</sub> O <sub>3</sub> | 29,51          | 29,76              | 33,40         | 34,43                         | 33,91        | 29,96                    | 30,53          |
| Fe <sub>2</sub> O <sub>3</sub> | 0,79           | 0,92               | 0,76          | 0,58                          | 0,71         | 0,90                     | 0,74           |
| MgO                            | 0,08           | 0,09               | 0,07          | 0,09                          | 0,06         | 0,10                     | 0,06           |
| CaO                            | 13,25          | 13,52              | 17,59         | 18,60                         | 17,90        | 13,89                    | 14,47          |
| Na <sub>2</sub> O              | 3,46           | 3,60               | 1,62          | 0,92                          | 1,21         | 3,45                     | 3,13           |
| K <sub>2</sub> O               | 0,36           | 0,37               | 0,11          | 0,01                          | 0,06         | 0,39                     | 0,45           |
| Total                          | 98,70          | 99,55              | 99,90         | 99,20                         | 99,67        | 99,60                    | 99,27          |
| Si                             | 2,36           | 2,35               | 2,14          | 2,08                          | 2,12         | 2,33                     | 2,30           |
| Al                             | 1,60           | 1,61               | 1,82          | 1,89                          | 1,85         | 1,62                     | 1,66           |
| Fe <sub>3</sub>                | 0,03           | 0,03               | 0,03          | 0,02                          | 0,03         | 0,03                     | 0,03           |
| Ti                             | 0,00           | 0,00               | 0,00          | 0,00                          | 0,00         | 0,00                     | 0,00           |
| Mg                             | 0,01           | 0,01               | 0,01          | 0,01                          | 0,00         | 0,01                     | 0,00           |
| Na                             | 0,31           | 0,32               | 0,15          | 0,08                          | 0,11         | 0,31                     | 0,28           |
| Ca                             | 0,66           | 0,66               | 0,87          | 0,93                          | 0,89         | 0,68                     | 0,72           |
| K                              | 0,02           | 0,02               | 0,01          | 0,00                          | 0,00         | 0,02                     | 0,03           |
| ->                             | 4,99           | 5,00               | 5,01          | 5,01                          | 5,00         | 5,00                     | 5,01           |
| OR                             | 0,02           | 0,02               | 0,01          | 0,00                          | 0,00         | 0,02                     | 0,03           |
| AB                             | 0,31           | 0,32               | 0,14          | 0,08                          | 0,11         | 0,30                     | 0,27           |
| AN                             | 0,67           | 0,66               | 0,85          | 0,92                          | 0,89         | 0,68                     | 0,70           |

## Moines

| Cyl 07-10<br>macro phenocryst<br>interm | Cyl 07-10<br>rim | Cyl 07-10<br>microlith | Cyl 07-10<br>microlith | Cyl 07-10<br>microlith | Cyl 07-10<br>phenocryst<br>core |
|---|------------------|------------------------|------------------------|------------------------|---------------------------------|
| 51,26                                   | 50,74            | 64,70                  | 53,13                  | 50,16                  | 52,58                           |
| 0,05                                    | 0,06             | 0,19                   | 0,10                   | 0,06                   | 0,05                            |
| 28,84                                   | 29,19            | 19,22                  | 28,78                  | 30,18                  | 28,58                           |
| 0,68                                    | 0,97             | 0,30                   | 1,12                   | 0,76                   | 0,80                            |
| 0,11                                    | 0,14             | 0,02                   | 0,13                   | 0,14                   | 0,11                            |
| 12,90                                   | 13,52            | 0,94                   | 12,54                  | 14,30                  | 12,17                           |
| 3,75                                    | 3,54             | 4,21                   | 4,08                   | 3,14                   | 4,13                            |
| 0,64                                    | 0,52             | 9,69                   | 0,49                   | 0,43                   | 0,64                            |
| 98,22                                   | 98,69            | 99,26                  | 100,35                 | 99,17                  | 99,05                           |
| 2,38                                    | 2,35             | 2,95                   | 2,41                   | 2,31                   | 2,41                            |
| 1,58                                    | 1,59             | 1,03                   | 1,54                   | 1,64                   | 1,55                            |
| 0,02                                    | 0,03             | 0,01                   | 0,04                   | 0,03                   | 0,03                            |
| 0,00                                    | 0,00             | 0,01                   | 0,00                   | 0,00                   | 0,00                            |
| 0,01                                    | 0,01             | 0,00                   | 0,01                   | 0,01                   | 0,01                            |
| 0,34                                    | 0,32             | 0,37                   | 0,36                   | 0,28                   | 0,37                            |
| 0,64                                    | 0,67             | 0,05                   | 0,61                   | 0,71                   | 0,60                            |
| 0,04                                    | 0,03             | 0,56                   | 0,03                   | 0,03                   | 0,04                            |
| 5,01                                    | 5,01             | 4,99                   | 4,99                   | 5,00                   | 5,00                            |
| 0,04                                    | 0,03             | 0,57                   | 0,03                   | 0,03                   | 0,04                            |
| 0,33                                    | 0,31             | 0,38                   | 0,36                   | 0,28                   | 0,37                            |
| 0,63                                    | 0,66             | 0,05                   | 0,61                   | 0,70                   | 0,60                            |

## Site 3: Canyon des Moines

| Cyl 07-11<br>macro phenocryst<br>core | Cyl 07-11<br>rim | Cyl 07-11<br>phenocryst<br>core |
|---------------------------------------|------------------|---------------------------------|
| 51,64                                 | 58,69            | 52,91                           |
| 0,04                                  | 0,08             | 0,04                            |
| 29,28                                 | 23,14            | 29,01                           |
| 0,68                                  | 0,39             | 0,73                            |
| 0,11                                  | 0,10             | 0,10                            |
| 12,70                                 | 6,13             | 12,02                           |
| 3,70                                  | 5,43             | 4,15                            |
| 0,73                                  | 3,91             | 0,77                            |
| 98,88                                 | 97,86            | 99,74                           |
| 2,38                                  | 2,71             | 2,41                            |
| 1,59                                  | 1,26             | 1,56                            |
| 0,02                                  | 0,01             | 0,03                            |
| 0,00                                  | 0,00             | 0,00                            |
| 0,01                                  | 0,01             | 0,01                            |
| 0,33                                  | 0,49             | 0,37                            |
| 0,63                                  | 0,30             | 0,59                            |
| 0,04                                  | 0,23             | 0,05                            |
| 5,00                                  | 5,01             | 5,00                            |
| 0,04                                  | 0,23             | 0,05                            |
| 0,33                                  | 0,48             | 0,37                            |
| 0,63                                  | 0,30             | 0,59                            |

| Cyl 07-11<br>cryst rim | Cyl 07-11<br>micro phenocryst | 77-35-3<br>lath | 77-35-3<br>phenocryst<br>core | 77-35-3<br>rim | 77-35-3<br>phenocryst<br>core | 77-35-3<br>rim | 77-35-3 | 77-35-3<br>microlith |
|------------------------|-------------------------------|-----------------|-------------------------------|----------------|-------------------------------|----------------|---------|----------------------|
| 49,70                  | 52,65                         | 50,97           | 51,04                         | 53,16          | 51,31                         | 50,04          | 45,02   | 53,27                |
| 0,08                   | 0,09                          | 0,06            | 0,05                          | 0,07           | 0,04                          | 0,03           | 0,03    | 0,09                 |
| 30,47                  | 28,35                         | 29,89           | 30,06                         | 28,98          | 29,62                         | 30,73          | 34,05   | 28,08                |
| 1,03                   | 0,97                          | 0,76            | 0,62                          | 0,77           | 0,82                          | 0,73           | 0,55    | 0,87                 |
| 0,11                   | 0,13                          | 0,11            | 0,11                          | 0,11           | 0,11                          | 0,13           | 0,05    | 0,11                 |
| 14,43                  | 12,20                         | 13,77           | 14,34                         | 12,56          | 13,86                         | 14,75          | 18,57   | 12,18                |
| 3,00                   | 4,25                          | 3,74            | 3,46                          | 4,39           | 3,54                          | 3,29           | 0,93    | 4,47                 |
| 0,34                   | 0,65                          | 0,13            | 0,13                          | 0,18           | 0,10                          | 0,10           | 0,00    | 0,21                 |
| 99,16                  | 99,29                         | 99,44           | 99,80                         | 100,22         | 99,40                         | 99,80          | 99,20   | 99,27                |
| 2,29                   | 2,41                          | 2,34            | 2,33                          | 2,41           | 2,35                          | 2,29           | 2,10    | 2,44                 |
| 1,66                   | 1,53                          | 1,62            | 1,62                          | 1,55           | 1,60                          | 1,66           | 1,87    | 1,51                 |
| 0,04                   | 0,03                          | 0,03            | 0,02                          | 0,03           | 0,03                          | 0,03           | 0,02    | 0,03                 |
| 0,00                   | 0,00                          | 0,00            | 0,00                          | 0,00           | 0,00                          | 0,00           | 0,00    | 0,00                 |
| 0,01                   | 0,01                          | 0,01            | 0,01                          | 0,01           | 0,01                          | 0,01           | 0,00    | 0,01                 |
| 0,27                   | 0,38                          | 0,33            | 0,31                          | 0,39           | 0,31                          | 0,29           | 0,08    | 0,40                 |
| 0,71                   | 0,60                          | 0,68            | 0,70                          | 0,61           | 0,68                          | 0,72           | 0,93    | 0,60                 |
| 0,02                   | 0,04                          | 0,01            | 0,01                          | 0,01           | 0,01                          | 0,01           | 0,00    | 0,01                 |
| 5,00                   | 5,01                          | 5,01            | 5,00                          | 5,00           | 4,99                          | 5,01           | 5,00    | 4,99                 |
| 0,02                   | 0,04                          | 0,01            | 0,01                          | 0,01           | 0,01                          | 0,01           | 0,00    | 0,01                 |
| 0,27                   | 0,37                          | 0,33            | 0,30                          | 0,38           | 0,31                          | 0,29           | 0,08    | 0,39                 |
| 0,71                   | 0,59                          | 0,67            | 0,69                          | 0,61           | 0,68                          | 0,71           | 0,92    | 0,59                 |



Site 6: Propriano High

Site 6: P1

| Cyl 02-01<br>phenocryst | Cyl 02-01<br>automorp | Cyl 02-01<br>phenocry: | Cyl 02-01<br>phenocryst | Cyl 02-01<br>microlith | Cyl 02-01<br>microlith | Cyl 02-01<br>macro | Cyl 02-01<br>phenocryst | Cyl 02-01<br>phenocryst | Cyl 02-02<br>pheno |
|-------------------------|-----------------------|------------------------|-------------------------|------------------------|------------------------|--------------------|-------------------------|-------------------------|--------------------|
| core                    | rim                   | core                   | rim                     |                        |                        | core               | interm                  | rim                     | core               |
| 49,79                   | 57,72                 | 54,92                  | 55,43                   | 51,88                  | 56,74                  | 56,94              | 56,35                   | 58,60                   | 53,04              |
| 0,03                    | 0,04                  | 0,00                   | 0,00                    | 0,00                   | 0,02                   | 0,00               | 0,00                    | 0,00                    | 0,00               |
| 30,81                   | 26,76                 | 27,72                  | 28,56                   | 30,14                  | 27,21                  | 26,62              | 26,73                   | 26,55                   | 29,15              |
| 0,38                    | 0,25                  | 0,15                   | 0,37                    | 0,53                   | 0,45                   | 0,27               | 0,18                    | 0,20                    | 0,36               |
| 0,04                    | 0,00                  | 0,03                   | 0,07                    | 0,07                   | 0,00                   | 0,00               | 0,02                    | 0,03                    | 0,05               |
| 14,40                   | 8,97                  | 10,39                  | 10,73                   | 12,82                  | 9,55                   | 9,12               | 9,35                    | 8,40                    | 12,02              |
| 3,13                    | 6,10                  | 5,31                   | 4,87                    | 4,02                   | 5,59                   | 6,06               | 5,69                    | 5,94                    | 4,42               |
| 0,14                    | 0,38                  | 0,30                   | 0,35                    | 0,42                   | 0,44                   | 0,41               | 0,41                    | 0,46                    | 0,27               |
| 98,71                   | 100,22                | 98,83                  | 100,37                  | 99,87                  | 99,99                  | 99,41              | 98,72                   | 100,17                  | 99,31              |
| 2,30                    | 2,58                  | 2,50                   | 2,49                    | 2,36                   | 2,55                   | 2,57               | 2,56                    | 2,61                    | 2,42               |
| 1,68                    | 1,41                  | 1,49                   | 1,51                    | 1,62                   | 1,44                   | 1,42               | 1,43                    | 1,40                    | 1,57               |
| 0,01                    | 0,01                  | 0,01                   | 0,01                    | 0,02                   | 0,02                   | 0,01               | 0,01                    | 0,01                    | 0,01               |
| 0,00                    | 0,00                  | 0,00                   | 0,00                    | 0,00                   | 0,00                   | 0,00               | 0,00                    | 0,00                    | 0,00               |
| 0,00                    | 0,00                  | 0,00                   | 0,01                    | 0,01                   | 0,00                   | 0,00               | 0,00                    | 0,00                    | 0,00               |
| 0,28                    | 0,53                  | 0,47                   | 0,42                    | 0,36                   | 0,49                   | 0,53               | 0,50                    | 0,51                    | 0,39               |
| 0,71                    | 0,43                  | 0,51                   | 0,52                    | 0,63                   | 0,46                   | 0,44               | 0,46                    | 0,40                    | 0,59               |
| 0,01                    | 0,02                  | 0,02                   | 0,02                    | 0,02                   | 0,03                   | 0,02               | 0,02                    | 0,03                    | 0,02               |
| 5,00                    | 4,98                  | 4,99                   | 4,97                    | 5,01                   | 4,98                   | 4,99               | 4,98                    | 4,96                    | 5,00               |
| 0,01                    | 0,02                  | 0,02                   | 0,02                    | 0,02                   | 0,03                   | 0,02               | 0,02                    | 0,03                    | 0,02               |
| 0,28                    | 0,54                  | 0,47                   | 0,44                    | 0,35                   | 0,50                   | 0,53               | 0,51                    | 0,55                    | 0,39               |
| 0,71                    | 0,44                  | 0,51                   | 0,54                    | 0,62                   | 0,47                   | 0,44               | 0,46                    | 0,43                    | 0,59               |

ropriano High

Site 9: Monte Doria SW fla

| Cyl 02-02<br>cryst<br>rim | Cyl 02-02<br>microlith | Cyl 02-02<br>phenocryst<br>core | Cyl 02-02<br>rim | Cyl 02-02<br>microlith | Cyl 02-02<br>microlith | Cyl 02-02<br>phenocryst | Cyl 22-03<br>lath | Cyl 22-03<br>macro<br>core | Cyl 22-03<br>phenocryst<br>rim |
|---------------------------|------------------------|---------------------------------|------------------|------------------------|------------------------|-------------------------|-------------------|----------------------------|--------------------------------|
| 56,09                     | 55,60                  | 53,10                           | 56,08            | 53,16                  | 52,84                  | 53,71                   | 52,40             | 50,34                      | 51,14                          |
| 0,01                      | 0,01                   | 0,00                            | 0,00             | 0,02                   | 0,03                   | 0,00                    | 0,07              | 0,07                       | 0,05                           |
| 27,48                     | 27,64                  | 28,91                           | 27,27            | 29,43                  | 28,29                  | 29,05                   | 29,75             | 30,73                      | 30,13                          |
| 0,40                      | 0,37                   | 0,32                            | 0,26             | 0,32                   | 0,47                   | 0,44                    | 0,73              | 0,39                       | 0,66                           |
| 0,02                      | 0,05                   | 0,03                            | 0,02             | 0,01                   | 0,06                   | 0,02                    | 0,11              | 0,12                       | 0,12                           |
| 9,91                      | 10,18                  | 12,06                           | 9,93             | 12,12                  | 11,42                  | 11,84                   | 12,78             | 13,97                      | 13,53                          |
| 5,59                      | 5,53                   | 4,66                            | 5,77             | 4,35                   | 4,69                   | 4,62                    | 3,77              | 3,23                       | 3,54                           |
| 0,36                      | 0,35                   | 0,22                            | 0,38             | 0,25                   | 0,37                   | 0,27                    | 0,36              | 0,18                       | 0,25                           |
| 99,87                     | 99,73                  | 99,30                           | 99,71            | 99,67                  | 98,17                  | 99,94                   | 99,97             | 99,03                      | 99,42                          |
| 2,53                      | 2,51                   | 2,42                            | 2,53             | 2,42                   | 2,44                   | 2,43                    | 2,38              | 2,32                       | 2,34                           |
| 1,46                      | 1,47                   | 1,56                            | 1,45             | 1,58                   | 1,54                   | 1,55                    | 1,59              | 1,67                       | 1,63                           |
| 0,01                      | 0,01                   | 0,01                            | 0,01             | 0,01                   | 0,02                   | 0,02                    | 0,03              | 0,01                       | 0,02                           |
| 0,00                      | 0,00                   | 0,00                            | 0,00             | 0,00                   | 0,00                   | 0,00                    | 0,00              | 0,00                       | 0,00                           |
| 0,00                      | 0,00                   | 0,00                            | 0,00             | 0,00                   | 0,00                   | 0,00                    | 0,01              | 0,01                       | 0,01                           |
| 0,49                      | 0,48                   | 0,41                            | 0,51             | 0,38                   | 0,42                   | 0,41                    | 0,33              | 0,29                       | 0,32                           |
| 0,48                      | 0,49                   | 0,59                            | 0,48             | 0,59                   | 0,57                   | 0,57                    | 0,62              | 0,69                       | 0,66                           |
| 0,02                      | 0,02                   | 0,01                            | 0,02             | 0,02                   | 0,02                   | 0,02                    | 0,02              | 0,01                       | 0,02                           |
| 4,99                      | 5,00                   | 5,01                            | 5,00             | 4,99                   | 5,00                   | 5,00                    | 4,98              | 4,99                       | 5,00                           |
| 0,02                      | 0,02                   | 0,01                            | 0,02             | 0,02                   | 0,02                   | 0,02                    | 0,02              | 0,01                       | 0,02                           |
| 0,49                      | 0,49                   | 0,41                            | 0,50             | 0,39                   | 0,42                   | 0,41                    | 0,34              | 0,29                       | 0,32                           |
| 0,48                      | 0,49                   | 0,58                            | 0,48             | 0,60                   | 0,56                   | 0,58                    | 0,64              | 0,70                       | 0,67                           |

unk

Site 9: Monte Doria SW flank

| Cyl 22-03<br>microlith | Cyl 22-03 | Cyl 22-03<br>macro phenocryst<br>core | Cyl 22-03<br>rim | Cyl 22-08<br>lath | Cyl 22-08<br>microlith | Cyl 22-08<br>lath | Cyl 22-08<br>lath | Cyl 22-08<br>xenocryst |
|------------------------|-----------|---------------------------------------|------------------|-------------------|------------------------|-------------------|-------------------|------------------------|
| 52,49                  | 51,41     | 54,40                                 | 51,04            | 52,77             | 53,52                  | 52,05             | 50,26             | 51,35                  |
| 0,11                   | 0,07      | 0,04                                  | 0,07             | 0,13              | 0,14                   | 0,10              | 0,04              | 0,09                   |
| 29,12                  | 29,84     | 28,19                                 | 30,12            | 28,84             | 28,09                  | 28,60             | 30,69             | 29,33                  |
| 0,75                   | 0,66      | 0,43                                  | 0,73             | 1,01              | 0,88                   | 1,07              | 0,54              | 0,85                   |
| 0,12                   | 0,12      | 0,07                                  | 0,11             | 0,10              | 0,12                   | 0,43              | 0,08              | 0,10                   |
| 12,57                  | 13,31     | 10,85                                 | 13,33            | 12,25             | 11,37                  | 12,20             | 14,38             | 13,10                  |
| 4,04                   | 3,88      | 4,94                                  | 3,50             | 4,31              | 4,82                   | 4,18              | 3,24              | 3,61                   |
| 0,39                   | 0,43      | 0,51                                  | 0,27             | 0,26              | 0,39                   | 0,32              | 0,17              | 0,22                   |
| 99,57                  | 99,71     | 99,42                                 | 99,17            | 99,68             | 99,34                  | 98,95             | 99,39             | 98,65                  |
| 2,40                   | 2,35      | 2,47                                  | 2,34             | 2,41              | 2,44                   | 2,39              | 2,31              | 2,37                   |
| 1,57                   | 1,61      | 1,51                                  | 1,63             | 1,55              | 1,51                   | 1,55              | 1,66              | 1,59                   |
| 0,03                   | 0,02      | 0,02                                  | 0,03             | 0,04              | 0,03                   | 0,04              | 0,02              | 0,03                   |
| 0,00                   | 0,00      | 0,00                                  | 0,00             | 0,00              | 0,01                   | 0,00              | 0,00              | 0,00                   |
| 0,01                   | 0,01      | 0,01                                  | 0,01             | 0,01              | 0,01                   | 0,03              | 0,01              | 0,01                   |
| 0,36                   | 0,34      | 0,44                                  | 0,31             | 0,38              | 0,43                   | 0,37              | 0,29              | 0,32                   |
| 0,61                   | 0,65      | 0,53                                  | 0,66             | 0,60              | 0,56                   | 0,60              | 0,71              | 0,65                   |
| 0,02                   | 0,03      | 0,03                                  | 0,02             | 0,02              | 0,02                   | 0,02              | 0,01              | 0,01                   |
| 4,99                   | 5,02      | 5,00                                  | 4,99             | 5,00              | 5,01                   | 5,01              | 5,00              | 4,99                   |
| 0,02                   | 0,03      | 0,03                                  | 0,02             | 0,02              | 0,02                   | 0,02              | 0,01              | 0,01                   |
| 0,36                   | 0,34      | 0,44                                  | 0,32             | 0,38              | 0,42                   | 0,38              | 0,29              | 0,33                   |
| 0,62                   | 0,64      | 0,53                                  | 0,67             | 0,60              | 0,55                   | 0,61              | 0,70              | 0,66                   |

| Cyl 22-05    | Cyl 22-05<br>microlith | Cyl 22-05<br>pheno<br>core | Cyl 22-05<br>rim | Cyl 22-7a<br>lath | Cyl 22-7a<br>microlite |
|--------------|------------------------|----------------------------|------------------|-------------------|------------------------|
| 52.205       | 53.341                 | 51.435                     | 51.433           | 51.101            | 50.746                 |
| 0.032        | 0.108                  | 0.043                      | 0.082            | 0.092             | 0.077                  |
| 29.647       | 28.648                 | 29.949                     | 29.993           | 30.133            | 30.095                 |
| 0.532        | 0.894                  | 0.590                      | 0.641            | 0.656             | 0.732                  |
| 0.093        | 0.081                  | 0.068                      | 0.119            | 0.176             | 0.194                  |
| 12.759       | 11.931                 | 13.046                     | 13.266           | 13.562            | 13.635                 |
| 3.931        | 4.412                  | 3.951                      | 3.494            | 3.568             | 3.286                  |
| 0.313        | 0.408                  | 0.313                      | 0.266            | 0.300             | 0.369                  |
| 99.512       | 99.823                 | 99.396                     | 99.293           | 99.588            | 99.134                 |
| 2.383        | 2.425                  | 2.356                      | 2.355            | 2.339             | 2.334                  |
| 1.595        | 1.535                  | 1.617                      | 1.619            | 1.625             | 1.631                  |
| 0.018        | 0.031                  | 0.020                      | 0.022            | 0.023             | 0.025                  |
| 0.001        | 0.004                  | 0.001                      | 0.003            | 0.003             | 0.003                  |
| 0.006        | 0.006                  | 0.005                      | 0.008            | 0.012             | 0.013                  |
| 0.348        | 0.389                  | 0.351                      | 0.310            | 0.317             | 0.293                  |
| 0.624        | 0.581                  | 0.640                      | 0.651            | 0.665             | 0.672                  |
| 0.018        | 0.024                  | 0.018                      | 0.016            | 0.018             | 0.022                  |
| 4.993        | 4.994                  | 5.009                      | 4.984            | 5.001             | 4.993                  |
| <b>0.018</b> | <b>0.024</b>           | <b>0.018</b>               | <b>0.016</b>     | <b>0.018</b>      | <b>0.022</b>           |
| <b>0.351</b> | <b>0.391</b>           | <b>0.348</b>               | <b>0.318</b>     | <b>0.317</b>      | <b>0.297</b>           |
| <b>0.630</b> | <b>0.585</b>           | <b>0.634</b>               | <b>0.666</b>     | <b>0.666</b>      | <b>0.681</b>           |